University of Alberta

A novel mouse model of acute antibody-mediated transplant rejection shows simultaneous complement activating and anti-inflammatory effects of donor specific IgG antibodies

by

Aaron K.Y. Chow

A thesis submitted to the Faculty of Graduate Studies and Research
in partial fulfillment of the requirements for the degree of

Master of Science

in

Medical Sciences – Laboratory Medicine and Pathology

©Aaron K.Y. Chow

Fall 2013
Edmonton, Alberta

Permission is hereby granted to the University of Alberta Libraries to reproduce single copies of this thesis and to lend or sell such copies for private, scholarly or scientific research purposes only. Where the thesis is converted to, or otherwise made available in digital form, the University of Alberta will advise potential users of the thesis of these terms.

The author reserves all other publication and other rights in association with the copyright in the thesis and, except as herein before provided, neither the thesis nor any substantial portion thereof may be printed or otherwise reproduced in any material form whatsoever without the author's prior written permission.

Dedicated to friends and family who have encouraged and supported me unconditionally in all my pursuits, and to God, who has brought me through this amazing journey beyond my wildest dreams.

Abstract

We developed a small animal model of pure antibody-mediated rejection (ABMR) by utilizing fully major histocompatibility complex (MHC) mismatched kidney allografts in mice. By examining resultant ABMR pathology, we show that terminal complement products C5a and C5b-9 are crucial in establishing antibody-mediated allograft microvascular and tubular injury, and the presence of proximal complement product C4d alone is not indicative of ABMR. We demonstrate allorecognition capabilities in NK cells to induce micro-inflammation and apoptosis in MHC mismatched transplants. By gene expression profiling, we found that binding of donor specific antibodies (DSA) into kidney allograft tissues induces a 'self-protective' anti-inflammatory response in kidney parenchyma. The data suggests that the anti-inflammatory response associated with DSA may be regulated via inhibitory Fc receptors for immunoglobulin G. In summary, we established a mouse model demonstrating pure acute ABMR of kidney allografts mimicking some aspects of human ABMR pathology in the absence of T cell-mediated rejection.

Acknowledgements

I would like to express my deepest gratitude to Dr. Banu Sis for spending the time, effort, and patience in mentoring me as a graduate student. To the members of the Sis Lab, who played instrumental roles in my data presented here.

I would like to thank the Halloran Lab for the advice, contributions, and insight as I put this thesis together

I would like to thank my committee members Dr. Lisa Cameron, Dr. Judith Hugh, Dr. Allan Murray for their input and guidance in my pursuit of a Master's degree and in my continued endeavors towards additional education and training.

I would like to acknowledge the CIHR funding, without which none of this research would have been possible.

Table of Contents

List of Tables

List of Figures

List of Abbreviations

ABMR	Antibody-Mediated Rejection
APC	Antigen Presenting Cell
ALLO	Allograft (transplant)
ANOVA	Analysis of Variance
CD	Cluster of Differentiation
DSA	Donor Specific Antibody
ELISA	Enzyme-Linked Immunosorbent Assay
ESRD	End Stage Renal Disease
HLA	Human Leukocyte Antigen
I.P.	Intraperitoneal (injection)
ISO	Isograft (transplant)
IVIG	Intravenous Immunoglobulin
LS	Life-Supporting (transplant)
MAC	Membrane Attack Complex
MFI	Median Fluorescent Intensity
MHC	Major Histocompatibility Complex
NCBA	Normal CBA/J strain mouse
NK	Natural Killer

NLS	Non-Life Supporting (transplant)
NRAG	Normal C57BL/6 strain mouse (with knockout in Rag gene)
PBS	Phosphate Buffered Saline
S.C.	Subcutaneous (injection)
TCMR	T cell-Mediated Rejection

Chapter 1: Introduction

1.1 – Kidney failure and transplantation

Kidney failure, or end-stage renal disease (ESRD), is the most severe stage of kidney disease. Patients present with drastically lowered kidney function (less than 15% of normal kidney function) (1), and if left untreated, ESRD is fatal. In order to replace renal function needed to sustain life, patients must undergo either dialysis or kidney transplantation. Currently, kidney transplantation is the preferred method to treat ESRD, as it eliminates the patient's dependence on dialysis regimes and also alleviates financial pressures on the healthcare system (ongoing dialysis treatments for patients in the United States cost about $30 billion a year) (123). While modern immunosuppression therapies significantly lowered the incidence of acute T cell-mediated rejection, kidney transplant survival beyond first year has not improved (72). USRDS data shows that approximately 5000 kidney transplants in the USA fail each year, making renal allograft failure the fourth leading cause of ESRD (2). The lack of improvement in long-term graft survival is primarily due to donor specific antibodies (DSA) and recurrent primary diseases (25;28;39;94;99). Approximately 40% of pre-sensitized patients against donor MHC antigens before transplantation experience acute antibody-mediated rejection (ABMR) episodes, with 22% later developing chronic ABMR (84). Patients without DSA at time of transplantation are also at risk for developing de novo DSA after transplantation, which are associated with high frequency of acute rejection (36%) and kidney graft failure (127). Furthermore, insufficient numbers of kidney donors have led to a waitlist of 3,000 Canadians currently waiting for a kidney for transplantation. In addition to the growing waitlist, there are approximately 5,000 newly diagnosed ESRD patients a year, according to the Canadian Institute of Health Information Annual Report of 2011-2012 (3). With the limited availability of kidneys for transplant, the loss of graft tissue remains a very serious problem.

Kidney transplantation is a relatively new field, with the first successful kidney transplant accomplished in 1954 by Dr. Joseph Murray et al. (44). Prior to this study,

transplanted organs continually failed not only due to the lack of established surgery techniques for transplantation, but also due to the lack in understanding of the immune system and rejection. Although the role of the immune system was not completely understood at the time Dr. Murray conducted the first successful kidney transplant, his success was due to the fact that the kidney was transplanted between two identical twins. The genetically identical nature of the donor-recipient pair allowed for the avoidance of immune recognition and activation against the transplanted kidney (21).

1.2 – Allograft Rejection

1.2.1 – HLA/MHC mismatch

The basis of graft rejection lies in the incompatibilities of different antigens present on cell surfaces between donor and host tissue (38). Just as the immune system recognizes bacteria as foreign matter that must be eliminated, transplanted graft tissue with mismatched major histocompatibility complexes (MHC) (or human leukocyte antigen (HLA) in humans) compared to the host elicits the same response – destruction and elimination of the foreign matter. HLA molecules are present on the surface of all nucleated cells, and functions to provide, in essence, a scaffolding platform in which proteins can be presented from cell to cell (129). Two classes of HLA molecules (class I and class II) function to present different types of proteins into the extra cellular space. Class I HLA molecules are present on all nucleated cells, and are used to present proteins fragments (about 8-15aa in length) (113) originating from within the cell to Cd8+ T lymphocytes. This functions as a method of monitoring the wellbeing of a given cell, as presentation of abnormal peptides may denote an infection in the cell. Class II HLA molecules are important primarily for antigen presenting cells (APC) in order to place fragments (about 12-25aa in length) (36) of digested proteins typically originating from outside of the cell into the Class II HLA scaffold. Loaded MHC II proteins are then presented to Cd4+ T lymphocytes for recognition (35;129).

In humans, the genes encoding HLA molecules are located in multiple loci, each represented by numerous variant alleles (22;54). This makes HLA molecules highly polymorphic, leading to a higher probability of HLA differences between individuals (54). Due to this polymorphic nature, the HLA molecules present on the surface of donor tissue may appear foreign to the transplant recipient, and elicit an immune response. It is generally fragments of the foreign unrecognized HLA molecules that the immune system mounts a response against (38).

1.2.2 – Forms of rejection

Donor kidneys expressing mismatched HLA molecules compared to the recipient elicits injury and rejection of the transplanted graft. Graft injury and loss is primarily due to two forms of rejection in transplant recipients: T cell-mediated rejection (TCMR), and ABMR. TCMR is not the focus of this thesis, but briefly, TCMR begins with the recognition of donor antigens. Two pathways exist for detecting donor antigens: the direct or the indirect allorecognition pathway. Direct allorecognition refers to recipient T cells binding donor antigens presented on donor-derived antigen presenting cells (APC) that were present in the transplanted kidney. These donor APCs would be presenting normal donor-derived antigens as they migrate into secondary recipient lymphoid organs where they activate recipient T cells. Direct allorecognition-induced T cell activation plays an important role in early phases of TCMR, when donor APCs originating from the donor graft are still present. However, as donor APCs are not replenished and their numbers decrease, the direct allorecognition pathway plays less and less of a role in maintaining a T cell response (38;121).

In indirect allorecognition, recipient T cells bind onto donor-derived antigens as they are presented on recipient APCs. This is similar to how T cells would normally respond to foreign matter in the body. Recipient APCs process and present donor-derived antigens (typically peptides derived from donor MHC molecules (38)) on their MHC II molecules, and upon meeting recipient T cells in secondary lymphoid organs, the

T cell becomes activated against the presented antigen. Unlike direct allorecognition, the indirect allorecognition pathway can provide sustained activation signals for recipient T cells, as recipient APCs are constantly replenished. The indirect allorecognition pathway is also important in activating antibody production (22;83).

In contrast to TCMR, ABMR begins with the production and presence of antibodies against donor antigens. Binding of antibodies specific against donor antigens elicits various biochemical pathways such as the complement pathway to bring about tissue injury and rejection. The ABMR disease can be further into three forms: hyperacute ABMR, acute ABMR, and chronic ABMR. Hyperacute rejection can occur within minutes to hours of graft reperfusion, and occurs primarily in recipients who were highly pre-sensitized to donor HLA antigens prior to transplantation (84). This form of ABMR yields severe endothelial injury and arterial inflammation (84). Hyperacute ABMR progresses with such severity and speed that the transplanted kidney must often be removed from the recipient to avoid further graft injury and early graft loss (63;128). However, with the incorporation of HLA cross-match testing between donor and recipient prior to transplantation to detect highly pre-sensitized patients, this form of rejection has become extremely rare. Acute ABMR occurs within days, arising due to either pre-formed or de novo donor specific antibody (DSA), showing pathology of endothelial injury where DSA binds to and injures. Acute ABMR typically shows less severe pathology than that in hyperacute rejection, but is still a major concern in practice as it is a prevalent disease in kidney transplant patients, and can lead to chronic graft injury (66;71;90). According to the consensus Banff classification, the criterion for diagnosis of acute ABMR requires the presence of: 1. Morphological evidence of acute tissue injury (such as acute tubular injury or acute arteritis), 2. Positive C4d staining in peritubular capillaries, and 3. Evidence for circulating DSA antibodies (85;86). In contrast, chronic ABMR can manifest itself within months of transplantation, due to either pre-formed or de novo DSA, and is characterized by pathological features such as the duplication of the basement membrane of glomeruli and peritubular capillaries, also known as transplant

glomerulopathy (19). Currently, chronic ABMR is the major cause of late kidney transplant dysfunction and failure (23;39). In all three forms of ABMR, antibodies play a crucial role in triggering disease phenotypes.

It is important to note that both TCMR and ABMR are diseases that commonly occur in other transplanted organ systems as well, and is not a disease exclusive to the renal system.

1.3 – Antibodies

1.3.1 – Antibody forms

Antibodies, or immunoglobulins, exist as five different types, designated as: IgA, IgD, IgE, IgG, and IgM. These different classes (or isotypes) of antibodies are found in different areas of the body, each with different properties and functions (96;97). The specificity and epitopes recognized by the antibodies are determined by the B cell that manufactured it. The process of antibody production begins in peripheral lymphoid organs where B cells encounter, recognize, and bind onto antigens via the B cell receptors present on its cell surface (110). In addition to binding onto foreign antigens, the B cell requires a co-activation signal, provided as cytokines released by CD4+ T cells (also known as T helper cells). Once the antigen and co-stimulation signal is achieved, the B cell differentiates into a plasma cell, producing large quantities of antibodies specific to the recognized antigen. In the setting of ABMR, antigens recognized are typically MHC molecules presented on donor cells (118).

Antibodies produced against donor antigens are usually the IgG isotype variety. This form of immunoglobulins is the most relevant and is routinely tested for donor reactivity in human patients. Human IgG antibodies are further classified into four subclasses, IgG1, IgG2, IgG3, and IgG4. Similarly, mice have four IgG subclasses as well, designated as IgG1, IgG2a, IgG2b, and IgG3. IgG1 antibodies are not known to

activate the complement pathway (56;122). In comparison, both IgG2a and IgG2b antibodies are capable of initiating the complement pathway by binding C1q protein on their Fc region (122). Finally, unlike all previous IgG subclasses in mice, IgG3 antibodies do not recognize protein antigens, but instead recognize carbohydrate antigens (56).

1.3.2 – Donor Specific Antibody

Donor specific antibodies, or DSA, are immunoglobulins of any subtype that recognize and are capable of binding donor-specific antigens. Typically, DSA refer to the more common IgG antibody subtype. The antigens recognized as foreign are typically major histocompatibility complex molecules (either class I or class II) expressed on donor tissues. Recognition of other non-MHC molecules by donor specific antibodies occurs, but infrequently (61;118). In human transplant patients, DSA can be generated through the adaptive immune system following transplantation, but DSA may also be present in the circulation of a patient prior to transplantation due to a previous transplant, blood transfusion, or pregnancy.

The primary site for donor specific antibodies binding is typically the endothelial cells lining blood vessels, as DSA is present in circulation (19). Bound DSA can elicit damage to the endothelial cells through several means. Firstly, the bound antibodies can activate the complement system, eventually forming membrane attack complexes (MAC) on the surface of the bound cell, thereby lysing the affected cell (109). Bound DSA can also bind onto Fc receptors present in leukocytes and lymphocytes (114). Here, Fc regions of the bound DSA come into contact and interact with Fc receptors located on the surface of effector cells such as lymphocytes, NK cells, macrophages, neutrophils, and eosinophils. Interaction between the Fc portion of the antibody and the Fc receptor can induce different cellular responses, depending on the receptor bound (89). The binding can recruit these effector cells to the transplanted tissue and further contribute to graft injury.

1.4 – Complement

1.4.1 – The complement pathway

Activation of the complement pathway by bound DSA is the primary way by which ABMR injures and rejects allografts (109). It has been shown in animal experiments that by 'blocking' progression of the complement pathway (125), ABMR can be avoided. From these findings, drug development has since produced antibodies against complement proteins in order to disrupt the complement pathway, thereby interfering with graft injury progression and ABMR (109;111).

The complement system is a tightly regulated pathway composed of a series of inter-related proteins with chemotactic properties and the ability to form membrane pores to lyse target cells. Its function is to bring about the lysis and destruction of foreign material in the body. In transplantation, DSA bound on graft tissues activate the classical form of the complement pathway (Figure 1.1). The antibody-activated classical complement pathway begins with the assembly of the C1 complex, which is initiated by the recognition of the Fc region of IgG or IgM immune complexes by a C1q molecule. Binding onto antibody complexes causes the C1q molecule to undergo a conformational change (10;37;42). This allows two molecules of C1r to add onto the growing C1 complex. Once bound, the C1r proteases cleave and activate two molecules of C1s to complete the C1 complex. In all, the C1 complex is composed of one molecule of C1q, two molecules of C1r, and two molecules of C1s. The activated C1s portions in the complete $C1qr_2s_2$ complex have protease properties, allowing it to cleave both C2 into C2a and C2b, along with C4 into C4a and C4b. C4b portions bind the membrane surface, with C2a binding C4b to form a separate complex. Similar to C1s molecules in the C1 complex, the C2a portion of the C4b2a complex possess protease properties, allowing it to cleave both C3 and C5. The cleavage of C3 yields C3a and C3b portions, the latter of which incorporates into the C4b2a complex to form C4b2a3b. The addition of

C3b allows the C2a portion of the complex to bind to and cleave C5 into C5a and C5b. The presence of the C5b split product initiates the formation of the MAC, a polymerized protein structure on the surface of the pathogen marked for destruction. C5b binds onto complement proteins C6, C7 in the fluid phase before anchoring into the cell membrane. C8 binds onto the C5b67 complex and begins polymerizing complement protein C9 into a pore in the membrane of the pathogen, thereby forming the MAC to bring about cell lysis.

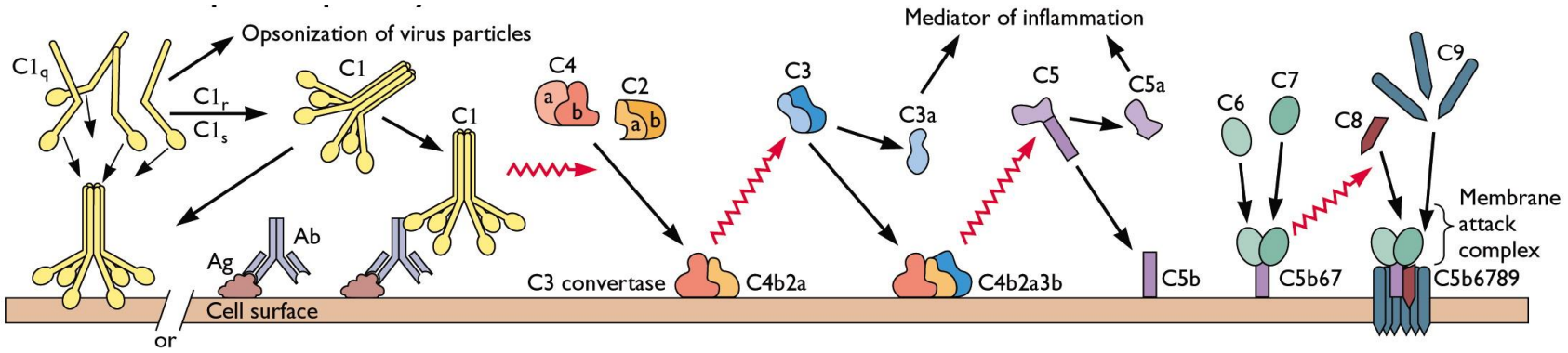

Figure 1.1 – Classical complement pathway. The classical complement pathway begins with the binding of antibodies onto antigens present on the target cell surface. The C1 complex assembles onto bound antigens, and begins cleavage and combination of C4 and C2 to form the C3 convertase. Subsequent addition of portions of C3 forms the C5 complex, implementing C5b into the cell membrane. Catalytic assembly of C6-C9 onto C5b on the cell surface forms the terminal complement complex, the membrane attack complex (MAC).

Image retrieved June 22, 2013 from: http://www.twiv.tv/classical-complement.jpg

1.4.2 – Complement split products enhance immune responses

In addition to forming the terminal MAC and causing lysis in cells bound with DSA, portions of the complement pathway have additional immunomodulatory properties. Complement split products C3a, C4a, and C5a, also known as anaphylatoxins, are potent pro-inflammatory proteins, capable of recruiting neutrophils to areas of complement activation (126). Furthermore, split products C3a and C5a have additional functions to induce mast cell and basophil degranulation, and activate the expression of adhesion molecules of endothelial cells in blood vessels such as Pecam1 (40;58;68). With the formation of chemotactic molecules together with the increase in adhesion molecules on the surface of endothelial cells, leukocytes in circulation migrate to the local area of cytokine release, and begin extravasation by first 'rolling' to a stop on endothelial cell surfaces by binding adhesion molecules, then penetrating through the capillary basement membrane between endothelial cells to infiltrate into the tissue (67;68) (Figure 1.2). Finally, split products C3a and C5a are also capable of inducing smooth muscle contraction and increasing the permeability of blood vasculature (45;126). In this way, the split products generated from complement activation further enhance the immune response against antibody bound antigens by inducing causing inflammation and recruitment of effector cells out of circulation and into the targeted tissue.

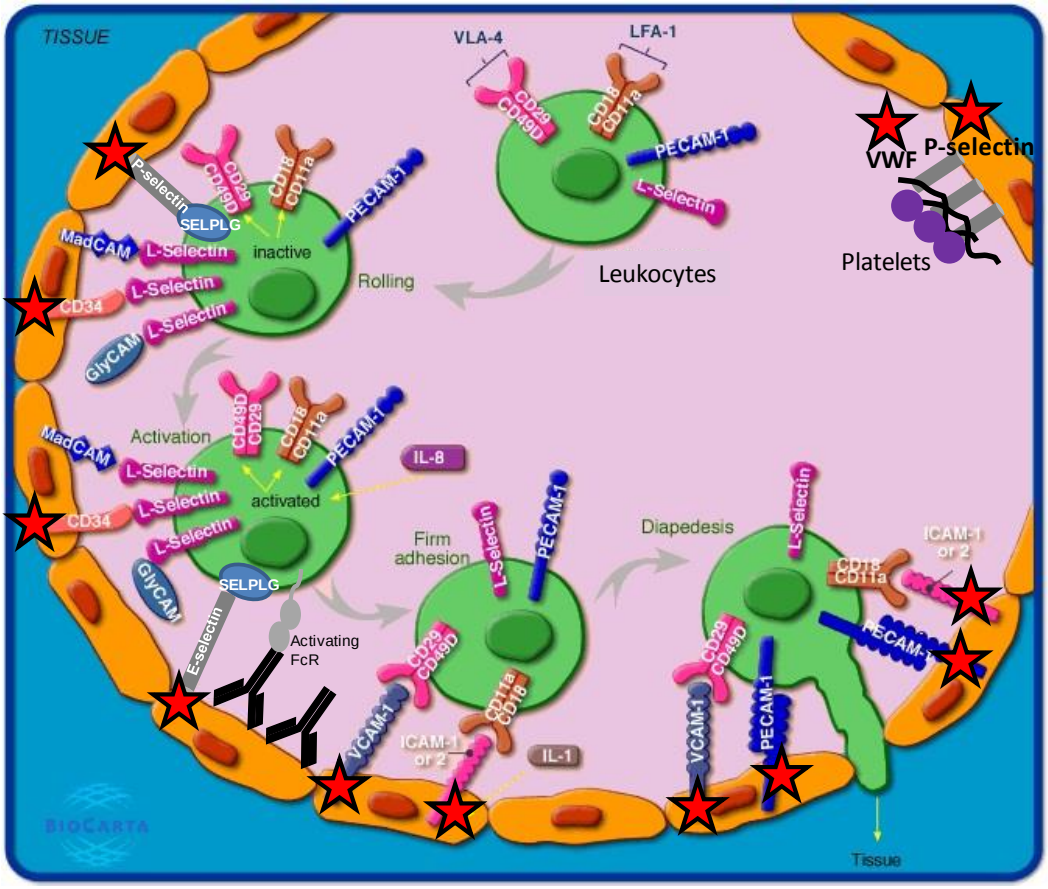

Upregulated endothelial genes in human antibody-mediated rejection

Figure 1.2 – Leukocyte adhesion and transmigration. Expression of adhesion molecules (marked by stars) are upregulated in renal biopsies in humans with ABMR. This schematic from the BioCarta database depicts the interactions between leukocyte and endothelial adhesion molecules to facilitate the arrest and transmigration of nearby leukocytes. (http://www.biocarta.com/genes/index.asp) (99)

1.4.3 – Complement regulation

Due to the potency and potential systemic effects that result from complement activation, the pathway itself is tightly regulated in order to prevent accidental activation and lysis of 'self' tissue. Inhibitory proteins are positioned throughout the complement pathway in order to regulate the extent of complement activation as it progresses through the cascade. There are several major locations in the complement pathway in which complement regulatory proteins typically act upon: the initial activation of the complement cascade beginning with C1 (such as C1-inhibitor protein), the cleavage and activation of C3 (such as membrane cofactor protein), the cleavage and activation of C5 (such as complement factor H-related 1), and the formation of the terminal complement complex, or MAC formation (such as cd59 protein) (131). There is a high number and variety of C3 convertase regulators, since the activated C3 complex is regarded as a catalyst for downstream complement activation, and it is also where all three forms of the complement cascade converge, where the classical pathway, lectin binding pathway, and alternative complement pathway all share common complement proteins. Furthermore, the split products from activated complement proteins beginning at C3 (such as C3a, C4a, C5a) are potent immunomodulatory molecules; the activation of these pro-inflammatory proteins at inappropriate times can lead to detrimental effects. For these reasons, complement regulation at C3 allows for the effective control at the 'bottleneck' of complement activation before the activated cascade becomes too difficult to manage. In addition to the location of the complement pathway with which the regulator acts upon, there are two forms of regulators: membrane bound and secreted complement regulators. There are 7 secreted complement regulators acting on the classical complement pathway: Carboxy-peptidase N, C4BP, C1q, C1INH, CFHR1, Clusterin, and Vitronectin (131), and 8 membrane bound complement regulators: CR1, CR2, CR3, CR4, CRIg, CD46, CD55, and CD59 (131). Unlike the membrane bound complement regulators that act upon either C3 protein or the terminal C5b-9 complex, secreted

complement regulators tend to work in the early stages of complement activation, and therefore are specific to one of the three complement pathways (131). In this way, the variety of complement proteins allows for the efficient control of complement activation to prevent inappropriate 'self' activation.

1.4.4 – Detectable markers of complement activation

Since ABMR is driven primarily by the complement pathway, the detection of complement activation is important in determining the risk of ABMR which transplant patients face. Originally observed by Feucht et al., complement split product C4d deposition in peritubular capillaries in biopsies of transplanted kidneys correlates well with impaired graft function (32;33). From this finding came the development of C4d as a biomarker for complement activation and the onset of ABMR. Complement C4d works well as a biomarker due to its behavior in patient biopsy samples. After the complement pathway is activated and C4 protein is cleaved into C4a and C4b, where C4a is a fluid phase protein and C4b is deposited onto the endothelium in the vicinity where complement was activated. C4b proteins eventually become converted into C4d, an inert molecule which covalently bind onto the endothelium, and can remain bound for roughly several days before being cleared (19;93). C4d is easily visualized in biopsies by immunohistochemistry, and is a fairly specific test having low false positive results (13), with a few exceptions (46;73;102;103). As such, it has since been incorporated as a diagnostic criterion in the Banff classification of ABMR. However, despite the usefulness of this biomarker, there are shortcomings to using C4d deposition as an indicator for ABMR. Exceptions to the high specificity of C4d typically occur in ABO blood group mismatched transplants, where fully functioning and uninjured grafts show diffuse C4d deposition (46;73). Haas *et al.* has shown that 80% of protocol biopsies from kidneys maintaining long term function post-transplant are C4d positive.

In addition to the low specificity of C4d staining in ABO incompatible transplants, there are occasional patient cases of C4d negative ABMR, turning the C4d biomarker insensitive to certain situations of ABMR (102;103).

In addition to C4d as a marker for complement activation, we examine the presence of fluid phase complement C5a split product and complement C5b-9 as an indicator of the activation of the complement pathway to terminal MAC formation. We utilize previously developed antibodies against C5a and C5b-9 to the application of enzyme linked immunoassays (ELISA) analysis for quantitative measurements. In this way, we examine the presence of C4d as a histopathological marker, and C5a / C5b-9 as a fluid phase marker for complement activation.

1.5 – Fc receptors

In addition to the activation of complement as a means to injure tissues in ABMR, antibodies bound onto target antigens can elicit inflammatory responses from the immune system. The activation and recruitment of leukocytes can be triggered by pro-inflammatory cytokines such as C3a, C4a, and C5a, but leukocytes can also directly interact with the Fc portions found on antibodies via Fc receptors found on the surface of the leukocyte.

Fc receptors exist in many different forms, each with different properties. Fc receptors are classified into different groups based on the type of immunoglobulin that it interacts with. Fc receptors interacting with IgA antibodies are termed Fc-alpha receptors (FcαR). Those binding IgE antibodies are Fc-epsilon receptors (FcεR), while Fc-gamma receptors (FcγR) bind IgG. IgM antibodies bind onto a specialized Fc-alpha/mu receptor (Fcα/μR) (14;89;122). Furthermore, there are also neonatal forms of Fc receptors (FcRn), typically involved in the transfer of IgG from mother to fetus (92). In this thesis, we only examine mouse FcγR and its effects on ABMR phenotypes.

Within the FcγR family, there are further classifications to identify receptors based on their downstream effects. There are 4 forms of the mouse FcγR: FcγR1, FcγR2b, FcγR3, and FcγR4. Their properties are described in Table 1.1 (14;122). Briefly, only FcγR2b is an inhibitory receptor, while all other Fcγ receptors activate their respective leukocytes to perform downstream effector abilities.

Table 1.1 – Fc-gamma receptor properties. Mouse Fc-gamma receptor ligands, effects, and distribution in mouse leukocytes.

Fc receptor	IgG recognition	Activating / Inhibitory	Relevant Distribution
FcγR1	IgG2a IgG2b IgG3	Activating	Monocytes / Macrophages Neutrophils Dendritic Cells
FcγR2b	IgG1 IgG2a IgG2b	Inhibitory	Monocytes / Macrophages Neutrophils Dendritic Cells Basophils Mast Cells Eosinophils
FcγR3	IgG1 IgG2a IgG2b	Activating	NK cells Monocytes / Macrophages Neutrophils Dendritic Cells Basophils Mast Cells Eosinophils
FcγR4	IgG2a IgG2b	Activating	Monocytes / Macrophages Neutrophils

1.6 – Cell types

1.6.1 – NK Cells

With FcγR3 expressed on NK cells, one of the ways NK cells become activated is through Fc receptor interactions. However, unlike other leukocytes whose general function is to induce inflammation when activated, NK cells carry out its effector functions by inducing apoptosis.

In addition to Fc receptor binding, NK cells also recognize cell surface antigens to become activated or inhibited, depending on which receptor is bound. These receptors present on NK cells fall into one of two categories: activating or inhibitory receptors. When these receptors bind onto ligands present on target cells, the NK cell becomes either inhibited or activated to inducing apoptosis to the target cell, depending on the balance and proportion of receptors bound from each category (65). Both forms of NK cell receptors primarily recognize MHC class I molecules present on potential target cells.

Inhibitory receptors such as the majority of the Ly49 family of receptors in mice (with exception to Ly49D and Ly49H in B6 mice) (64;65), or killer immunoglobulin-like receptors (KIR) associated with immunoreceptor tyrosine-based inhibitory motif (ITIM) adapters in humans, recognize antigens present on potential target cells that denote normal cell function, such as expression of normal self MHC I (107). The binding of these antigens inhibit NK cell activation, thereby avoiding apoptosis and autoimmune reactions (107). In contrast, activating receptors present on NK cells such as NKG2D bind onto stress-related antigens on cell surfaces such as MICA and MICB (112) in order to activate the NK cell to induce apoptosis in the bound target cell. In instances where both inhibitory and activating receptors on NK cells are bound to ligands on potential

target cells, the overall activation status of the NK cell is dependent on the relative proportions of activating receptors versus inhibitory receptors bound. From these findings, the NK cell "missing self-hypothesis" was developed to show that, in addition to binding activating receptors, NK cells can become activated when there is a lack of binding onto inhibitory receptors. However, in situations where neither activating or inhibitory receptors are bound, such as normal red blood cells that do not express MHC I molecules or activating surface antigens, NK cells experience an inhibitory effect to avoid autoimmune activation (65;107).

When NK cells are activated to destroy a target cell, they do so by inducing the target cell to undergo apoptosis. There are two primary methods by which NK cells achieve this: the Fas receptor / Fas ligand pathway, or the perforin / granzyme pathway. In the Fas receptor / Fas ligand pathway, NK cells induce increased expression of Fas receptor via secretion of interferon gamma. Fas ligand present on the NK cell binds Fas receptors present on the target cell. The binding of the receptor-ligand pair of these "death receptors" directly induce the apoptosis of the target cell. The other method by which NK cells cause apoptosis in target cells is through the perforin / granzyme pathway. When NK cells become activated, they can release perforin proteins in the proximity of cells targeted for apoptosis. Perforin proteins interact with the cell membrane of the target cell to form pores within the membrane. Following pore formation, granzyme release by NK cells enter the target cell, and induce the caspase cascade to activate the apoptosis pathway (107;117). In addition to the activation of direct apoptotic cell death, NK cells can also enhance immune reactions with expression of cytokines such as interferon gamma and tumor necrosis alpha (15).

1.6.2 – Monocytes / Macrophages / Neutrophils

Monocytes, macrophages and neutrophils are a part of the innate immune system, acting as phagocytes to engulf and remove pathogens from the bloodstream and body tissues. These phagocytes also act as antigen presenting cells, digesting

phagocytized compounds into small peptide chains. These cells then present the digested peptides onto MHC II molecules on their cell surface, in order to activate T helper cells. Activation of T helper cells leads to the activation of B cells and T killer cells to react against the specific peptide antigen.

In the context of transplantation, these leukocytes not only can present donor derived peptides on their MHC II molecules, but also respond to cytokines such as activated complement components, in order to migrate to sites of complement activation to inflict further injury to antibody bound cells.

1.7 – Gene microarray and gene expression analysis

Injury to transplanted kidney tissues due to ABMR have generally been diagnosed by histopathology, immunohistochemical staining, and markers of fluid phase DSA (85;86). However, with the incorporation of gene expression analysis, it has been shown that certain forms of rejection-induced injury to transplanted tissues may not be detectable by conventional histopathological and biochemical analyses, such as in C4d-negative ABMR (102;103). Furthermore, utilizing gene expression signatures as a means of classifying diseases have not only revealed the heterogeneous nature of certain diseases (such as cancer) displaying similar phenotypes, but have also been used successfully as a predictor for disease outcome (6;91).

In this thesis, we examine not only the expression of individual genes, but we utilize previously established gene lists representing major biological processes in order to describe events occurring in ABMR. These lists are based on mouse transplant experiments, human transplants, cell culture experiments, and literature-based. Gene lists relevant to this thesis include: cytotoxic T lymphocyte-associated transcripts (26), interferon gamma associated transcripts (31), macrophage-associated transcripts (30),

injury and repair induced transcripts (30), renal transcripts (24), solute carriers (24), endothelial activation associated transcripts (103), and NK cell receptors based on literature (5;65;79;80).

1.8 – Current animal models of antibody-mediated transplant rejection

There are currently several small animal models developed with the goal of reproducing ABMR disease phenotypes. Fairchild *et al.* (78) studied heart transplants in mice mismatched on a single MHC I locus. Hearts from wildtype C57BL/6 expressing H-2^b antigens were heterotopically transplanted into the abdomens of transgenic C57BL/6 mice with CCR5 gene knockout and expressing K^d antigens. Donor specific antibodies were either generated in recipient C57BL/6 $CCR5^{-/-}$ mice or injected via I.V. DSA was generated by transplanting MHC I mismatched heart without eliminating T or B lymphocytes in recipients. I.V. injections of DSA were done with either purchased monoclonal antibody, or injections of serum from sensitized mice. This model shows little pathology as serum from sensitized mice was injected, and the pathology present represents a mixed TCMR and ABMR phenotype. Pathology findings were also limited to gene expression changes and neutrophil recruitment.

Fairchild *et al.* (77) also developed a heterotopic cardiac transplant model between A/J mice donors (expressing H-2^a) and C57BL/6$RAG^{-/-}$ recipients (expressing H-2^b). Donor specific antibodies were generated in C57BL/6 $CCR5^{-/-}$ mice by transplantation of cardiac allograft from A/J mouse donors. Serum from sensitized mice was injected into B6.RAG recipients of A/J cardiac allografts. This model shows recruitment of neutrophils and macrophages into allograft tissue when sensitized serum was injected into the allograft recipient, but other accompanying ABMR lesions were not shown.

Reed *et al.* (60) heterotopically transplanted cardiac allografts from BALB/c mice expressing H-2^d antigens into B6.$RAG^{-/-}$ mice expressing H-2^b antigens, thereby

establishing an MHC I mismatched allograft condition. Donor specific antibodies were generated via hybridoma (HB-159) production of IgG antibodies specific against H-2K^{d} antigens. The use of B6.RAG$^{-/-}$ recipients allows for the elimination of the production of TCMR, but the pathology presented in these animals are limited to smaller scale injury involving microvascular changes, with accompanying C4d deposition and gene expression changes.

In primates, Colvin *et al.* (106) demonstrated chronic ABMR phenotypes in kidney transplant recipients treated with cyclosporine and whole body / thymic irradiation (to eliminate T cells). Kidney transplants were performed heterotopically, and donor specific antibodies were generated in allograft recipients. Severe chronic glomerulopathy showing duplication of glomerular basement membrane, C4d deposition, and glomerulitis was observed in this model. However, as the model is developed in a primate model system, it is impractical to use when studying the mechanism of disease and potential interventions in the generation of ABMR pathology. Colvin *et al.* also demonstrated antibody-mediated arteriopathy in a mouse model of ABMR in heart transplantation. Here, hearts from B10.BR mice expressing H-2^{k} antigens were transplanted heterotopically into B6.C3$^{-/-}$RAG$^{-/-}$ mice, and purchased monoclonal IgG1 and IgG2a antibodies were injected into recipient mice. Although this model demonstrates proliferation of arteries in a chronic fashion, further ABMR pathology is not generated.

Finally, Nadasdy *et al.* (12) have utilized pre-sensitization transplants in mice in order to elicit strong donor specific antibody generation. In their model, skin from DBA/2 mice expressing H-2^{d} antigens were first transplanted onto recipient C57BL/6 mice expressing H-2^{b} antigens to sensitize the recipients. After sensitization, kidney transplants were performed, with depletion of CD8+ cells performed multiple times pre- and post- transplantation. Graft rejection and renal dysfunction was demonstrated within 11 days post-transplant, with mild and diffuse infiltration of mononuclear cells into the interstitial space, acute tubular necrosis, and peritubular capillary margination. However,

despite the presence of histopathologic evidence for ABMR, there are also TCMR phenotypes shown in this model, such as interstitial inflammation, tubulitis, and endarteritis. In this way, the model does not reflect a pure ABMR phenotype.

1.9 - Thesis outline and objectives

Currently, there are no adequate small animal models of pure acute ABMR, hampering the study of this disease. All current animal models either show mixed ABMR / TCMR rejection or chronic ABMR rejection. In this thesis, our main objective is to develop a mouse model demonstrating purely acute ABMR, without contamination of TCMR. We aim to describe the role of both the complement pathway and inflammatory responses in the progression of injury in our animal model. By comparing histopathology, gene expression and biochemical properties of our model to clinical observations in human patients with ABMR, we demonstrate potential mechanisms by which ABMR pathology progresses.

With the establishment of a working animal model of ABMR, future studies can be performed to examine molecular signs of disease as a diagnostic, identify potential targets for disease intervention, which can eventually lead to drug development and discovery for the treatment of ABMR.

Chapter 2: Materials and Methods

2.1 – General Materials and Methods

Mice

CBA/J (CBA) and B6.129S7-Rag1^{tm1Mom}/J (B6.RAG1$^{-/-}$) were purchased from Jackson Laboratories (Bar Harbor, ME) and colonies were established. Male mice between 15 and 25 weeks of age were used in all transplantation experiments. Mouse maintenance and experiments adhered to animal care protocols approved by the University of Alberta Health Sciences Animal Policy and Welfare Committee.

Kidney transplantation

We performed major histocompatibility complex-mismatched kidney transplantation by implanting kidneys from donor CBA mice (H-2^{k}) into recipient B6.RAG1$^{-/-}$ mice (H-2^{b}) (abbreviated as B6.RAG), which lack mature T and B cells (Figure 2.1). In addition to MHC-mismatched kidney transplants, we performed MHC-matched kidney transplantation (isograft) by implanting kidneys from donor CBA (H-2^{k}) or B6.RAG (H-2^{b}) mice into recipient CBA (H-2^{k}) or B6.RAG (H-2^{b}) mice, respectively. The donor kidney was anastomosed heterotopically to the aorta, inferior vena cava and bladder on the right side, without removing the host's left kidney (non-life supporting kidney transplantation) (Figure 2.1), as previously described (101). Transplantation surgeries were performed by micro-surgeon Dr. Lin-Fu Zhu.

In addition to non-life supporting transplants, we also performed life-supporting MHC mismatched transplants via the same method, but removed the host's left kidney during surgery (Figure 2.1). No immunosuppressive therapy was administered at any time during transplantation experiments.

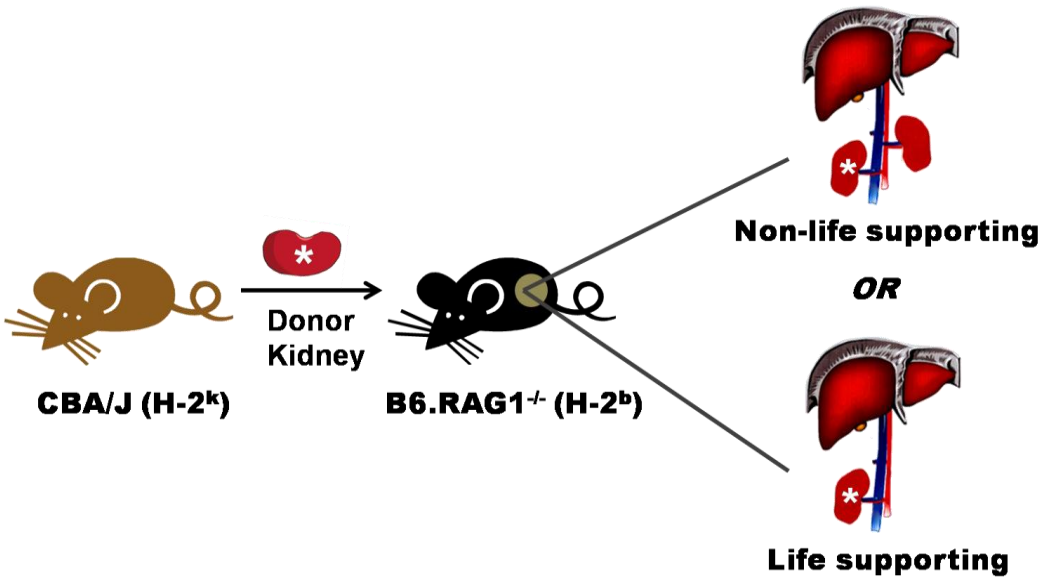

Figure 2.1 – Kidney transplantation. Kidneys from CBA/J strain mice are transplanted into the right side portion of recipient B6 strain mice. Recipient B6 mice have a knockout in the Rag1 gene. In non-life supporting transplants, the recipient's left kidney remains intact. In life-supporting transplants, recipient left kidney is removed

Generation of monoclonal DSA by growth of hybridoma cell lines via cell culture

Hybridoma clones 16-1-2N, 15-1-5P, and AF3-12.1.3 were purchased from American Type Culture Collection (ATCC, Manassas, VA) and cultured according to the supplier's directions. Lines were gradually adapted to 50 to 80 % serum free medium (BD Biosciences, Mississauga, ON or Lonza Walkersville, Walkersville, MD) in a balance of RPMI (ATCC, Manassas, VA), L-glutamine (LifeTechnologies, Carlsbad, CA), penicillin and streptomycin (LifeTechnologies, Carlsbad, CA) with 10 to 15 % Ultra Low IgG Fetal Bovine Serum (LifeTechnologies, Carlsbad, CA). Once counts reached 30 million viable cells these were transferred to the lower chamber of a CELLine Device (BD Biosciences, Mississauga, ON), and the appropriate serum free medium supplemented with L-glutamine, penicillin and streptomycin, was added to the upper chamber. Flasks were placed in a humidified 37 °C incubator under 5 % CO_2 with a balance of air and cultured for two weeks. Cells were harvested from the lower chamber, the supernatant was filtered through 0.45 µm then 0.22 µm syringe filters (Millipore, Tullagreen, Ireland), and filtrates stored at -75 °C. Monoclonal antibodies from thawed filtrates were purified using dedicated HiTrap columns and a MAb Trap Kit (GE Healthcare, Piscataway, NJ). Sterile filtered monoclonal antibodies were quantified on the NanoDrop (Thermo Scientific, Wilmington, DE) using the IgG settings, and stored at -75°C in appropriately sized aliquots until use.

Generation of polyclonal DSA by mouse sensitization

B cell lymphoma clone CH1 T cell lymphoma clone BW5147.3 were purchased from American Type Culture Collection (ATCC, Manassas, VA) and cultured according to the supplier's directions. The cell lines were cultured for 7 days, and then cells were harvested. $1x10^7$ cells ($5x10^6$ each of B cell and T cell lymphoma cells) were injected into wild-type C57BL/6 mice via I.P. injection, in combination with 25µL of Freund's adjuvant (complete Freud's adjuvant was used for the first injection. Subsequent injections utilized Freund's incomplete adjuvant) twice weekly. Blood samples from

immunized mice were taken roughly every 30 days to determine donor reactivity in the mouse serum. Donor reactivity was determined by flow cytometry, as described below. Once mice are successfully immunized, blood was collected, and donor specific IgG antibodies were isolated by purification in HiTrap Protein G columns (GE Healthcare, Piscataway, NJ).

Detection of donor specific antibody reactivity by flow cytometry

Circulating donor specific antibodies were tested for alloreactivity via flow cytometric crossmatch (60). Briefly, CBA spleens were homogenized and red blood cells removed with RBC lysis buffer (STEMCELL Technologies, Vancouver, BC). $1x10^6$ splenocytes were first incubated with antibody to Cd16/32 (eBioscience, San Diego, CA) to block Fc receptors, followed by recipient serum, then Alexa-Fluor 488 conjugated anti-mouse IgG antibody (Invitrogen, Burlington, ON). Cells were examined with a LSR II flow cytometer (BD biosciences, Mississauga, ON), gating on lymphocytes based on forward and side scatter, measuring the amount of anti-donor IgG antibodies bound on lymphocytes, and analyzed with FCS Express V3 (De Novo Software, Los Angeles, CA). MFI values were corrected against CBA splenocytes incubated with normal B6.RAG serum prior to staining with secondary fluorescent antibodies. Resultant correct values are reported as median fluorescent intensity.

Adoptive transfer of donor specific antibodies and injectables

All transplant recipient mice were injected twice daily via subcutaneous (SC) injections with 500 µg of Ampicillin from day of transplant until day 6 post-transplant. Mouse IgG2a and IgG2b monoclonal antibodies that react with H-$2K^k$ were produced as described above. Clone 36-7-5, which is a mouse IgG1 isotype that reacts with H-$2K^k$, was purchased (BioLegend, San Diego, CA). B6.RAG mice which had received CBA donor kidneys were given injections of either: one injection of 100µg DSA (IgG2a) on day 6 post-transplant, three injections of 300µg DSA (IgG2a) on days 5, 6, and 7 post-

transplant, one injection of 750µg DSA (IgG2a) on day 6 post-transplant, two injections of 2000µg DSA on days 6 and 7 post-transplant, or three injections of 3000µg (1000µg IgG1, 1000µg IgG2a, 1000µg IgG2b) DSA on days 5, 6, and 7 post-transplant. DSA injections were administered by intraperitoneal injection (IP) with addition (in certain transplants) of 0.25mL rabbit complement injected SC daily from day 5 post-transplant to either day 7 post-transplant (in non-life supporting transplants), or until serum creatinine increased by 20% or more and was sustained over 2 days (in life-supporting transplants). Typical harvest days for life-supporting transplants fell within the range of approximately day 25 – 40 post-transplant. Sham control groups included B6.RAG mice which had received CBA kidneys with injections of either PBS or 3000µg mouse non-immune IgG (Alpha Diagnostic International , San Antonio, TX) by I.P. from day 5 to day of harvest. Control mice were day-matched with DSA treated experimental groups, and harvested on the same day as when the corresponding treated mouse showed sustained renal dysfunction. In non-life supporting transplants, the left native kidney that remained in allograft recipients served as another group of controls.

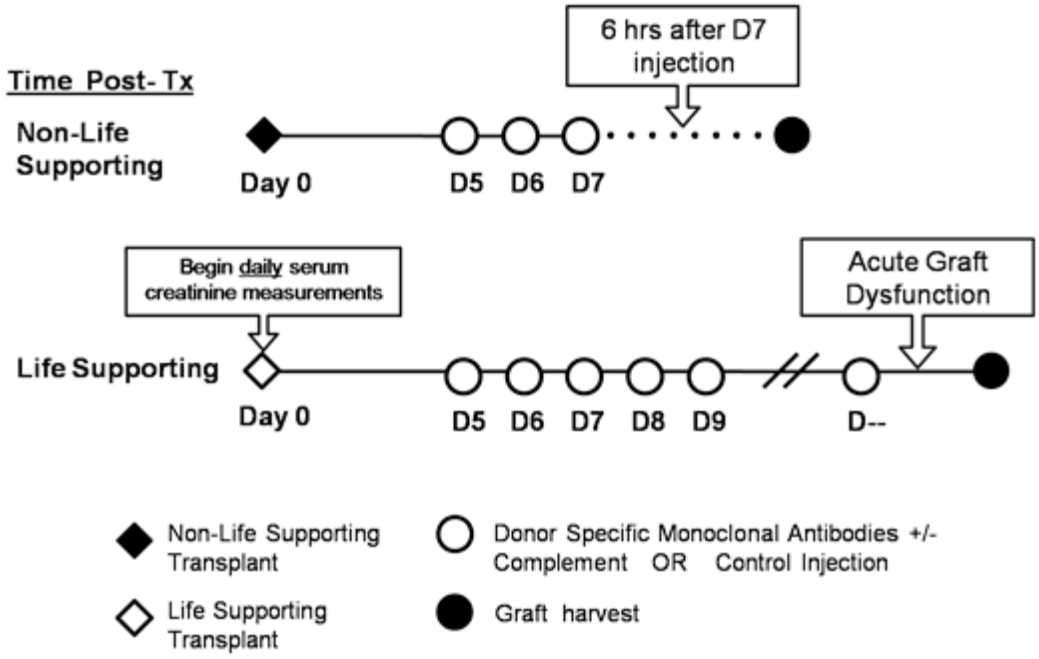

Figure 2.2 – Adoptive transfer of DSA, injectables, and organ harvest. Non-life supporting transplants were injected via I.P. with treatment or control injections on days 5, 6, and 7 post-transplant. Organ harvest took place 6 hours after last injection. Life-supporting transplants were injected via I.P. with treatment or control injections daily from day 5 post-transplant, until graft dysfunction occurred. Serum creatinine was measured (from tail vein blood) daily in mice with life supporting transplants from day of transplant to day of harvest. Baseline serum creatinines were also measured prior to transplantation.

Graft Harvest

For non-life supporting transplants, the kidneys, spleen and blood were harvested on day 7, 6 hours after the last injection. For life-supporting transplants, the kidney, spleen, and blood were harvested when serum creatinine was elevated by more than 20% of baseline serum creatinine and the elevation was sustained over 2 days. At time of harvest, kidney tissue was divided into three pieces: one piece was snap-frozen in liquid nitrogen and stored at −70^{o}C, one piece formalin-fixed and paraffin embedded, one stored in 2% glutaraldehyde, and one piece embedded in Tissue-Tek® OCT compound (Sakura Finetek Inc., Torrence, CA), snap-frozen in liquid nitrogen, and stored at -70^{o}C. Whole blood was incubated at room temperature for 30min, and then centrifuged at 12,000 rpm to collect serum. Serum aliquots were stored at −70^{o}C.

Quantitative Histopathology

Paraffin embedded tissue sections (2 μm) were stained with hematoxylin and eosin, and periodic acid-Schiff using standard techniques and assessed by two renal pathologists (Dr. Sufia Husain and Dr. Paula Blanco) who were blinded to experimental conditions. The histological features were semi-quantitatively graded according to Banff renal allograft histology scoring criteria (100). In addition to Banff scores, several injury features were quantitatively or semi-quantitatively scored: % cortical tubular cytoplasmic vacuolization, % flattening/thinning of cortical tubular epithelium, % loss/thinning of cortical tubular brush border, % cortical tubules with granular casts, % cortical tubular necrosis, cortical PTC dilation, endothelial cell swelling etc. A detailed description of individual histopathology features and their scoring criteria are available in our laboratory.

Data analysis

Data analyses were performed using SPSS 19.0 statistical software package (SPSS Inc., Chicago, IL) and GeneSpring™ GX 7.3.1 (Agilent, Palo Alto, CA). The

differences between the experimental groups were investigated using t-test, Mann-Whitney U test, Kruskal-Wallis, and ANOVA, where applicable. Microarray data analysis was done using Benjamini and Hochberg false discovery rate set at 0.05 as a multiple test correction: a corrected p-value of 0.05 signifies that 5% of the probe sets identified as significant at the 0.05 level will be false positives. The level of significance was set at $p<0.05$.

Immunoperoxidase staining for C4d

C4d was detected by immunoperoxidase staining of frozen kidney sections using a rat monoclonal antibody against mouse C4 that reacts with C4b/C4d (Clone 16D2; Abcam Inc., Cambridge, MA). Here, we will refer to the molecule stained by 16D2 as C4d, as previously reported in mice studies and human literature of C4d, because C4 is not cell bound and C4b is short-lived, with an in-vitro half-life measured in minutes (120). Negative control kidney sections were stained with purified rat isotype IgG2a (BD Biosciences, Mississauga, ON). ImmPRESS peroxidase-labeled anti-rat IgG (mouse adsorbed) (Vector Labs, Burlingame, CA) was applied as the secondary antibody and color developed using ImmPACT NovaRED peroxidase substrate (Vector Labs, Burlingame, CA). C4d staining in peritubular capillaries was scored as follows; diffuse (score-3: >50% of renal cortex that has a linear, circumferential staining in peritubular capillaries), focal (score-2: 10-50%), minimal focal (score-1: 1-9%), and negative (score-0: 0%) (100). The glomerular capillary loop staining was also assessed and recorded as absent or present.

Immunohistochemistry staining and quantification

Paraffin embedded tissue sections (2 μm) were stained with hematoxylin and eosin, and periodic acid-Schiff and assessed by two renal pathologists. The histological features were graded according to Banff renal allograft histology scoring criteria (100).

To examine localization of cell recruitment, graft infiltrating leukocytes were labeled by double IHC stain, and are presently being quantitatively evaluated as a whole tissue digital slide by Definiens Tissue Studio analysis software (Definiens, Carlsbad, CA)

Cleaved caspase 3 (Rabbit polyclonal anti-CC3, Asp175, Cell Signaling, Whitby, ON) immunohistochemistry was used to identify apoptotic cells. Biotinylated goat polyclonal anti-rabbit was applied as the secondary and the color developed with sequential addition of streptavidin HRP (BD Biosciences, Mississauga, ON) and the peroxidase substrate ImmPACT DAB (Vector Labs, Burlingame. CA).

Numbers of Ly49G2+ and CC3+ cells were quantified in entire sample cortex. Total numbers were divided by total cortical area, and represented as # positive cells / mm^2. Cd68+ cells were quantified in 20 fields of view at 40X magnification. Total cells were divided by area of 20 fields of view at 40X magnification, and represented as # positive cells / mm^2.

Quantification of C5a

Freshly thawed serum samples were analyzed via ELISA to quantify complement split product C5a. C5a in the harvested serum was quantified with Mouse Complement Component C5a DuoSet (R&D systems, Minneapolis, MN) ELISA kit.

Gene expression by Microarrays

RNA extraction, amplification, and hybridization to GeneChip Mouse Genome 430 2.0 arrays (Affymetrix, Santa Clara, CA) were performed according to the Affymetrix® technical manual (www.affymetrix.com). Microarray data were pooled into one batch and preprocessed using robust multi-chip averaging and implemented in GeneSpring™ GX 7.3.1 (Agilent, Palo Alto, CA). This nonspecific filtering step was used to remove genes with no or little variation across all samples. Microarray data were grouped according to experimental condition and compared between groups.

Gene expression by Nanostring

RNA from frozen kidney allograft samples were processed by Nanostring nCounter analysis. Briefly, RNA was extracted by homogenizing tissue samples in Trizol® reagent (Life Technologies, Burlington, ON), and total RNA was obtained by chloroform extraction, via a modified version of manufacturer's protocol. Total RNA was purified with the QiAamp DNA Mini Kit (Qiagen, Toronto, ON). RNA quality was confirmed via absorption spectra by NanoDrop 2000 (Thermo Scientific, Wilmington, DE). 200ng of total RNA was analyzed with the nCounter Gene Expression assay (NanoString Technologies, Seattle, WA). Gene expression of all samples was normalized as per manufacturer's instructions.

Measurement of kidney function by serum creatinine

Serum creatinine measurements were performed on mice who received a life-supporting kidney allograft transplant. Tail vein bleeds were performed on the mice daily, starting one day prior to transplantation. 50µL of whole blood was taken daily, and centrifuged to collect serum. Serum creatinine was analyzed by the enzymatic Mouse Creatinine Assay Kit (Chrystal Chem, Downer's Grove, IL) with slight modifications to the manufacturer's instructions.

Transmission electron microscopy

Three kidneys collected at day 22 and day 24 after transplant with immunomorphological findings of ABMR (including diffuse PTC C4d staining and the characteristic light microscopic findings of capillary injury such as capillary dilatation, endothelial swelling, and small vessel microthrombus) were selected for ultrastructural examination. Time matched mouse kidney allografts treated with non-immune IgG were served as controls. Tissue from the renal cortex was cut into 1-mm cubes and immersion-fixed in 3% buffered glutaraldehyde immediately after euthanasia. The tissues were routinely processed for electron microscopy using osmium tetroxide after

fixation, Epon embedding, and uranyl acetate and lead citrate contrasting. Semi-thin sections were stained with toluidine blue and representative areas were selected for electron microscopy. Ultrathin sections were examined with an H7650 transmission electron microscope (Hitachi, Japan). Electron microscopic evaluation was performed to assess glomerular changes including the ultrastructure of glomerular endothelial cells, glomerular basement membrane, mesangium, podocytes, and peritubular capillaries including their lining endothelial cells, basement membrane multilayering, and microvascular thrombi.

Quantification of C5b-9

Freshly thawed serum samples were analyzed via ELISA to quantify complement split product C5b-9 levels. C5b-9 in the harvested serum was quantified with Mouse C5b-9 ELISA Kit (Uscn Life Science Inc., Houston, TX) ELISA kit.

Chapter 3:

Experimental results

3.1 –Activation of complement in the absence of C5a and C5b-9 formation is not associated with kidney allograft injury

3.1.1 - Overview

ABMR of transplanted kidneys is a major problem in human patients, and it injures transplanted kidney tissues primarily through the complement pathway, directed against kidney microvascular endothelial cells (19). The complement pathway, when fully activated, forms the membrane attack complex (MAC) composed of C5b-9 to cause cell lysis of endothelial cells bound with donor specific antibodies (DSA). In addition to the lytic activity of the complement pathway, activated fluid phase complement split products C3a and C5a further enhance tissue injury by triggering additional immune reactions. C3a and C5a are potent pro-inflammatory chemotactic molecules that attract leukocytes to the allograft and induce allograft inflammation (126). Furthermore, endothelial cells binding C3a and C5a molecules via complement receptors become activated themselves, which induce the expression and release of additional pro-inflammatory molecules (51;68). This further increases leukocyte recruitment, platelet adherence, and vascular permeability.

Another complement split product C4d, derived from complement C4, has been developed into a biomarker to indicate the location of complement activation. C4d covalently binds onto endothelium for several days when the complement pathway proceeds past C4, and therefore, the presence of this molecule denotes the previous activation of the complement pathway at that given location. Since ABMR injury is regarded as primarily driven by the classical complement pathway, C4d is used for the detection of complement activation in kidney allograft tissues. However, there are several limitations to the use of C4d as a biomarker. Firstly, Haas et al. (46) and Fidler et

al.(34) showed that C4d deposition is not very specific for ABMR, as there was diffuse C4d in peritubular capillaries in the absence of graft pathology in 25-80% of ABO blood group incompatible renal allografts, where only 4-12% developed acute rejection. Furthermore, C4d deposition has been shown in 2% of stable kidney transplants in ABO blood group incompatible transplants with no signs of graft inflammation or injury.

Although the occurrence of C4d positivity in the absence of graft injury has been documented, the basis for this phenomenon is largely unknown. Here, we tested the hypothesis that antibody-induced activation of the complement pathway fails to produce allograft injury if the complement pathway does not proceed to terminal C5a and C5b-9 formation. We transplanted wild-type H-2k donor kidneys into T-cell/B-cell-null Rag1-/- H-2b recipients. The following doses of donor specific anti-class-I monoclonal antibodies with rabbit complement were transferred into transplant recipients: intraperitoneal injection of 100µg anti-H-2Kk IgG2a on day 6 post-transplant and harvesting of kidneys 24 hours later, three injections of 1000µg anti-H-2Kk IgG2a plus 1000µg anti-H-2KkDk IgG2b plus 1000µg anti-H-2Kk IgG1 on days 5, 6, and 7 post-transplant and harvesting kidneys 6 hours after the last injection.

Adoptive transfer of low dose donor specific anti-class-I antibodies into allograft recipients induced intragraft antibody deposition and diffuse C4d staining in peritubular capillaries, which were absent in control allograft and normal kidneys. C4d positive allografts following low dose antibody transfer showed normal histology and no molecular signs of injury, inflammation, or endothelial activation by expression microarrays. Also, there was no molecular evidence for acquired graft resistance to alloantibody (accommodation): no gene expression changes were present in C4d positive allografts following low dose antibody transfer. In contrast, C4d positive allografts following high dose antibody transfer showed acute microvascular endothelial and tubular injury and weak inflammation. Surprisingly, serum levels of distal complement effector products C5a and C5b-9 were significantly increased in mice with C4d positive allografts following high

dose antibody transfer, but not in mice with C4d positive allografts following low dose antibody transfer, control allograft recipient mice, and naïve mice. These data indicate that alloantibody-induced complement activation with C4d deposition does not produce allograft injury when distal complement effector products are not generated.

Table 3.1 – Transplant and condition abbreviations applicable to section 3.1

Donor	Recipient	Condition	Treatment	Abbrev.	Day post tx	N of mice
CBA ($H\text{-}2^{k}$)	-	Normal CBA kidney	-	NCBA	-	29
B6.RAG1$^{-/-}$ ($H\text{-}2^{b}$)	-	Normal B6.RAG1$^{-/-}$ kidney	-	NRAG	-	5
B6.RAG1$^{-/-}$ ($H\text{-}2^{b}$)	-	Normal B6.RAG1$^{-/-}$ kidney	0.25mL rabbit complement / day, 3 day treatment	NRAG + C’	-	5
CBA ($H\text{-}2^{k}$)	B6.RAG1KO ($H\text{-}2^{b}$)	Non-life supporting CBA/RAG allograft	No treatment OR 0.2mL PBS / day, 3 day treatment	CBA/ B6.RAG allo NLS	D7	8
CBA ($H\text{-}2^{k}$)	B6.RAG1KO ($H\text{-}2^{b}$)	Non-life supporting CBA/RAG allograft	0.25mL rabbit complement / day, 3 day treatment	CBA/ B6.RAG allo + C’ NLS	D7	5
CBA ($H\text{-}2^{k}$)	B6.RAG1KO ($H\text{-}2^{b}$)	Non-life supporting CBA/RAG allograft	100µg DSA, 1 day treatment	CBA/B6.RAG allo + 0.1mg NLS	D7	15
CBA ($H\text{-}2^{k}$)	B6.RAG1KO ($H\text{-}2^{b}$)	Non-life supporting CBA/RAG allograft	100µg DSA + 0.25mL rabbit complement, 1 day treatment	CBA/B6.RAG allo + 0.1mg + C’ NLS	D7	5
CBA ($H\text{-}2^{k}$)	B6.RAG1KO ($H\text{-}2^{b}$)	Non-life supporting CBA/RAG allograft	300µg DSA / day, 3 day treatment	CBA/B6.RAG allo + 3x0.3mg NLS	D7	10
CBA ($H\text{-}2^{k}$)	B6.RAG1KO ($H\text{-}2^{b}$)	Non-life supporting CBA/RAG allograft	750µg DSA, 1 day treatment	CBA/B6.RAG allo + 0.75mg NLS	D7	3
CBA ($H\text{-}2^{k}$)	B6.RAG1KO ($H\text{-}2^{b}$)	Non-life supporting CBA/RAG allograft	2000µg DSA / day, 3 day treatment	CBA/B6.RAG allo + 3x2mg NLS	D7	5
CBA ($H\text{-}2^{k}$)	B6.RAG1KO ($H\text{-}2^{b}$)	Non-life supporting CBA/RAG allograft	3mg DSA / day, 3 day treatment	CBA/B6.RAG allo + 3x3mg NLS	D7	6
CBA ($H\text{-}2^{k}$)	B6.RAG1KO ($H\text{-}2^{b}$)	Non-life supporting CBA/RAG allograft	3mg DSA / day + 0.25mL rabbit complement / day, 3 day treatment	CBA/B6.RAG allo + 3x3mg + C’ NLS	D7	9

3.1.2 – Results

Intraperitoneally transferred donor specific antibody successfully entered into circulation and was reactive for donor cells

Since ABMR is driven primarily by the complement pathway, we utilized our mouse ABMR model generated earlier as a positive control for observable histopathology. We tested our hypothesis using this model and examined whether or not the complement pathway can be partially activated, but without showing histopathological phenotypes.

We adoptively transferred 100µg IgG2a anti-class I donor specific antibody into B6.RAG recipients with allografts by a single I.P. injection. To determine the effectiveness of antibody migration into the circulation from the intraperitoneal space, we used ELISA to measure serum IgG levels from tail vein bleeds 24 hours post I.P. injection. Serum IgG levels were significantly higher in B6.RAG recipients treated with antibody when compared to control B6.RAG recipients without antibody treatment (8.91 ± 4.19 µg/mL versus 2.20 ± 0.47 µg/mL, respectively) (Figure 3.1a). Thus I.P. injected donor specific antibody successfully entered into the bloodstream of allograft recipients.

To determine the ability of circulating donor specific antibody to bind onto donor cells, we performed a flow cytometric crossmatch: we incubated donor splenocytes with serum from B6.RAG recipients which received allografts and donor specific antibody. We found increased serum IgG bound on donor splenocytes in B6.RAG recipients treated with antibody when compared to control B6.RAG recipients without antibody treatment, confirming the reactivity of injected antibody against donor cells (Figure 3.1b).

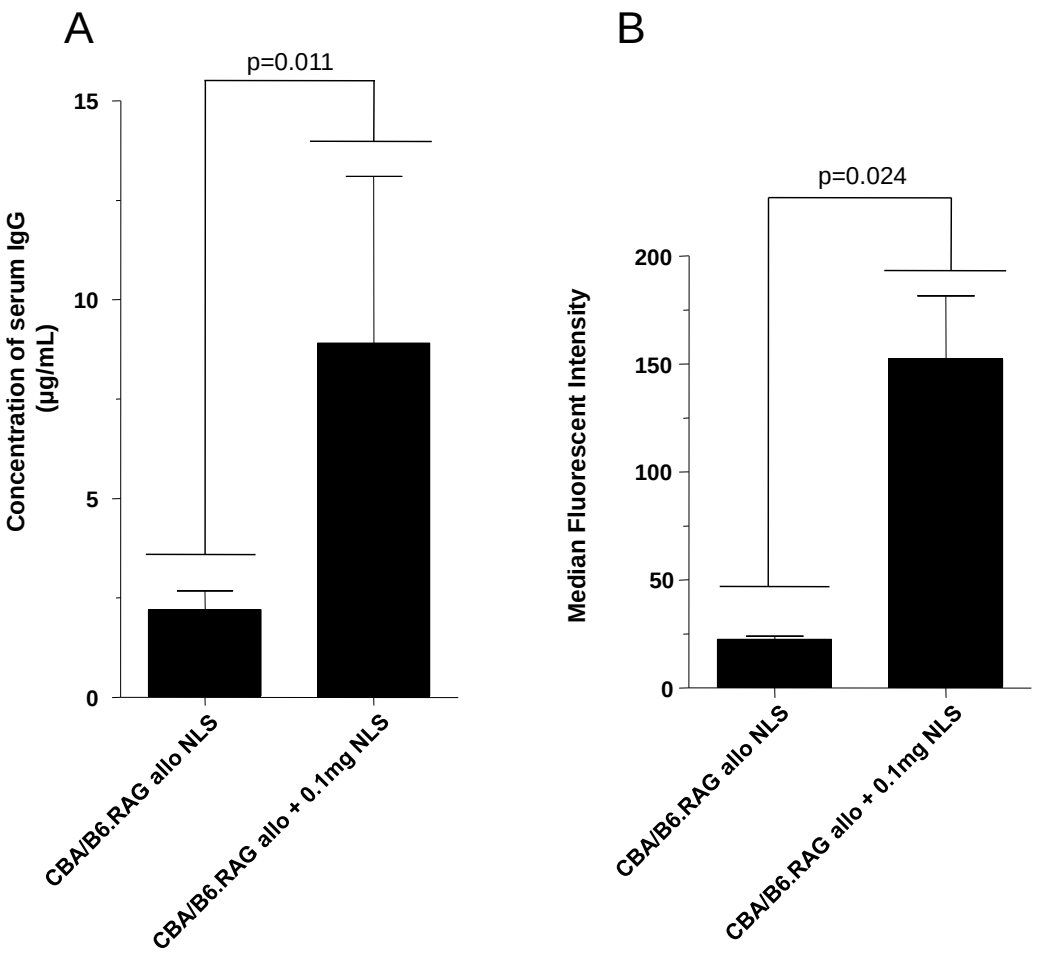

Figure 3.1 – Injected DSA successfully enters circulation. **(A)** By ELISA, significantly (p=0.011) higher levels of fluid phase IgG is present in DSA treated allografts compared to allograft controls. **(B)** By flow cytometry, serum of 0.1mg DSA treated allograft recipients contains IgG with significantly (p=0.024) higher levels of reactivity to donor strain splenocytes. Values are represented as mean ± SD. Significance in differential serum levels of C5a or donor reactivity determined by Mann-Whitney U-test.

Adoptive transfer of 100µg donor specific antibody did not induce histopathological signs of allograft rejection

Microscopic sections of kidneys were assessed using international the consensus Banff scoring system for histopathological signs of rejection and injury in the transplanted graft tissue (Table 3.2, Figure 3.2). Wild-type CBA (H-2^k) donor kidneys transplanted into T-cell/B-cell-null B6.RAG (H-2^b) recipients were not rejected and did not show inflammatory cell infiltration and parenchymal injury when compared to normal CBA kidneys and left native kidneys of B6.RAG recipients with allografts (Figure 3.2a and 3.2d).

In contrast to our expectations, CBA allografts in B6.RAG recipients which were transferred with 100µg anti-class I donor specific antibody (with and without rabbit complement) did not show histological signs of rejection: there was no increased inflammation in any histological compartment including the microcirculation and no signs of microvascular endothelial changes (swelling, denudation, apoptosis, capillary congestion) or acute tubular injury (Figure 3.2g and 3.2j).

Thus, a single dose of donor specific antibody transfer did not induce histologically detectable intragraft inflammation and injury.

Adoptive transfer of 100µg donor specific antibody triggered diffuse C4d deposition in peritubular capillaries

To assess whether 100µg of transferred donor specific antibody acted on donor antigens and caused complement activation, we determined intragraft C4d deposition by immunostaining, which is an in-situ tissue biomarker of classical complement activation triggered by tissue bound antibody (18). The C4d staining results are illustrated in Figure 3.2 b, e, h, and k.

We observed diffuse linear C4d staining of peritubular capillaries in allografts of donor specific antibody treated (with or without rabbit complement) recipients (Figure

3.2h 3.2k, and Table 3.2). In contrast, left native kidneys of mice which received donor specific antibody, control allografts without antibody treatment, and normal kidneys were negative for C4d staining in peritubular capillaries (Figure 3.2b, 3.2e, and Table 3.2).

We also assessed glomerular C4d staining. Antibody treated allografts with peritubular capillary C4d staining also showed diffuse glomerular capillary and mesangial staining. However, glomerular staining was also seen in all control kidneys (normal or allograft), mainly as a mesangial staining heavily expanding into the glomerular capillaries. Therefore, we did not detect differences in glomerular C4d staining between antibody treated allografts and controls. Other renal histological compartments (tubules and larger vessels) did not show C4d staining.

In summary, donor specific antibody transfer induced C4d deposition in peritubular capillaries of allografts.

Intragraft accumulation of donor specific antibody

To assess whether 100µg of I.P. injected donor specific antibody entered into the kidney allograft, we performed IgG immunostaining. The intrarenal IgG staining results are illustrated in Figure 3.2 c, e, i, and l.

Allograft kidneys in B6.RAG recipients transferred with donor specific antibody (with or without rabbit complement) (Figure 3.2i and 3.2l) showed intragraft accumulation of IgG in peritubular interstitium including peritubular capillary walls and basolateral aspects of the tubular epithelial cells, confirming entry of transferred alloantibody from the circulation into the allograft tissue. In contrast, control allografts without antibody treatment, left native kidneys from the allograft recipients, and normal donor kidneys were negative for IgG staining (Figure 3.2c and 3.2f).

Thus, intraperitoneally transferred donor specific antibody had accumulated in the transplanted donor kidneys and this was accompanied by C4d deposition along peritubular capillaries.

Table 3.2 – 0.1mg DSA treatment in allograft recipients does not result in development of pathological lesions. Kidney hematoxylin & eosin slides were scored for histopathology based on consensus Banff scoring criteria. Each kidney was given a score from 0-3 for each lesion. No histopathological lesions were seen in any of the kidneys, with the only exception of C4d deposition in 0.1mg DSA treated allograft recipients. Values are represented as mean ± SD.

Histology scores	NCBA	CBA/B6.RAG allo NLS		CBA/B6.RAG allo + 0.1mg NLS		CBA/B6.RAG allo + 0.1mg + C' NLS	
	Native	Allo	Native	Allo	Native	Allo	Native
C4d staining (score)	0.0 ± 0.0	0.0 ± 0.0	NA	3.0 ± 0.0	0.0 ± 0.0	2.0 ± 0.0	0.0 ± 0.0
Capillary endothelial swelling (score)	0.0 ± 0.0	0.3 ± 0.5	0.0 ± 0.0	0.3 ± 0.5	0.1 ± 0.3	0.0 ± 0.0	0.0 ± 0.0
Capillary dilation (score)	0.0 ± 0.0	1.6 ± 1.4	0.6 ± 0.5	0.7 ± 0.6	0.1 ± 0.3	0.4 ± 0.5	0.0 ± 0.0
% Capillaritis	0.0 ± 0.0	0.0 ± 0.0	0.0 ± 0.0	0.3 ± 1.3	0.0 ± 0.0	0.0 ± 0.0	0.0 ± 0.0
Glomerulitis (score)	0.0 ± 0.0	0.0 ± 0.0	0.0 ± 0.0	0.0 ± 0.0	0.0 ± 0.0	0.0 ± 0.0	0.0 ± 0.0
Peritubular capillaritis (score)	0.0 ± 0.0	0.0 ± 0.0	0.0 ± 0.0	0.0 ± 0.0	0.0 ± 0.0	0.0 ± 0.0	0.0 ± 0.0
Tubulitis (score)	0.0 ± 0.0	0.0 ± 0.0	0.0 ± 0.0	0.0 ± 0.0	0.0 ± 0.0	0.0 ± 0.0	0.0 ± 0.0
Tubular atrophy (score)	0.0 ± 0.0	0.0 ± 0.0	0.0 ± 0.0	0.0 ± 0.0	0.0 ± 0.0	0.0 ± 0.0	0.0 ± 0.0
% Tubular cytoplasmic vacuolation	0.0 ± 0.0	12.9 ± 13.5	0.7 ± 1.9	15.3 ± 11.4	4.0 ± 10.2	7.0 ± 2.7	0.0 ± 0.0
% Necrotic tubules	0.0 ± 0.0	0.0 ± 0.1	0.0 ± 0.0	0.0 ± 0.0	0.0 ± 0.0	0.0 ± 0.0	0.0 ± 0.0
% Tubular epithelial flattening	0.0 ± 0.0	8.6 ± 6.3	0.7 ± 1.9	12.7 ± 11.3	2.0 ± 7.7	6.0 ± 2.2	0.0 ± 0.0
Transplant glomerulopathy (score)	0.0 ± 0.0	0.0 ± 0.0	0.0 ± 0.0	0.0 ± 0.0	0.0 ± 0.0	0.0 ± 0.0	0.0 ± 0.0
Interstitial inflammation (score)	0.0 ± 0.0	0.0 ± 0.0	0.0 ± 0.0	0.0 ± 0.0	0.0 ± 0.0	0.0 ± 0.0	0.0 ± 0.0
Interstitial fibrosis (score)	0.0 ± 0.0	0.0 ± 0.0	0.0 ± 0.0	0.0 ± 0.0	0.0 ± 0.0	0.0 ± 0.0	0.0 ± 0.0
Intimal arteritis (score)	0.0 ± 0.0	0.0 ± 0.0	0.0 ± 0.0	0.0 ± 0.0	0.0 ± 0.0	0.0 ± 0.0	0.0 ± 0.0
Arterial fibrous intimal thickening (score)	0.0 ± 0.0	0.0 ± 0.0	0.0 ± 0.0	0.0 ± 0.0	0.0 ± 0.0	0.0 ± 0.0	0.0 ± 0.0
Arteriolar hyalinosis (score)	0.0 ± 0.0	0.0 ± 0.0	0.0 ± 0.0	0.0 ± 0.0	0.0 ± 0.0	0.0 ± 0.0	0.0 ± 0.0
% Global glomerular sclerosis	0.0 ± 0.0	0.0 ± 0.0	0.0 ± 0.0	0.0 ± 0.0	0.0 ± 0.0	0.0 ± 0.0	0.0 ± 0.0

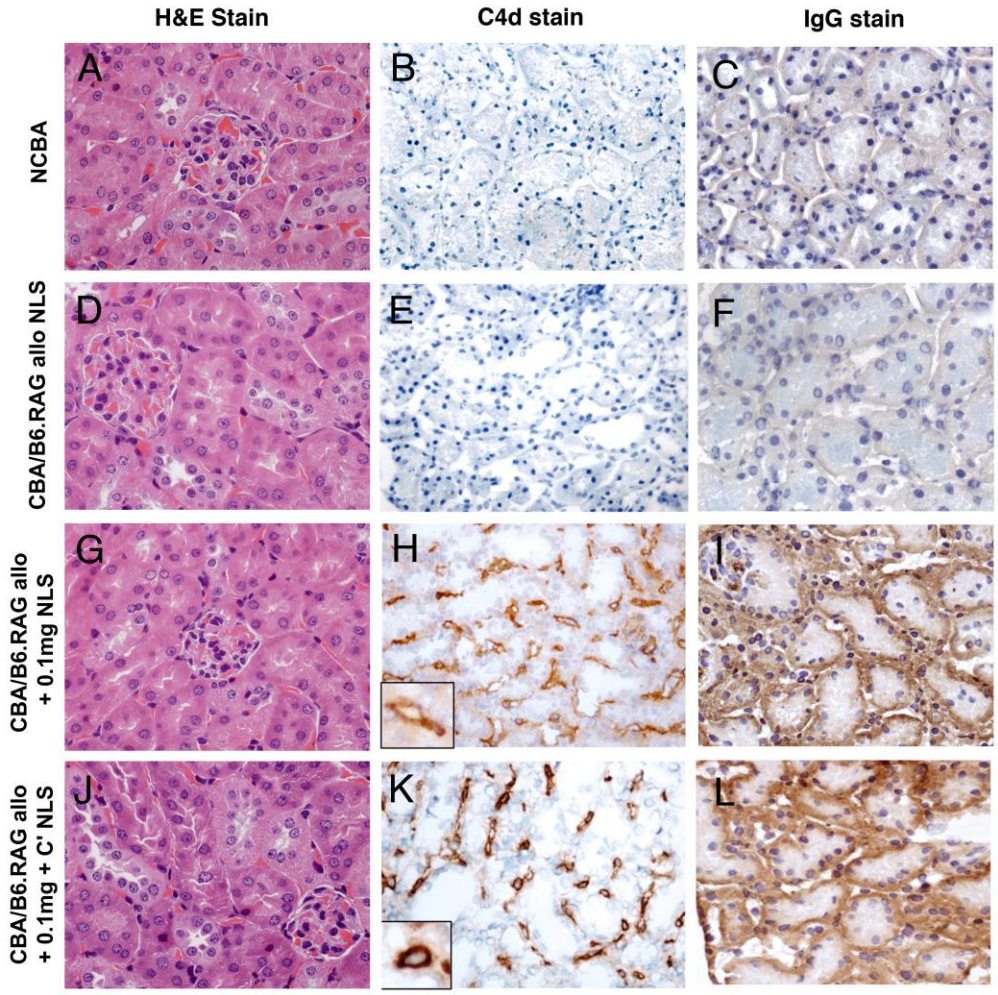

Figure 3.2 – No pathological lesions present in DSA treated allograft recipients despite presence of IgG and C4d. A-C: Normal CBA kidneys from naïve mice show (A) normal histology, (B) no staining for C4d in peritubular capillaries, and (C) no staining for IgG **D-F:** CBA/B6.RAG allografts with no antibody treatment show (D) normal histology, (E) no staining for C4d in peritubular capillaries, and (F) no staining for IgG. **G-I:** CBA/B6.RAG allografts with donor specific antibody treatment show (G) normal histology, *H) diffuse C4d staining in peritubular capillaries, and (I) IgG staining in peritubular interstitium including peritubular capillary walls and basolateral aspects of tubular epithelial cells. **J-L:** CBA/B6.RAG allografts treated with donor specific antibody plus rabbit complement show (J) normal histology, (K) diffuse C4d staining in peritubular capillaries, and (L) IgG staining. (Hematoxylin and eosin or immunoperoxidase, original magnification x600 or x400)

Lack of distal effector complement C5a activation in recipients with C4d positive allografts treated with 100µg DSA

Because intragraft C4d deposition was not accompanied by graft inflammation, we asked if potent chemoattractant complement effectors i.e., C5a that recruit inflammatory cells were generated. To determine whether initiation of complement activation induced by bound antibody was amplified and progressed to generation of bioactive complement effector fragments, we measured distal complement effector product C5a in serum by ELISA.

As we predicted, complement split product C5a levels were not increased in sera from 100µg donor specific antibody treated B6.RAG recipients with C4d positive allografts when compared to baseline levels in sera of naïve B6.RAG mice and control B6.RAG recipients with C4d negative allografts and no donor specific antibody treatment (Figure 3.3).

Thus, bound antibody induced initiation of complement activation (as indicated by intragraft C4d staining) but this process did not progress to distal stages of the complement cascade and terminated prior to the conversion of C5 to C5a and C5b.

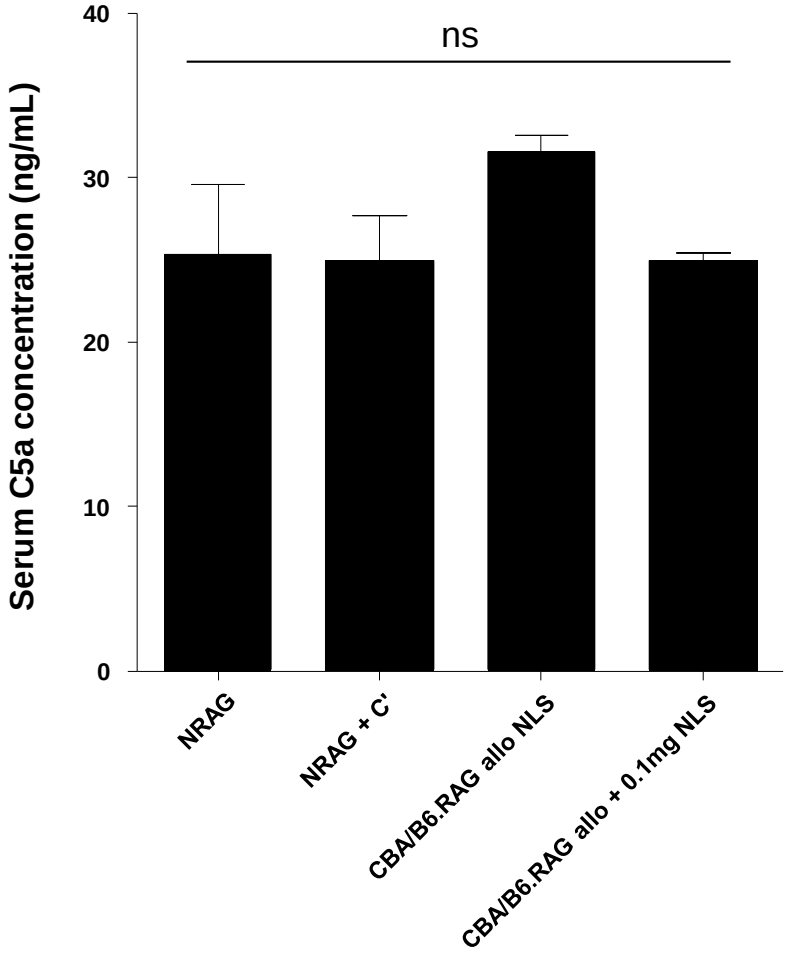

Figure 3.3 – No increase in fluid phase C5a after treating allograft recipients with 0.1mg DSA. By ELISA, serum collected at time of allograft harvest was analyzed for fluid phase C5a. No significant differences (denoted by ns, not significant, $p>0.05$) in C5a levels were detected between DSA treated allograft recipients and allograft controls or normal kidney controls. Values are presented as mean ± SEM. Significance of differential expression was determined by Kruskal-Wallis one-way analysis of variance.

Lack of molecular signs of inflammation and injury in C4d positive allografts

We questioned whether some C5a was generated in C4d positive allograft tissues without increasing serum C5a levels. We reasoned if C5a was locally generated in C4d positive allograft tissues, this would change intragraft expression of downstream molecules inducible by C5a.

First, we examined intragraft expression of pro-inflammatory cytokines (Il1, Ifng, Tnf, Il6, Ccl2, Ccl5, Ifng) some of which are shown to be inducible by C5a (55;95) and C5a-inducible endothelial adhesion/activation molecules (Icam1, Icam2, Pecam1, Selp, Sele, Vwf) (4;43;49). As illustrated in Figures 3.4a and 3.4b, intragraft expression of pro-inflammatory cytokine and endothelial adhesion/activation transcripts was not increased in C4d positive allografts in recipients with donor specific antibody treatment (with or without rabbit complement) when compared to C4d negative allografts in untreated recipients.

As an additional method of measuring allograft inflammation and injury, we examined expression of transcript sets representing intragraft interferon-gamma effects, macrophage-, NK cell-, and endothelial cell-associated transcripts, and kidney parenchymal transcripts among groups. By expression microarrays, we found no molecular signs of injury, inflammation, and endothelial activation in C4d positive allografts compared to control allografts (Figure 3.4c). Class comparison analyses using individual transcripts in each transcript set also did not reveal significant differences between C4d positive and control allografts ($p>0.05$).

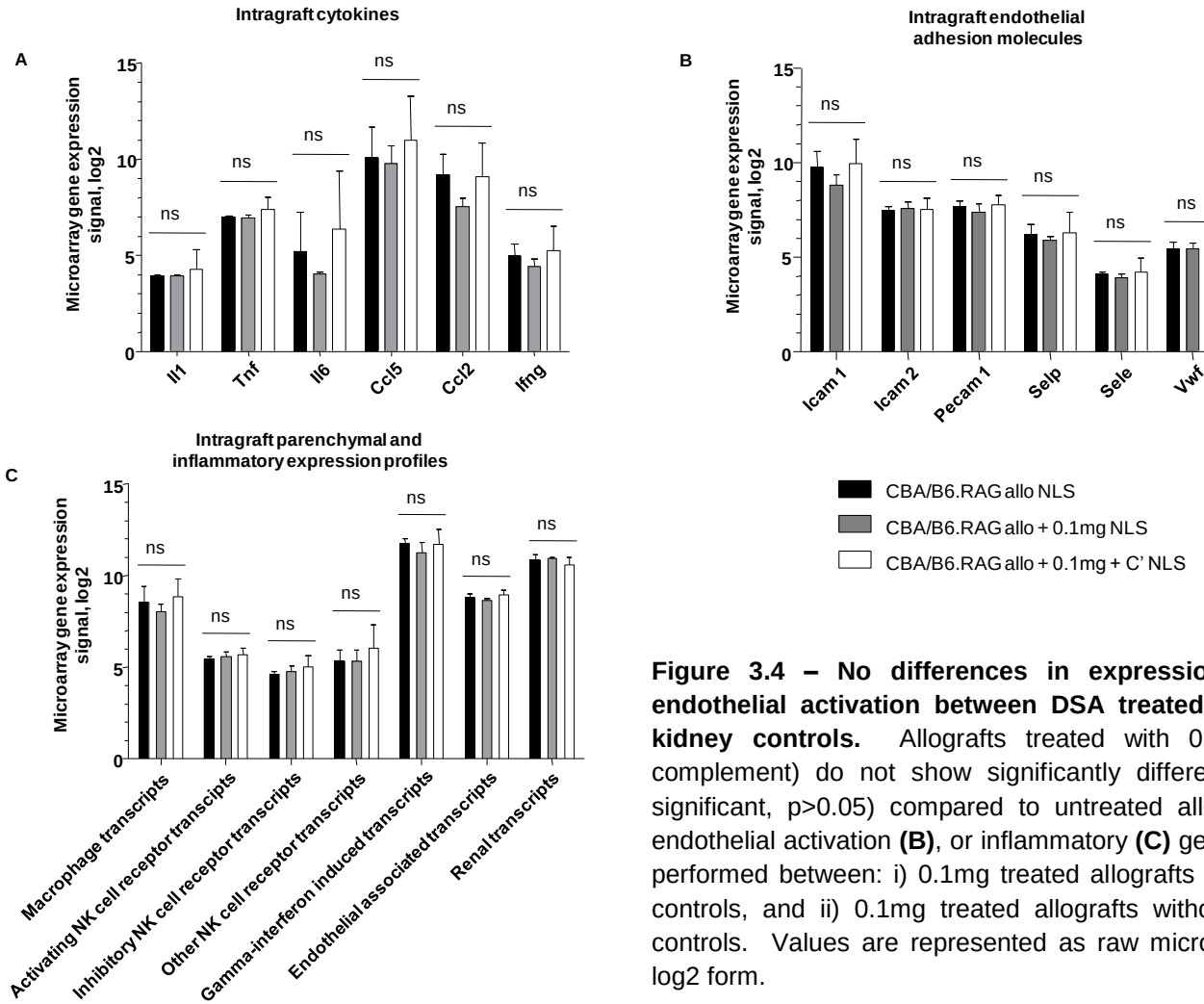

Figure 3.4 – No differences in expression of cytokine, inflammatory, or endothelial activation between DSA treated and untreated controls / normal kidney controls. Allografts treated with 0.1mg DSA (with or without rabbit complement) do not show significantly different expression (denoted by ns, not significant, $p>0.05$) compared to untreated allograft controls in any cytokine **(A)**, endothelial activation **(B)**, or inflammatory **(C)** gene sets. Mann-Whitney U-tests were performed between: i) 0.1mg treated allografts with rabbit complement and allograft controls, and ii) 0.1mg treated allografts without rabbit complement and allograft controls. Values are represented as raw microarray expression signals ± SEM, in log2 form.

No molecular evidence for acquired graft resistance to alloantibody (accommodation) in C4d positive allografts

Because C4d deposition in allografts was not accompanied by inflammation and injury, we asked if C4d positive allografts were protected against injurious effects of bound donor specific antibody and activation of complement.

To determine if termination of the complement activation prior to the conversion of C5 to C5a and C5b was due to heightened resistance of allografts to complement by improved complement control, we studied intragraft gene expression of complement regulators. By microarrays, intragraft transcript expression of membrane-bound (Cd59a, Cr1l, Cd46, Daf1, Daf2, Cr2) and secreted (C4bp, Cfh, Cfi, Serping1) complement regulators was not increased in C4d positive kidney allografts when compared to C4d negative allografts and normal kidneys (Figure 3.5). Thus, C4d positive allografts did not show increased ability to control complement compared to control kidneys.

To examine whether lack of tissue injury in C4d positive allografts was due to a protective molecular phenotype, we studied large scale intragraft gene expression profiles in C4d positive allografts and compared them to controls. First, we checked cytoprotective and survival genes that were previously associated with accommodation of experimental xenografts and some allografts in patients. Transcript levels of survival genes bcl2 and bcl2l1, cytoprotective gene heme-oxygenase (hmox1), and tumor necrosis factor-alpha induced protein 3 (tnfaip3, also known as A20), denoted in literature to be associated with graft accommodation (59;62;130) were not different between C4d positive allografts exposed to donor specific antibody and control allografts with no C4d deposition and antibody treatment (Figure 3.6). Furthermore, a class-comparison analysis using genome-wide transcript expression profiles, did not reveal any differentially expressed genes between C4d positive allografts with antibody treatment and control allografts with no C4d deposition and antibody treatment (corrected $p>0.05$).

Thus, C4d positive allografts did not show a modified protective molecular phenotype compared to control kidneys.

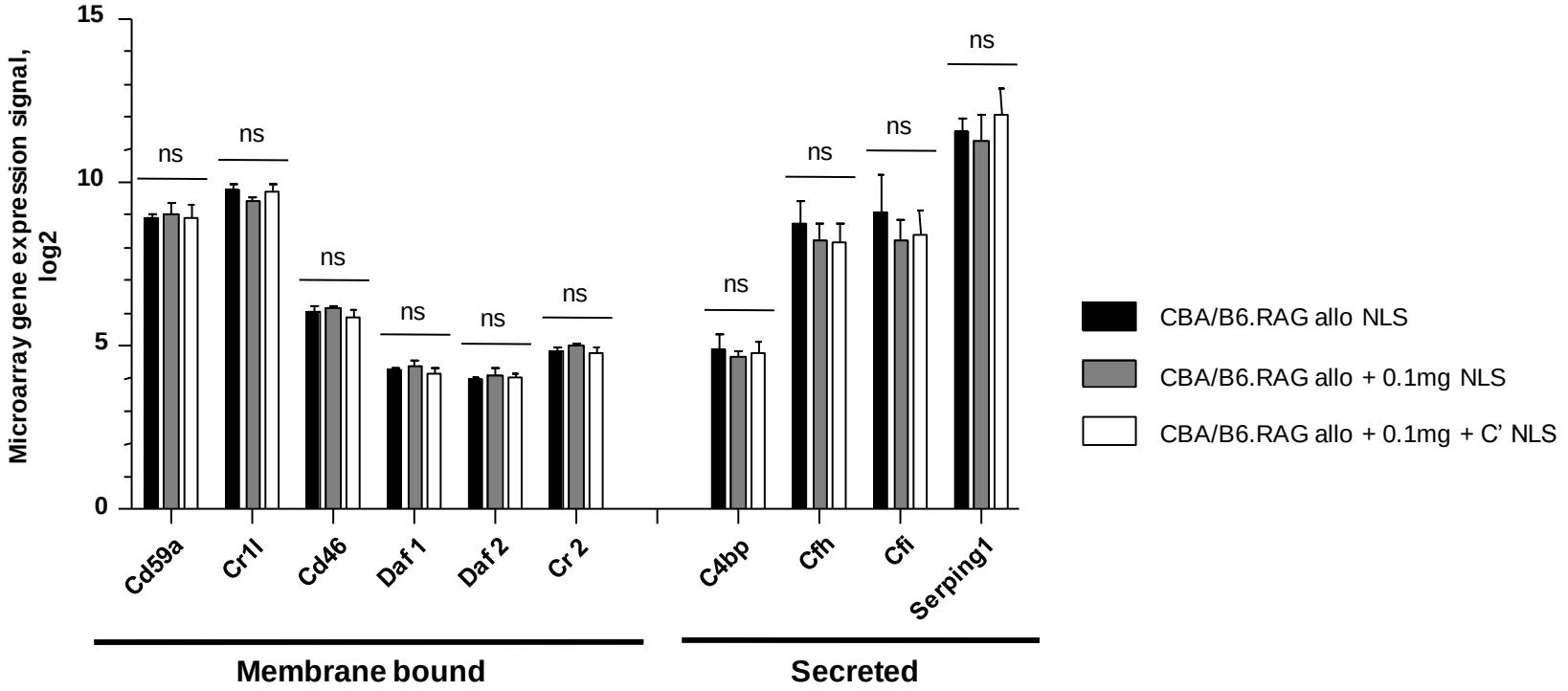

Figure 3.5 – No increases in expression of complement regulators in C4d positive DSA-treated allograft recipients compared to allograft controls. By microarray, allograft recipients treated with 0.1mg DSA with or without rabbit complement do not show significantly different expression (denoted by ns, not significant, $p>0.05$) of complement regulatory proteins compared to allograft controls. Mann-Whitney U-tests were performed between: i) 0.1mg treated allografts with rabbit complement and allograft controls, and ii) 0.1mg treated allografts without rabbit complement and allograft controls. Values are represented as raw microarray expression signals ± SEM, in log2 form.

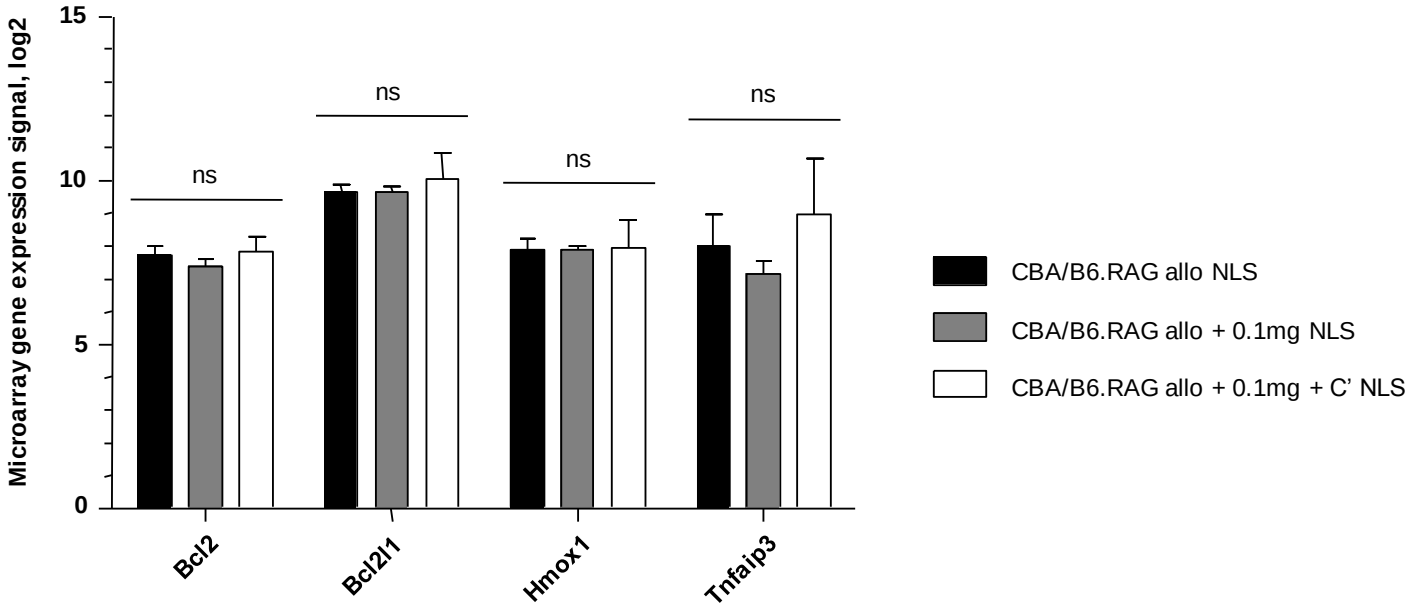

Figure 3.6 – No increases in expression of cytoprotective 'accommodation' genes in DSA treated allografts (with or without rabbit complement) compared to allograft controls. Kidneys from 0.1mg DSA treated allografts (with or without rabbit complement) do not show significantly different expression (denoted by ns, not significant, $p>0.05$) in any of the pre-selected genes (Bcl2, Bcl2l1, Hmox1, and Tnfaip3) associated with accommodation. Mann-Whitney U-tests were performed between: i) 0.1mg treated allografts with rabbit complement and allograft controls, and ii) 0.1mg treated allografts without rabbit complement and allograft controls. Values are represented as raw microarray expression signals ± SEM, in log2 form.

Serum C5a increases with DSA dosage

In addition to one injection of low dose 100µg DSA to allograft recipients, we examined the serum C5a levels and pathology of allograft recipients treated with increasing dosages of monoclonal DSA. We hypothesized that increasing DSA dosages further enhances complement activation to the point of achieving the terminal complement effectors C5a and C5b-9, thereby causing injury to transplanted tissue.

By ELISA, multiple injections of high dose consisting of 3000µg DSA induced a significant ($p=0.014$ and $p=0.021$) increase in serum C5a levels. We found a roughly 10 and 20 fold increase in serum C5a concentration (25ng/mL vs. 273ng/mL and 580ng/mL) between recipients of low dose 100µg DSA injections compared with high dose 3000µg, or 3000µg DSA with added rabbit complement injections, respectively. Medium doses of DSA (multiple injections of 300µg, single injection of 750µg, or multiple injections of 2000µg) did not show significant increases in serum C5a levels compared to low dose 100µg DSA injections or untreated allograft controls.

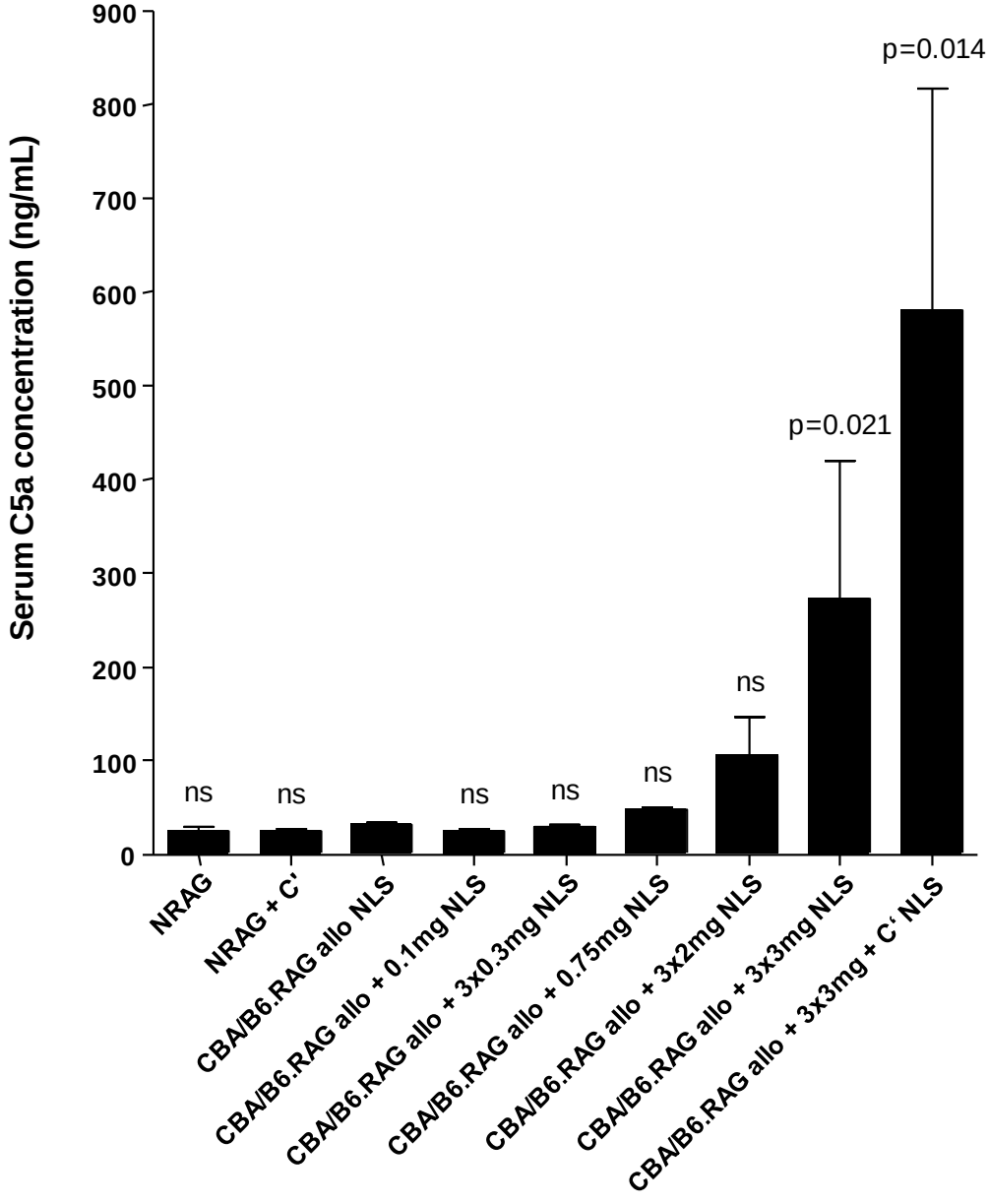

Figure 3.7 – Serum C5a levels increase with increasing DSA treatment dosage. By ELISA, serum samples from allograft recipients treated with varying dosages of DSA was measured and compared to allograft controls or normal B6.RAG kidneys. Fluid phase C5a levels in each condition were compared to allograft controls by Mann-Whitney U-test. No significant increases (denoted by ns, not significant, $p>0.05$) of serum C5a was measured in majority of DSA dosages. Only allograft recipients treated with 3 doses of 3mg DSA (with or without rabbit complement) showed significant differences to allograft controls ($p=0.014$ and $p=0.021$, respectively). Values are represented as mean ± SEM.

Pathology correlated with DSA dosage

We examined pathology generated in allograft tissues treated with increasing dosages of DSA. We hypothesized that a greater activation of terminal portions of the complement pathway (generation of C5a and C5b-9) increases observable pathology by conventional histopathological stains. Kidneys were scored based on Banff diagnostic criteria, and conditions were compared between treatment conditions. Pathology was examined as a function of DSA dosage, and was evaluated by determining correlativity. Untreated allografts and left kidneys were used as controls.

By quantitative pathology, we found significant correlation between increasing DSA dosage to increasing degree of pathology in acute tubular injury (tubular cytoplasmic vacuolization, epithelial cell flattening and tubular epithelial cell necrosis and acute microvascular injury (capillary endothelial swelling, capillary dilatation). However, we found only minimal inflammation of capillaries in all allograft tissues; no correlation between capillaritis and DSA dosage could be found (Figure 3.8).

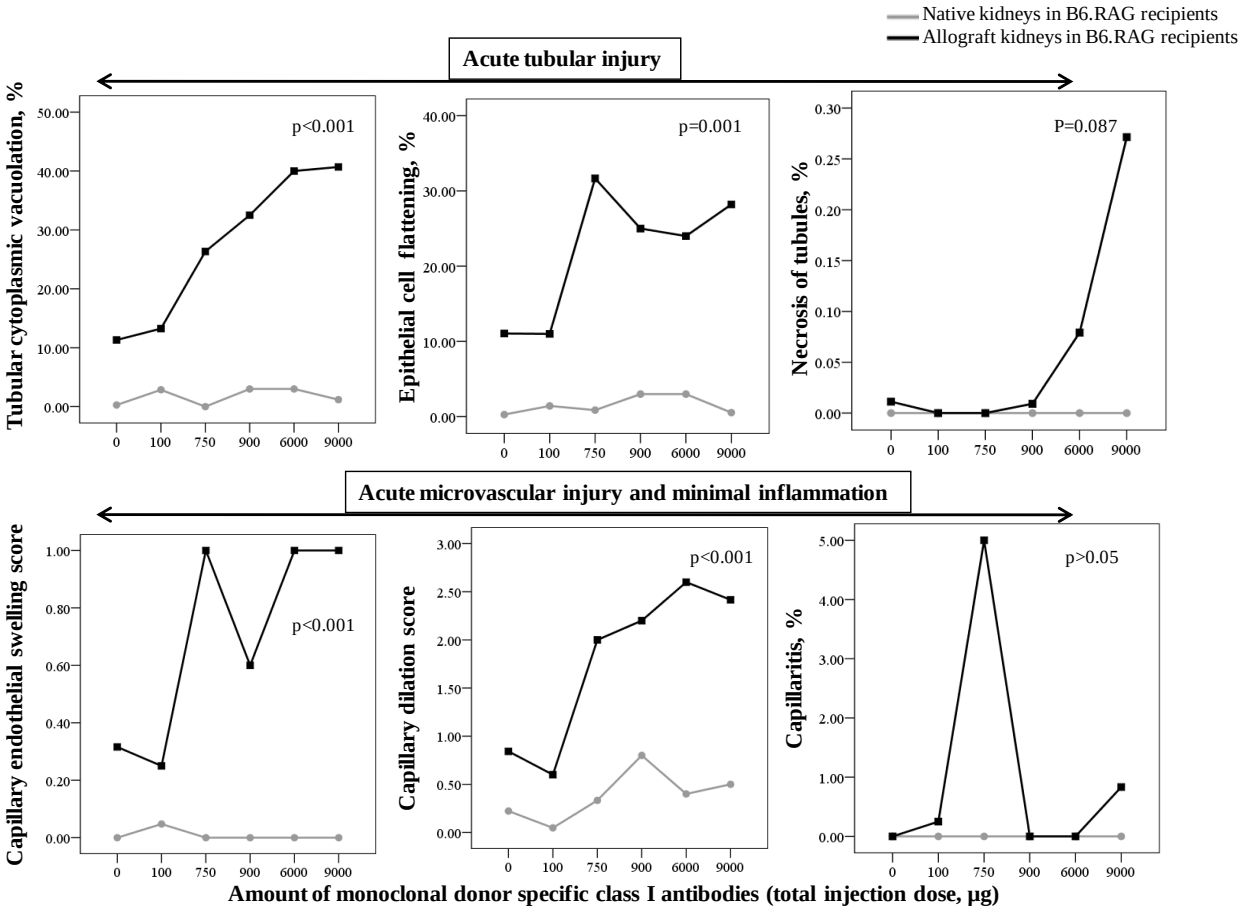

Figure 3.8 – Correlation between acute allograft injury and DSA treatment dosage. Histopathological lesions were scored in allografts treated with varying DSA dosages. Significant correlativity between histopathology and DSA dose ($p<0.05$) was seen in acute graft injury lesions, but no significant correlation exists between DSA dose and inflammation ($p>0.05$).

Table 3.3 - Histopathology in kidneys of normal mouse CBA/J and C57BL/6 strain controls

Histology scores	NCBA	NRAG
	Native	Native
C4d staining (score)	0.0 ± 0.0	0.0 ± 0.0
Capillary endothelial swelling (score)	0.0 ± 0.0	0.0 ± 0.0
Capillary dilation (score)	0.0 ± 0.0	0.0 ± 0.0
% Capillaritis	0.0 ± 0.0	0.0 ± 0.0
Glomerulitis (score)	0.0 ± 0.0	0.0 ± 0.0
Peritubular capillaritis (score)	0.0 ± 0.0	0.0 ± 0.0
Tubulitis (score)	0.0 ± 0.0	0.0 ± 0.0
Tubular atrophy (score)	0.0 ± 0.0	0.0 ± 0.0
% Tubular cytoplasmic vacuolation	0.0 ± 0.0	0.0 ± 0.0
% Necrotic tubules	0.0 ± 0.0	0.0 ± 0.0
% Tubular epithelial flattening	0.0 ± 0.0	0.0 ± 0.0
Transplant glomerulopathy (score)	0.0 ± 0.0	0.0 ± 0.0
Interstitial inflammation (score)	0.0 ± 0.0	0.0 ± 0.0
Interstitial fibrosis (score)	0.0 ± 0.0	0.0 ± 0.0
Intimal arteritis (score)	0.0 ± 0.0	0.0 ± 0.0
Arterial fibrous intimal thickening (score)	0.0 ± 0.0	0.0 ± 0.0
Arteriolar hyalinosis (score)	0.0 ± 0.0	0.0 ± 0.0
% Global glomerular sclerosis	0.0 ± 0.0	0.0 ± 0.0

Table 3.4 - Histopathology findings in early allograft and native kidneys of mice undergoing non-life supporting kidney transplantation treated with control injections

Histology scores	CBA/B6.RAG allo + PBS NLS		CBA/B6.RAG allo + C' NLS	
	Allo	Native	Allo	Native
C4d staining (score)	0.0 ± 0.0	NA	0.0 ± 0.0	NA
Capillary endothelial swelling (score)	0.3 ± 0.5	0.0 ± 0.0	0.6 ± 0.5	0.0 ± 0.0
Capillary dilation (score)	1.6 ± 1.4	0.6 ± 0.5	0.8 ± 0.4	0.0 ± 0.0
% Capillaritis	0.0 ± 0.0	0.0 ± 0.0	0.0 ± 0.0	0.0 ± 0.0
Glomerulitis (score)	0.0 ± 0.0	0.0 ± 0.0	0.0 ± 0.0	0.0 ± 0.0
Peritubular capillaritis (score)	0.0 ± 0.0	0.0 ± 0.0	0.0 ± 0.0	0.0 ± 0.0
Tubulitis (score)	0.3 ± 0.5	0.0 ± 0.0	0.0 ± 0.0	0.0 ± 0.0
Tubular atrophy (score)	0.0 ± 0.0	0.0 ± 0.0	0.0 ± 0.0	0.0 ± 0.0
% Tubular cytoplasmic vacuolation	12.9 ± 13.5	0.7 ± 1.9	21.0 ± 18.8	0.0 ± 0.0
% Necrotic tubules	0.0 ± 0.1	0.0 ± 0.0	0.0 ± 0.0	0.0 ± 0.0
% Tubular epithelial flattening	8.6 ± 6.3	0.7 ± 1.9	25.0 ± 26.9	0.0 ± 0.0
Transplant glomerulopathy (score)	0.0 ± 0.0	0.0 ± 0.0	0.0 ± 0.0	0.0 ± 0.0
Interstitial inflammation (score)	0.0 ± 0.0	0.0 ± 0.0	0.0 ± 0.0	0.0 ± 0.0
Interstitial fibrosis (score)	0.0 ± 0.0	0.0 ± 0.0	0.0 ± 0.0	0.0 ± 0.0
Intimal arteritis (score)	0.0 ± 0.0	0.0 ± 0.0	0.0 ± 0.0	0.0 ± 0.0
Arterial fibrous intimal thickening (score)	0.0 ± 0.0	0.0 ± 0.0	0.0 ± 0.0	0.0 ± 0.0
Arteriolar hyalinosis (score)	0.0 ± 0.0	0.0 ± 0.0	0.0 ± 0.0	0.0 ± 0.0
% Global glomerular sclerosis	0.0 ± 0.0	0.0 ± 0.0	0.0 ± 0.0	0.0 ± 0.0

Table 3.5 - Histopathology findings in early allograft and native kidneys of mice undergoing non-life supporting kidney transplantation treated with donor specific antibodies. Histopathology was compared to allografts with control PBS injections or control complement injections (* and † denote p<0.05 when compared to allografts treated with PBS control or complement control injection, respectively.)

Histology scores	CBA/B6.RAG allo + 0.1mg NLS		CBA/B6.RAG allo + 0.1mg + C' NLS		CBA/B6.RAG allo + 3x0.3mg NLS		CBA/B6.RAG allo + 0.75mg NLS		CBA/B6.RAG allo + 3x2mg NLS		CBA/B6.RAG allo + 3x3mg + C' NLS	
	Allo	**Native**	**Allo**	**Native**	**Allo**	**Native**	**Allo**	**Native**	**Allo**	**Native**	**Allo**	**Native**
C4d staining (score)	***†3.0 ± 0.0**	NA	***†2.0 ± 0.0**	NA	***†3.0 ± 0.0**	NA	***†2.0 ± 1.7**	NA	***†3.0 ± 0.0**	NA	***†3.0 ± 0.0**	NA
Capillary endothelial swelling (score)	0.3 ±0.5	0.1 ±0.3	0.0 ±0.0	0.0 ±0.0	0.6 ±0.5	0.0 ±0.0	***1.0 ±0.0**	0.0 ±0.0	***1.0 ±0.0**	0.0 ±0.0	***†1.0 ±0.0**	0.0 ±0.0
Capillary dilation (score)	0.7 ±0.6	0.1 ±0.3	0.4 ±0.5	0.0 ±0.0	**†2.2 ±0.4**	0.8 ±0.4	**†2.0 ±0.0**	0.3 ±0.6	**†2.6 ±0.5**	0.4 ±0.5	**†2.3 ±0.7**	0.5 ±0.7
% Capillaritis	0.3 ±1.3	0.0 ±0.0	0.0 ±0.0	0.0 ±0.0	0.0 ±0.0	0.0 ±0.0	5.0 ±8.7	0.0 ±0.0	0.0 ±0.0	0.0 ±0.0	1.1 ±2.2	0.0 ±0.0
Glomerulitis (score)	0.0 ±0.0	0.0 ±0.0	0.0 ±0.0	0.0 ±0.0	0.0 ±0.0	0.0 ±0.0	0.0 ±0.0	0.0 ±0.0	0.0 ±0.0	0.0 ±0.0	0.0 ±0.0	0.0 ±0.0
Peritubular capillaritis (score)	0.0 ±0.0	0.0 ±0.0	0.0 ±0.0	0.0 ±0.0	0.0 ±0.0	0.0 ±0.0	0.3 ±0.6	0.0 ±0.0	0.0 ±0.0	0.0 ±0.0	0.0 ±0.0	0.0 ±0.0
Tubulitis (score)	0.0 ±0.0	0.0 ±0.0	0.0 ±0.0	0.0 ±0.0	0.0 ±0.0	0.0 ±0.0	0.0 ±0.0	0.0 ±0.0	0.0 ±0.0	0.0 ±0.0	0.1 ±0.3	0.0 ±0.0
Tubular atrophy (score)	0.0 ±0.0	0.0 ±0.0	0.0 ±0.0	0.0 ±0.0	0.0 ±0.0	0.0 ±0.0	0.0 ±0.0	0.0 ±0.0	0.0 ±0.0	0.0 ±0.0	0.0 ±0.0	0.0 ±0.0

…table 3.5 continued on next page

…table 3.5 continued

Histology scores	CBA/B6.RAG allo + 0.1mg NLS		CBA/B6.RAG allo + 0.1mg + C' NLS		CBA/B6.RAG allo + 3x0.3mg NLS		CBA/B6.RAG allo + 0.75mg NLS		CBA/B6.RAG allo + 3x2mg NLS		CBA/B6.RAG allo + 3x3mg + C' NLS	
	Allo	**Native**	**Allo**	**Native**	**Allo**	**Native**	**Allo**	**Native**	**Allo**	**Native**	**Allo**	**Native**
% Tubular cytoplasmic vacuolation	15.3 ±11.4	4.0 ±10.2	7.0 ±2.7	0.0 ±0.0	***32.5 ±20.6**	3.0 ±2.6	***26.3 ±7.1**	0.0 ±0.0	***40.0 ±18.7**	3.0 ±2.7	***42.7 ±27.2**	1.2 ±2.9
% Necrotic tubules	0.0 ±0.0	0.0 ±0.0	0.0 ±0.0	0.0 ±0.0	0.0 ±0.0	0.0 ±0.0	0.0 ±0.0	0.0 ±0.0	0.0 ±0.0	0.0 ±0.0	0.3 ±0.7	0.0 ±0.0
% Tubular epithelial flattening	12.7 ±11.3	2.0 ±7.7	6.0 ±2.2	0.0 ±0.0	***25.0 ±13.7**	3.0 ±2.6	***31.7 ±24.7**	0.9 ±1.5	***24.0 ±12.4**	3.0 ±2.7	***29.0 ±15.1**	0.5 ±1.3
Transplant glomerulopathy (score)	0.0 ±0.0	0.0 ±0.0	0.0 ±0.0	0.0 ±0.0	0.0 ±0.0	0.0 ±0.0	0.0 ±0.0	0.0 ±0.0	0.0 ±0.0	0.0 ±0.0	0.0 ±0.0	0.0 ±0.0
Interstitial inflammation (score)	0.0 ±0.0	0.0 ±0.0	0.0 ±0.0	0.0 ±0.0	0.0 ±0.0	0.0 ±0.0	0.0 ±0.0	0.0 ±0.0	0.0 ±0.0	0.0 ±0.0	0.0 ±0.0	0.0 ±0.0
Interstitial fibrosis (score)	0.0 ±0.0	0.0 ±0.0	0.0 ±0.0	0.0 ±0.0	0.0 ±0.0	0.0 ±0.0	0.0 ±0.0	0.0 ±0.0	0.0 ±0.0	0.0 ±0.0	0.0 ±0.0	0.0 ±0.0
Intimal arteritis (score)	0.0 ±0.0	0.0 ±0.0	0.0 ±0.0	0.0 ±0.0	0.0 ±0.0	0.0 ±0.0	0.0 ±0.0	0.0 ±0.0	0.0 ±0.0	0.0 ±0.0	0.0 ±0.0	0.0 ±0.0
Arterial fibrous intimal thickening (score)	0.0 ±0.0	0.0 ±0.0	0.0 ±0.0	0.0 ±0.0	0.0 ±0.0	0.0 ±0.0	0.0 ±0.0	0.0 ±0.0	0.0 ±0.0	0.0 ±0.0	0.0 ±0.0	0.0 ±0.0

…table 3.5 continued on next page

…table 3.5 continued

Histology scores	CBA/B6.RAG allo + 0.1mg NLS		CBA/B6.RAG allo + 0.1mg + C' NLS		CBA/B6.RAG allo + 3x0.3mg NLS		CBA/B6.RAG allo + 0.75mg NLS		CBA/B6.RAG allo + 3x2mg NLS		CBA/B6.RAG allo + 3x3mg + C' NLS	
	Allo	**Native**	**Allo**	**Native**	**Allo**	**Native**	**Allo**	**Native**	**Allo**	**Native**	**Allo**	**Native**
Arteriolar hyalinosis (score)	0.0 ±0.0	0.0 ±0.0	0.0 ±0.0	0.0 ±0.0	0.0 ±0.0	0.0 ±0.0	0.0 ±0.0	0.0 ±0.0	0.0 ±0.0	0.0 ±0.0	0.0 ±0.0	0.0 ±0.0
% Global glomerular sclerosis	0.0 ±0.0	0.0 ±0.0	0.0 ±0.0	0.0 ±0.0	0.0 ±0.0	0.0 ±0.0	0.0 ±0.0	0.0 ±0.0	0.0 ±0.0	0.0 ±0.0	0.0 ±0.0	0.0 ±0.0

3.2 – A mouse model that reproduces human acute antibody-mediated kidney transplant rejection

3.2.1 - Overview

Despite immunosuppression regimes for human kidney transplant patients, antibody-mediated rejection of transplanted kidney grafts remains a major problem. The mechanisms of ABMR are not well understood, mainly due to the lack of a small animal model of this disease reproducing the same pathological features as those found in human ABMR patients (87). The absence of a satisfactory animal model of ABMR is primarily due to the nature of kidney allograft rejection. Typical rejection in human patients is a mix between ABMR and T cell-mediated rejection (TCMR). With the exception of hyperacute ABMR, acute TCMR usually elicits allograft injury and rejection in the same timeframe to the development of ABMR phenotypes. In this way, TCMR phenotypes tend to mask ABMR phenotypes in rejecting kidneys.

In order to avoid TCMR phenotypes in a histocompatibility complex-mismatched kidney transplantation model, we transplanted kidneys from male CBA/J mice (H-2k: Kk, Dk, I-Ak) into male B6.Rag1 knock-out mice (H-2b: Kb, Db, I-Ab) which lack T-cells and B-cells. To induce allograft injury, we adoptively transferred 3000µg monoclonal donor specific IgG antibodies into B6.Rag1 knock-out kidney allograft recipient mice via I.P. injections. Injections were performed from day 5 post-transplant until day of harvest. Kidneys from allograft recipients were harvested either on day 7 post-transplant (in non-life-supporting transplants) or when serum creatinine rises above 20% of baseline, sustained over 2 days (in life-supporting transplants). Controls included kidney allografts in recipients which were treated with PBS or non-immune IgG. Control allografts were harvested on the same day post-transplant as recipient allografts treated with DSA.

Treatment with DSA induced the activation of the complement pathway to terminal C5a and C5b-9 MAC generation, while inducing acute microvascular endothelial and tubular injury, as evidenced by traditional histopathology and transmission electron microscopy. Injury to kidney allografts also induces renal dysfunction in life-supporting transplants at later time points (i.e. past D20 post-transplant). By gene expression analysis, DSA treatment to allograft recipients also induces the expression of endothelial adhesion molecules, denoting the activation of the microvascular endothelium. However, despite the presence of endothelial and tubular injury, minimal inflammation was detected.

In this section, we establish a working mouse model of ABMR, showing acute injury phenotypes mimicking those seen in human patients.

Table 3.6 – Transplant and condition abbreviations applicable to section 3.2

Donor	Recipient	Condition	Treatment	Abbrev.	Day post tx	N of mice
B6.RAG1$^{-/-}$ (H-2^{b})	-	Normal B6.RAG1$^{-/-}$ kidney	-	NRAG	-	5
B6.RAG1$^{-/-}$ (H-2^{b})	-	Normal B6.RAG1$^{-/-}$ kidney	0.25mL rabbit complement / day, 3 day treatment	NRAG + C’	-	5
CBA (H-2^{k})	B6.RAG1KO (H-2^{b})	Non-life supporting CBA/RAG allograft	No treatment, OR 0.2mL PBS / day, 3 day treatment	CBA/ B6.RAG allo NLS	D7	15
CBA (H-2^{k})	B6.RAG1KO (H-2^{b})	Non-life supporting CBA/RAG allograft	3mg DSA / day, 3 day treatment	CBA/B6.RAG allo + 3x3mg NLS	D7	6
CBA (H-2^{k})	B6.RAG1KO (H-2^{b})	Non-life supporting CBA/RAG allograft	3mg DSA / day + 0.25mL rabbit complement / day, 3 day treatment	CBA/B6.RAG allo + 3x3mg + C’ NLS	D7	9
CBA (H-2^{k})	B6 (H-2^{b})	Non-life supporting CBA/B6 allograft	3mg DSA / day + 0.25mL rabbit complement / day, 1 day treatment	CBA/B6 allo + 1x3mg + C’ WT NLS	varies (D1-3)	2
CBA (H-2^{k})	B6.RAG1KO (H-2^{b})	Life-supporting CBA/RAG allograft	3mg non-immune IgG / day	CBA/ B6.RAG allo LS	varies (D25-40)	5
CBA (H-2^{k})	B6.RAG1KO (H-2^{b})	Life-supporting CBA/RAG allograft	3mg DSA / day + 0.25mL rabbit complement / day	CBA/B6.RAG allo + 3x3mg + C’ LS	varies (D25-40)	5
CBA (H-2^{k})	B6.RAG1KO (H-2^{b})	Life-supporting CBA/RAG allograft	3mg pAb DSA / day + 0.25mL rabbit complement / day	CBA/B6.RAG allo + 3mg pAb + C’ LS	varies (D11-13)	2

3.2.2 – Results

Injected monoclonal antibodies against H-2K^k successfully enters circulation and is reactive against donor cells

Non-life supporting transplant recipients were injected via I.P. with either 3mg of DSA daily from day 5 post-transplant until day 7 or PBS for corresponding controls. Life supporting transplant recipients were injected I.P. with 3 mg of DSA from day 5 post-transplant until sustained elevations of serum creatinine were evident. Starting on day 5, life-supporting negative controls were injected with 3 mg of non-immune mouse IgG (Alpha Diagnostic International, San Antonio, TX) for the same number of days as the corresponding DSA treated recipient.

To determine whether or not injected DSA successfully enters the circulation and to determine the alloreactivity of the DSA injected, we performed a flow cytometric cross match against donor (CBA) strain splenocytes. Serum samples from allograft recipients treated with DSA show significantly increased MFI compared to B6.RAG allograft recipients treated with PBS or non-immune IgG, indicating significantly higher amounts of alloreactive IgG in DSA treated recipients compared to controls (Figure 3.9).

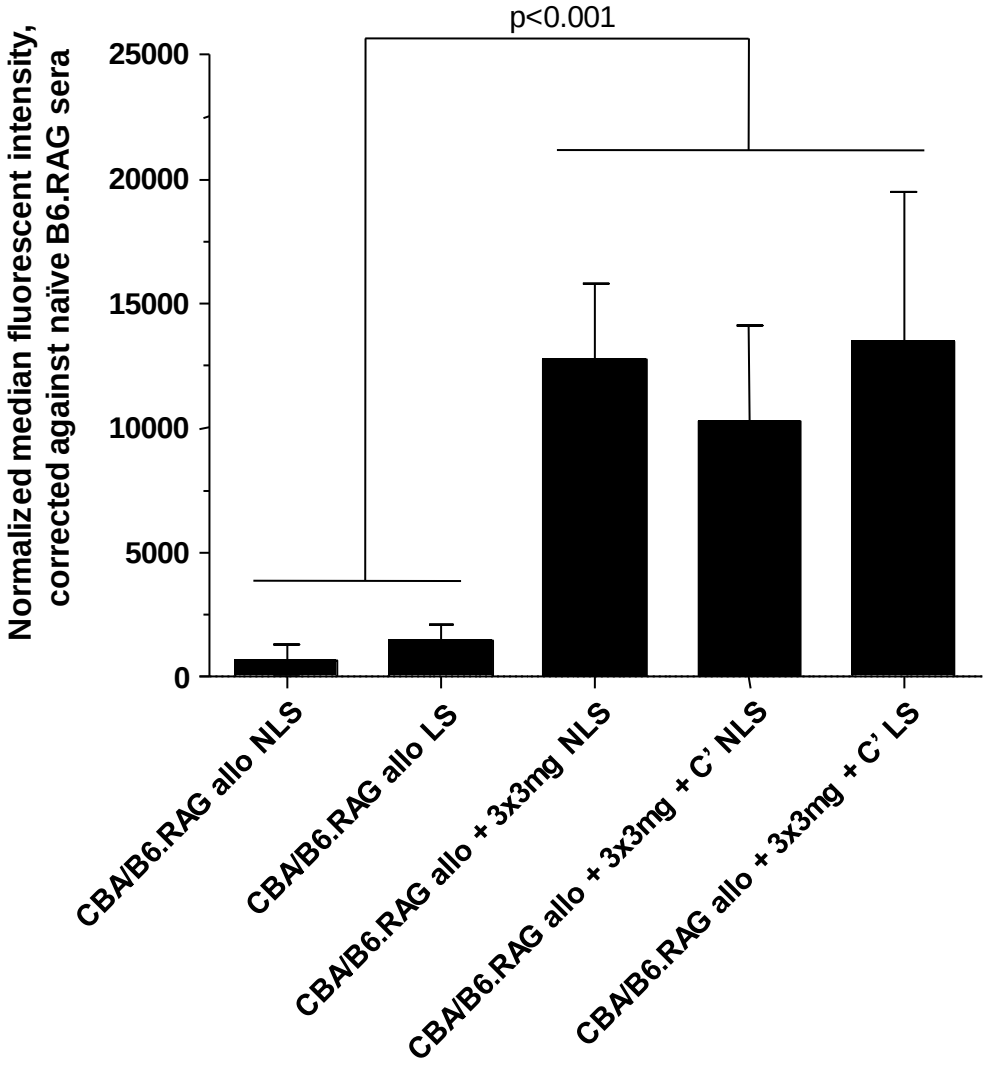

Figure 3.9 – Flow cytometric detection of fluid phase DSA. Fluid phase IgG reactive to donor (H-2K^k) splenocytes were significantly ($p<0.001$) higher in DSA treated allograft recipients than in either untreated, PBS treated, or non-immune IgG treated allografts recipients. MFI values are normalized against naïve B6.RAG sera. Values are reported as mean ± SEM. Significance in difference determined by Mann-Whitney U-test

Injected DSA was sufficient in inducing the activation of the complement pathway

Since DSA primarily elicit damage through activation of the complement pathway, we examined whether increased MFI values in flow cytometric crossmatch experiments translates into increased complement activation. After euthanization and harvest of transplant recipient mice, we measured levels of complement C5a split product and C5b-9 levels in freshly thawed serum.

By ELISA, transplant recipients treated with sham controls (PBS injections) showed the same levels of serum C5a levels compared to normal B6.RAG mice and normal B6.RAG mice treated with rabbit complement injections only. In contrast, we found a statistically significant increase in serum C5a levels in DSA treated mice compared to sham control mice or normal B6.RAG mice, with an approximately 20 fold increase in fluid phase C5a (Figure 3.10a). When examining MAC complex formation through C5b-9 ELISA, there was increased serum C5b-9 levels in DSA treated transplant recipients compared to sham treated groups and normal B6.RAG mice (Figure 3.10b).

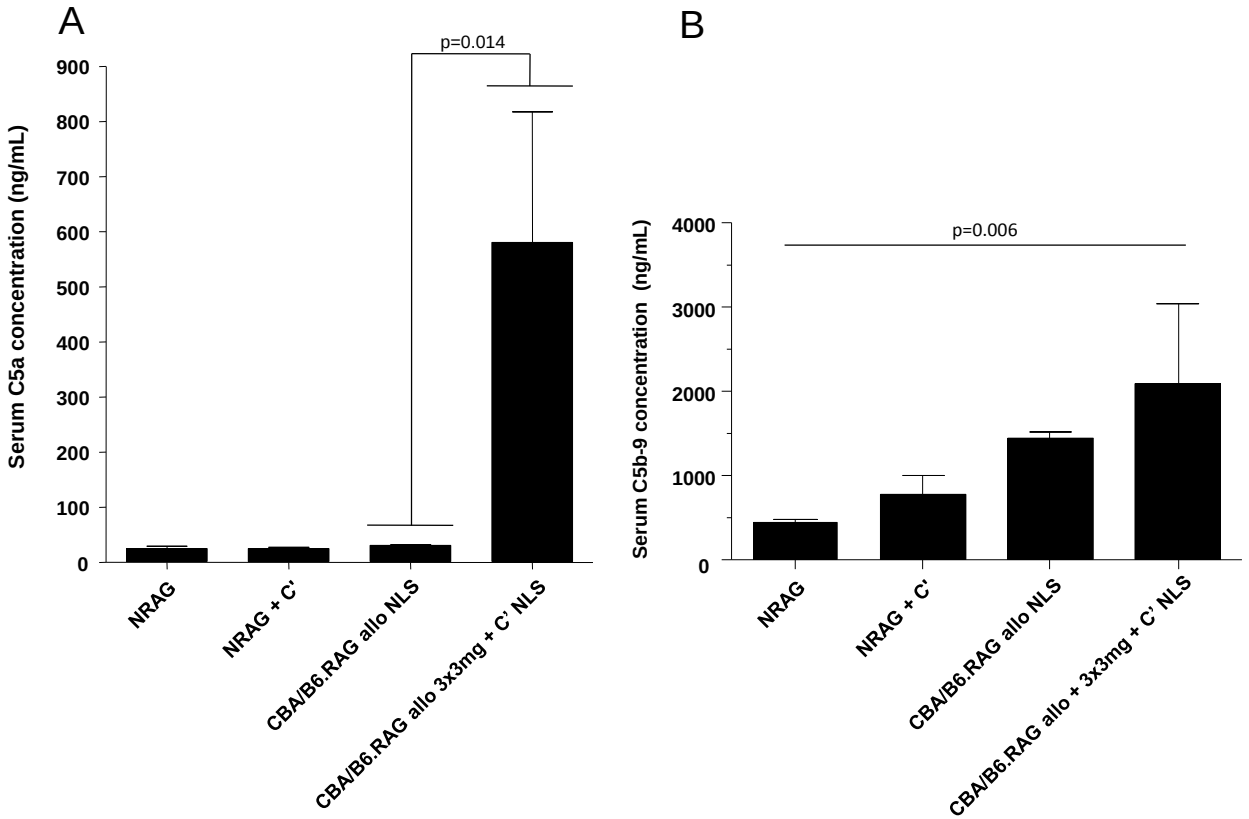

Figure 3.10 – Detection of serum C5a and C5b-9 by ELISA in allograft recipients treated with DSA, control injections, or normal kidney controls. Generation of terminal complement pathway product **(A)** C5a is significantly higher in DSA treated allograft recipients than untreated allograft recipients. **(B)** Generation of terminal C5b-9 complex shows a trend in increasing serum concentrations, with significantly differential (p=0.006) levels between conditions. Values represented as mean ± SEM. Significance in difference determined by **(A)** Mann-Whitney U-test, or **(B)** Kruskal-Wallis one-way analysis of variance

DSA treated allografts show acute microvascular and tubular injury with diffuse C4d staining

As another indicator for allograft injury in addition to measurements of renal function, FFPE sections of kidney tissue were stained with conventional histopathological stains and scored by two pathologists (Dr. Sufia Husain and Dr. Paula Blanco) based on the previously established Banff pathology scoring systems. In addition, transmission electron microscopy was performed on allograft kidneys of life-supporting transplants to further elucidate pathological signs of tissue injury.

By histopathology (Figure 3.11, Table 3.4), control allografts displayed unremarkable renal cortex and medulla with no rejection lesions (negative for tubulitis, arteritis, capillaritis, glomerulitis, capillary dilatation, vascular thrombi, and remarkable interstitial inflammation). However, allografts in recipients who received 3000 µg DSA with or without low toxicity rabbit complement showed increased acute microvascular and tubular injury with tubular epithelial cell cytoplasmic vacuolization, flattening of tubular epithelium, peritubular capillary dilation, capillary endothelial swelling/prominence, and mild aggregates of neutrophils and mononuclear leukocytes in lumens of peritubular capillaries (Table 3.5). Despite the presence of acute injury in microvascular network and tubular epithelial cells, high doses of DSA evoked only minimal light microscopic inflammation with focal leukocyte aggregation in capillary luminal and peritubular interstitium.

Immunostaining for complement C4d showed diffuse linear C4d deposition along peritubular capillaries and glomerular capillaries only in allografts with DSA treatment. Control allografts, contralateral native kidneys in mice with non-life supporting allografts, and baseline normal kidneys were negative for capillary C4d staining. By immunohistochemical IgG staining, we also demonstrated intragraft DSA deposition in allografts of mice that received adoptive transfer of DSA. IgG staining was negative in control allografts and baseline RAG kidneys.

Electron microscopy (Figure 3.12) showed presence of peritubular capillary injury with disruption and lysis of endothelial cells, adhesion of platelet aggregates onto disrupted microvascular endothelial surface, fibrin-like material deposition in capillary lumens, and focal capillary basement membrane multilayering in allograft kidneys after adoptive transfer of DSA. No such changes were observed in control allografts. (4 kidneys examined by electron microscopy). The glomeruli in kidneys from mice that received DSA showed electron dense immune complex deposits in the mesangium. Otherwise, there were no abnormal glomerular ultrastructural changes: well-preserved podocyte foot processes, endothelial morphology and preserved fenestrations, and normal mesangial cellularity were noted. Despite presence of mesangial immune complexes, there were no signs of glomerulonephritis: no increased cellularity and/or mesangial matrix were seen by electron microscopy and light microscopy. Glomerular immune complexes were not seen in control kidneys of mice that received non-immune IgG. In summary, electron microscopy confirmed the light microscopy findings and showed that DSA treatment induced acute peritubular capillary endothelial injury.

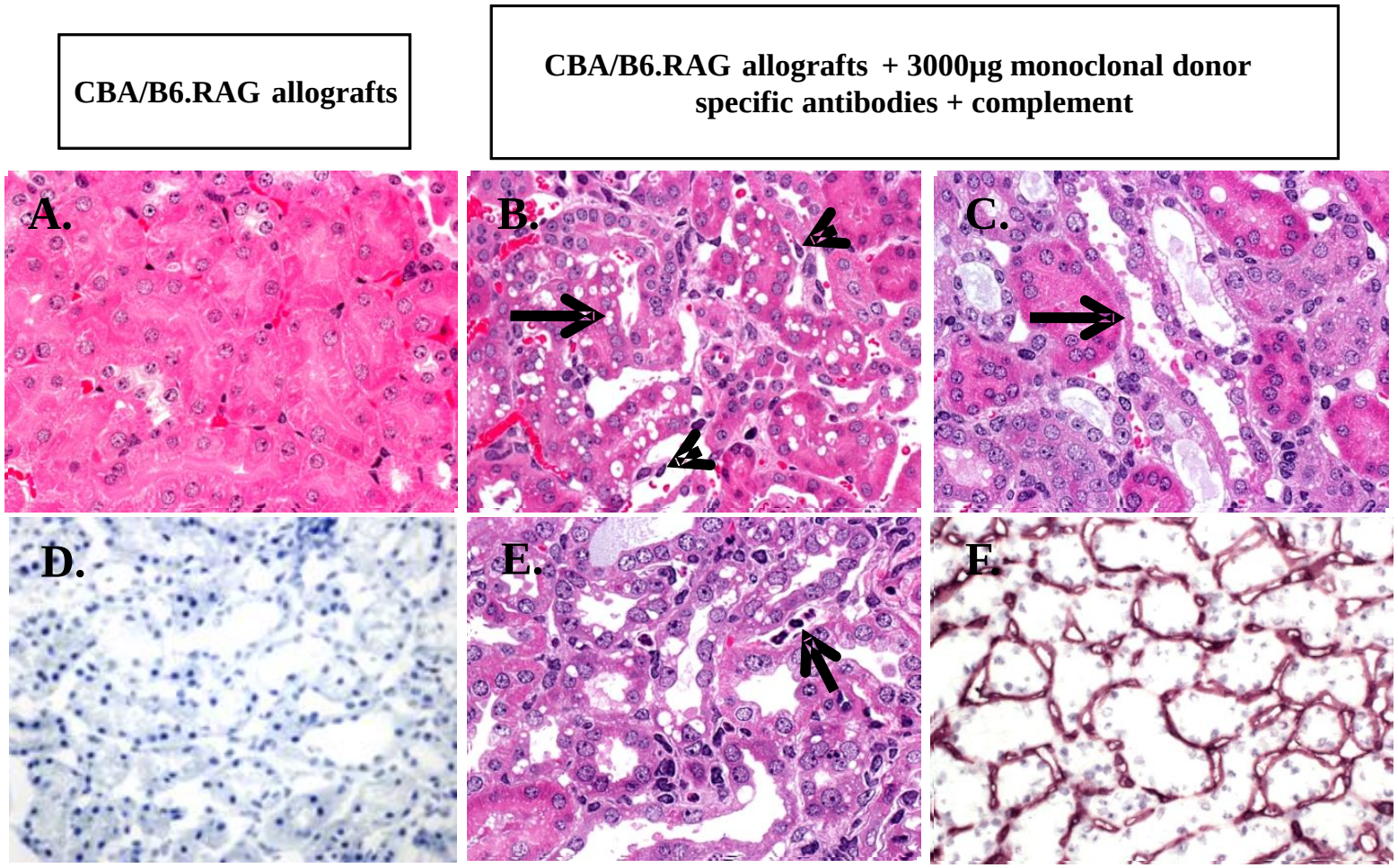

Figure 3.11 – Histopathology of allograft controls and DSA treated allografts.

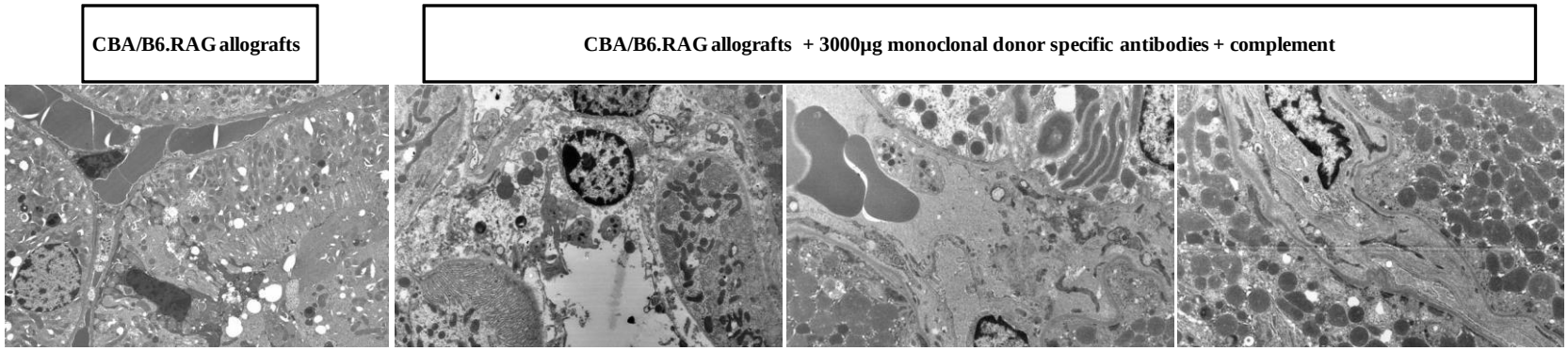

Figure 3.12 – Electron microscopy of DSA treated life-supporting allograft recipients and non-immune IgG treated life-supporting allograft recipients. Electron microscopy shows presence of peritubular capillary injury with disruption and lysis of endothelial cells, adhesion of platelet aggregates onto disrupted microvascular endothelial surface, fibrin-like deposition, and capillary basement membrane multilayering in allograft kidneys after adoptive transfer of DSA and complement. No such changes are observed in control allografts. (4 kidneys examined by EM).

Monoclonal DSA treated conditions show increased levels of serum creatinine

From mice receiving life-supporting transplants with I.P. injections of DSA or non-immune IgG, 50µL of whole blood was collected daily from one day prior to transplantation to the day of harvest. Serum was extracted from whole blood, and serum creatinine levels were measured to assess kidney function. Serum creatinine measurements from one day prior to transplantation served as baseline pre-treatment controls.

Serum creatinine in both DSA treated mice and sham treatment controls are comparable from day -1 to day 11 post-transplant, and although injections of DSA are administered beginning day 5 post-transplant, the effects of circulating DSA are not reflected in kidney function until day 11 post-transplant onwards. Although serum creatinine becomes significantly different between DSA treated and sham treatment control mice by day 11 post-transplant, graft dysfunction in DSA treated mice does not occur until roughly day 20 post-transplant (Figure 3.13).

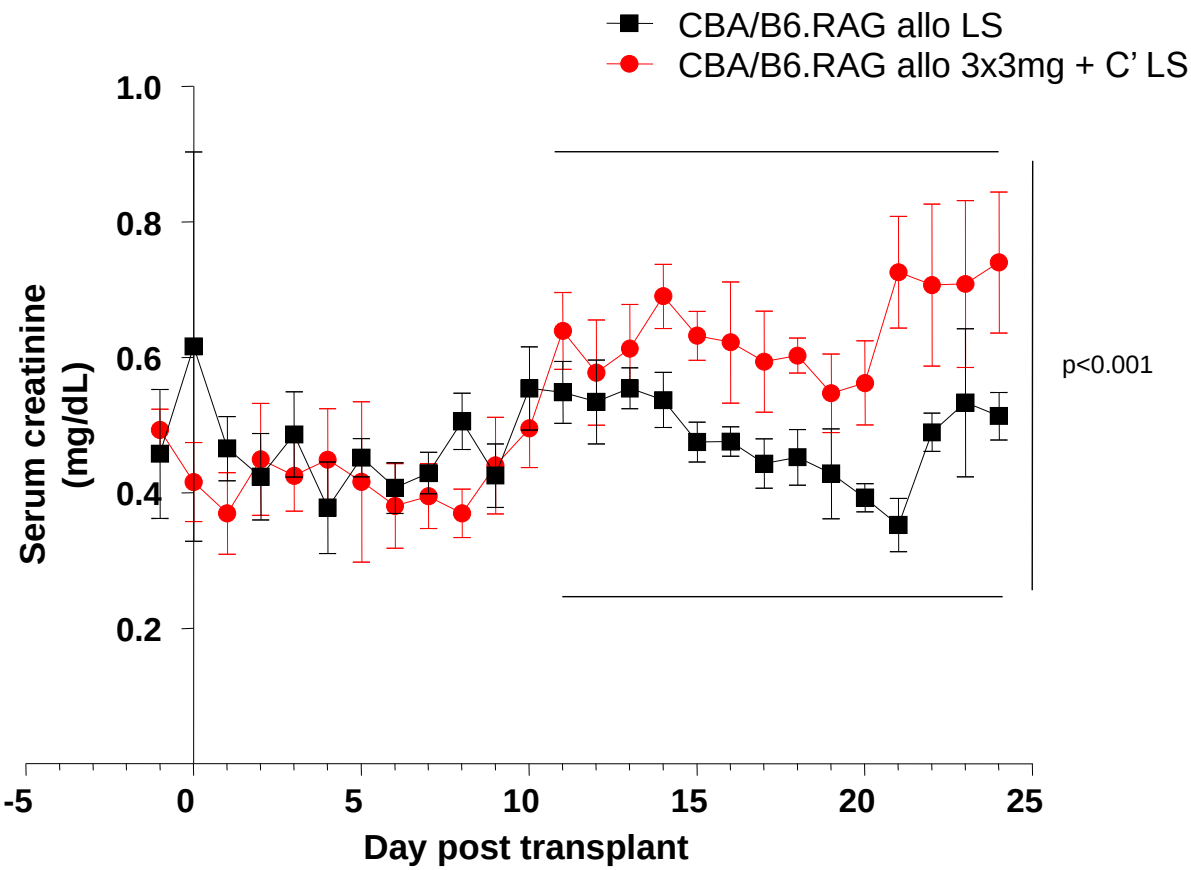

Figure 3.13 – Serum creatinine measurements of DSA treated life-supporting allograft recipients and IgG treated life-supporting allograft recipients. Significantly ($p<0.001$) higher serum creatinine levels were detected in DSA treated allograft recipients than non-immune IgG treated controls. Injections of either DSA or IgG control treatments were administered from day 5 post-transplant until graft dysfunction. Significance in difference calculated between all creatinine values from day 16 to 25 between DSA treated and non-immune IgG treated allograft recipients. Values are represented as mean ± SD. Significance tested by Mann-Whitney U-test.

Increased endothelial activation in DSA treated allografts

In human patients, endothelial activation and gene expression changes associated with graft injury arises prior to deterioration in graft function or the manifestation of histopathological signs of graft injury. Here, we examined the extent of gene expression changes in animals treated with DSA in which allograft tissue already shows signs of injury and dysfunction.

By ANOVA analysis on NanoString gene expression data, there was significant differential expression of endothelial adhesion and activation markers Pecam 1 and Cd34 between allograft tissues treated with monoclonal DSA, control allografts, and normal kidney controls, with increased expression of both Pecam1 and Cd34 in DSA treated allograft recipients than in allograft controls or normal kidney controls (Figure 3.14).

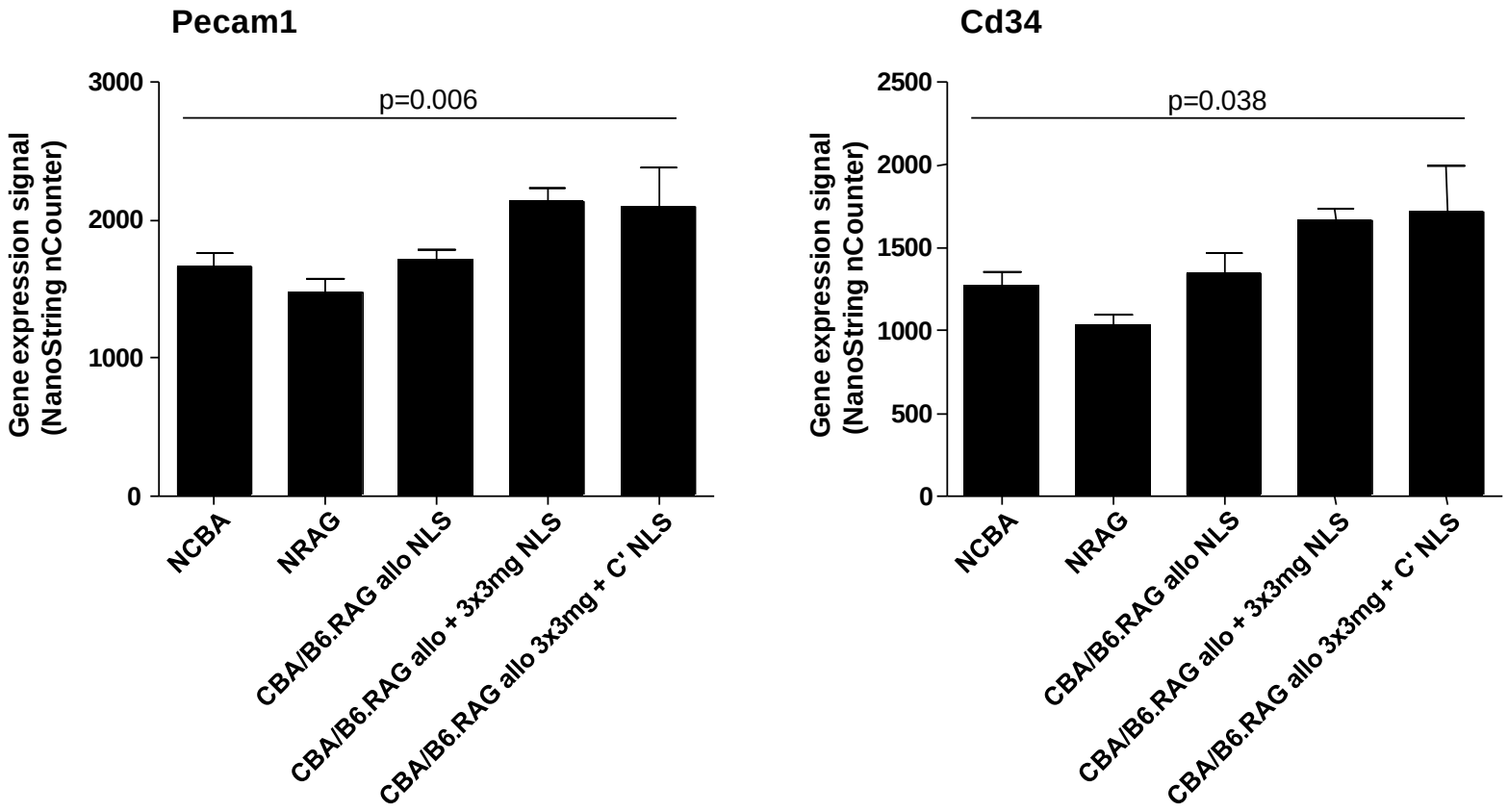

Figure 3.14 – Gene expression of endothelial adhesion molecules Pecam1 and Cd34 between DSA treated allografts, allograft controls, and normal kidney controls. DSA treated allografts show increased expression of both Pecam1 and Cd34 endothelial adhesion molecules compared to allograft controls and normal kidney controls. Differential expression of Pecam1 and Cd34 between all conditions reached statistical significance (p=0.006 and p=0.038, respectively). Values represented as mean ± SEM. Differential expression tested by Kruskal-Wallis one-way analysis of variance.

Polyclonal donor specific antibodies from immunized mice show reactivity against donor splenocytes

Since the adoptive transfer of 3mg of monoclonal DSA for 3 days induced endothelial and tubular injury, but failed to elicit inflammation or leukocyte recruitment into transplanted graft tissue, polyclonal DSA was examined to determine the effect of increased antigen recognition capabilities of DSA and resulting pathology generated.

Polyclonal IgG DSA was generated by immunizing wildtype C57BL/6 mice with H-2^k expressing B and T cell lymphoma cell lines twice weekly with adjuvant. By day 29 of immunization, serum from immunized mice show significantly increased reactivity to donor splenocytes than serum from naïve C57BL/6 mice (Figure 3.15). We purified IgG DSA from serum of sensitized mice after day 60 post exposure to allogeneic cells for injection into allograft recipients.

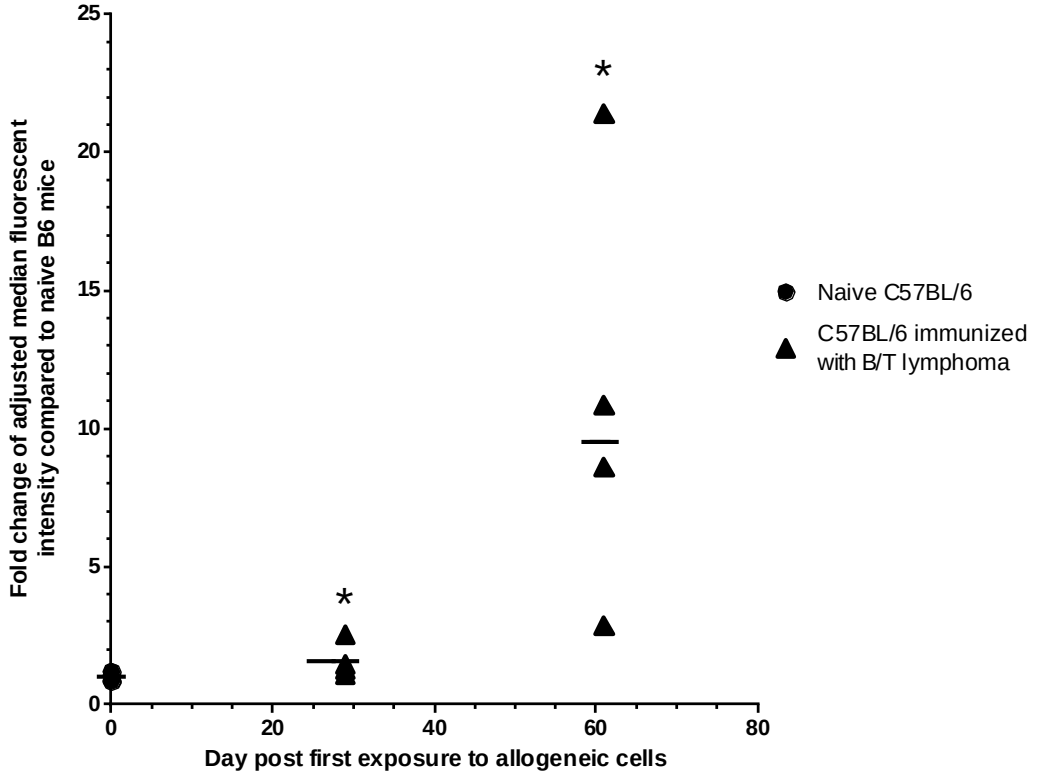

Figure 3.15 – C57BL/6 mice immunized with B / T lymphoma generate polyclonal DSA antibodies reactive against donor splenocytes. C57BL/6 mice were injected via I.P. with B and T lymphoma cell lines expressing donor H-2^k antigens. By day 29 post injection with lymphoma cell lines, MFI values, denoting donor reactivity, is significantly increased compared to naïve C57BL/6 mice that have not been exposed to allogeneic lymphoma cell lines (* denote $p<0.05$ when comparing mean median fluorescent intensity of donor reactivity between immunized C57BL/6 mice and naïve C57BL/6 mice)

Allograft between wild-type CBA/J donor and C57BL/6 recipient mice treated with DSA do not show immediate rejection

In order to determine if the lack of pathology in DSA treated allografts between CBA/J donors and B6.RAG recipients is due to the absence of T cells in RAG knoc*k*out C57BL/6 mouse allograft recipients, kidney allografts were performed between wild-type CBA/J donor mice and wild-type C57BL/6 recipient mice.

Experiments were designed to examine allografts from days 1 to 3 post-transplant in transplants between wildtype animals in order to avoid TCMR phenotypes, since histopathological signs of TCMR have been previously shown to manifest around day 5 post-transplant, beginning with interstitial inflammation by day 5 post-transplant and development of tubulitis from day 7 post-transplant. (27). Histopathological lesions in transplants in DSA treated wildtype recipient and those in kidney allografts in DSA treated B6.RAG recipient show comparable histopathological lesions, suggesting that the presence of T cells in allograft recipients do not increase the severity of rejection or the amount of histological lesions of ABMR.

Table 3.7 – Histopathology assessment shows no significant differences in early allografts transplanted into B6.RAG1 knockout versus wild-type C57BL/6 mice

Histology Scores	CBA/B6.RAG allo + 3x3mg + C' NLS		CBA/B6 allo + 1x3mg + C' WT NLS	
	Allo	Native	Allo	Native
C4d staining (score)	3.0 ± 0.0	NA	NA	NA
Capillary endothelial swelling (score)	1.0 ± 0.0	0.0 ± 0.0	0.5 ± 0.7	0.0 ± 0.0
Capillary dilation (score)	2.3 ± 0.7	0.5 ± 0.7	2.0 ± 0.0	0.0 ± 0.0
% Capillaritis	1.1 ± 2.2	0.0 ± 0.0	1.5 ± 0.7	0.0 ± 0.0
Glomerulitis (score)	0.0 ± 0.0	0.0 ± 0.0	0.0 ± 0.0	0.0 ± 0.0
Peritubular capillaritis (score)	0.0 ± 0.0	0.0 ± 0.0	0.0 ± 0.0	0.0 ± 0.0
Tubulitis (score)	0.1 ± 0.3	0.0 ± 0.0	0.0 ± 0.0	0.0 ± 0.0
Tubular atrophy (score)	0.0 ± 0.0	0.0 ± 0.0	0.0 ± 0.0	0.0 ± 0.0
% Tubular cytoplasmic vacuolation	42.7 ± 27.2	1.2 ± 2.9	12.5 ± 3.5	0.0 ± 0.0
% Necrotic tubules	0.3 ± 0.7	0.0 ± 0.0	0.0 ± 0.0	0.0 ± 0.0
% Tubular epithelial flattening	29.0 ± 15.1	0.5 ± 1.3	10 ± 7.1	0.0 ± 0.0
Transplant glomerulopathy (score)	0.0 ± 0.0	0.0 ± 0.0	0.0 ± 0.0	0.0 ± 0.0
Interstitial inflammation (score)	0.0 ± 0.0	0.0 ± 0.0	0.0 ± 0.0	0.0 ± 0.0
Interstitial fibrosis (score)	0.0 ± 0.0	0.0 ± 0.0	0.0 ± 0.0	0.0 ± 0.0
Intimal arteritis (score)	0.0 ± 0.0	0.0 ± 0.0	0.0 ± 0.0	0.0 ± 0.0
Arterial fibrous intimal thickening (score)	0.0 ± 0.0	0.0 ± 0.0	0.0 ± 0.0	0.0 ± 0.0
Arteriolar hyalinosis (score)	0.0 ± 0.0	0.0 ± 0.0	0.0 ± 0.0	0.0 ± 0.0
% Global glomerular sclerosis	0.0 ± 0.0	0.0 ± 0.0	0.0 ± 0.0	0.0 ± 0.0

Polyclonal donor specific antibodies induce graft dysfunction

Preliminary data shows that when examining graft function by measure of serum creatinine, treatment with low and high dose polyclonal DSA show elevated serum creatinine levels compared to pretreatment and control animals (Figure 3.16). The timeframe in which graft dysfunction was achieved between low and high dose polyclonal DSA treatment was similar, with high dose polyclonal DSA treatment eliciting graft dysfunction by day 12 post-transplant, whereas low dose polyclonal DSA treatment achieved graft dysfunction by day 16 post-transplant. Each condition is represented by n=1 animal, with error bars representing replicate serum creatinine readings each day post-transplant.

When compared to monoclonal DSA treatments, which required roughly 20 days post-transplant before graft dysfunction was achieved, treatments with polyclonal DSA show greater potency in generating graft dysfunction in transplanted kidney tissues.

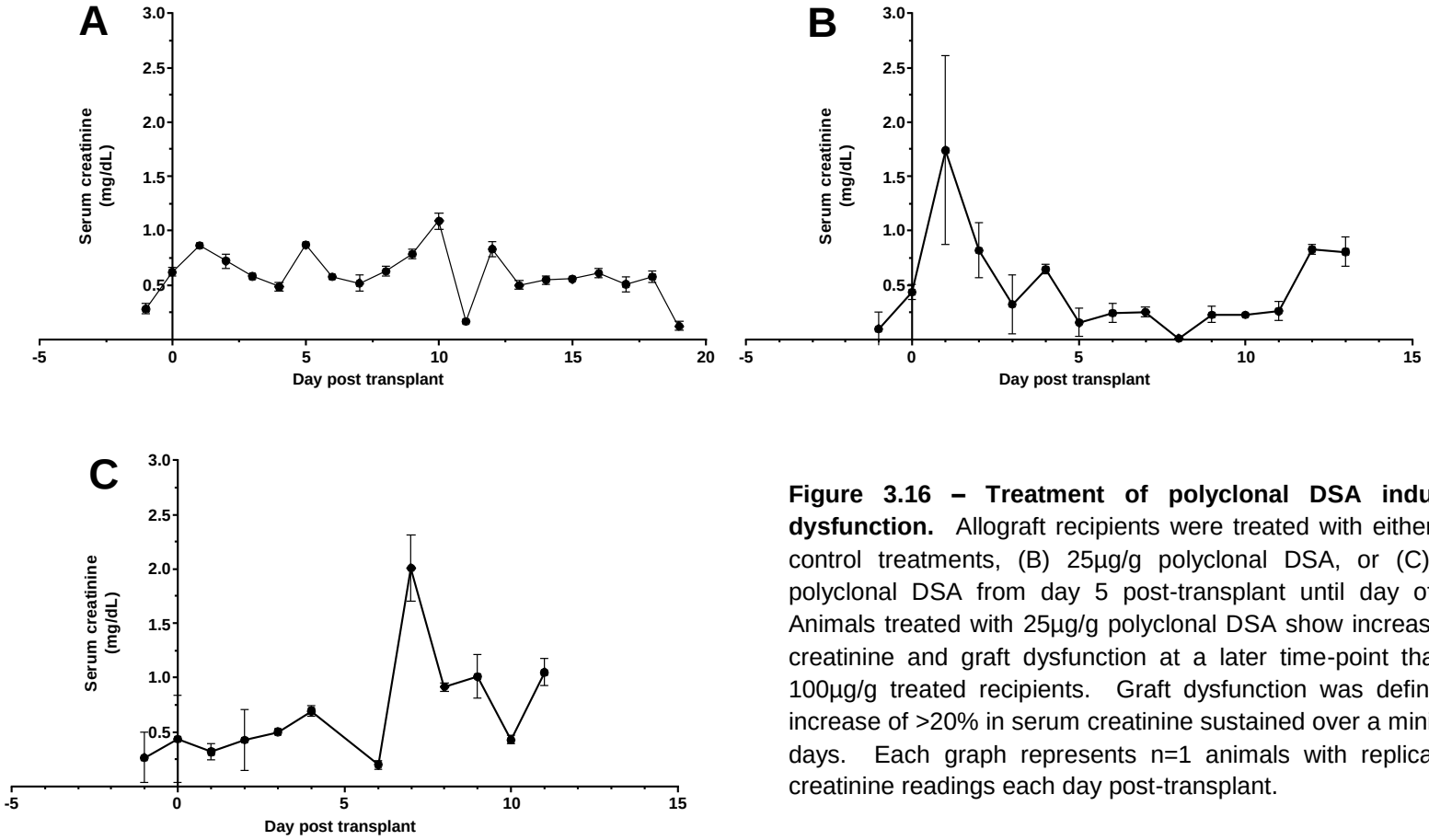

Figure 3.16 – Treatment of polyclonal DSA induce graft dysfunction. Allograft recipients were treated with either (A) PBS control treatments, (B) 25µg/g polyclonal DSA, or (C) 100µg/g polyclonal DSA from day 5 post-transplant until day of harvest. Animals treated with 25µg/g polyclonal DSA show increased serum creatinine and graft dysfunction at a later time-point than that of 100µg/g treated recipients. Graft dysfunction was defined as an increase of >20% in serum creatinine sustained over a minimum of 2 days. Each graph represents n=1 animals with replicate serum creatinine readings each day post-transplant.

Polyclonal donor specific antibodies promote leukocyte recruitment to allograft tissues

In addition to being more potent in generating allograft dysfunction, polyclonal DSA treatment also promoted increased recruitment of leukocytes into allograft tissues. Unlike control tissues and allografts treated with monoclonal DSA which do not show inflammation or any significant amount of leukocytes exiting circulation into graft tissue, allografts treated with polyclonal DSA show greater leukocyte staining in peritubular capillaries and interstitial spaces (Figure 3.17b). Furthermore, in addition to the recruitment of leukocytes to allograft tissue, treatment with polyclonal DSA over 14 days post-transplant also induced tubular basement membrane multilayering and glomerular double contours, indicative of the presence of chronic ABMR in these animals (Figure 3.17c). The results from polyclonal antibody treated transplant recipients are preliminary in nature, as mice demonstrating acute or chronic ABMR are composed of experimental group sizes of n=1 in each group. In this way, further experimentation to increase sample sizes is required prior to statistical analyses of these findings.

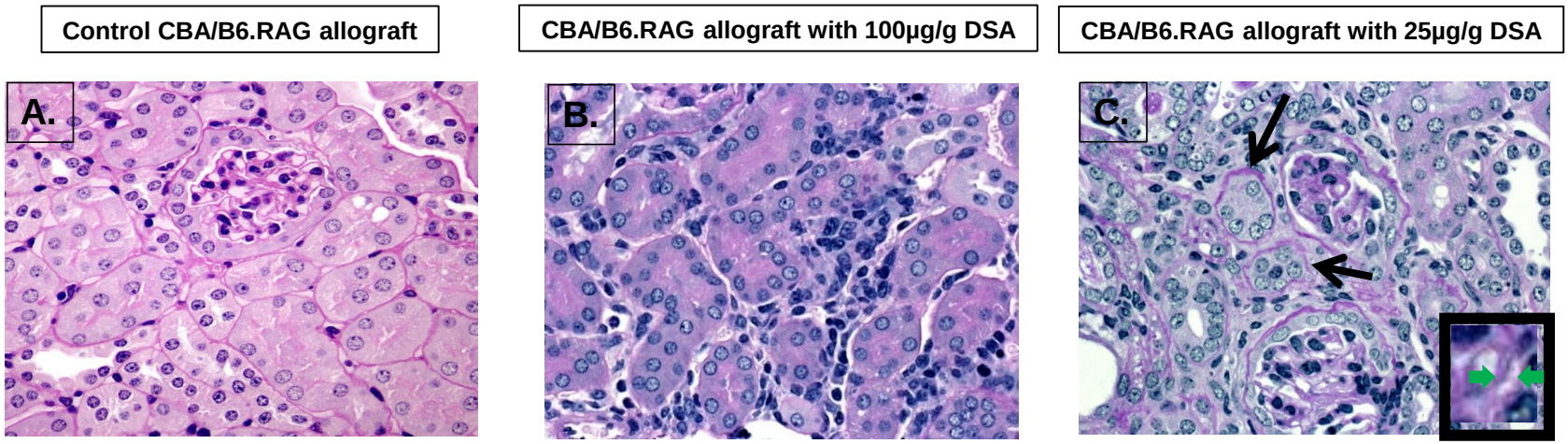

Figure 3.17 – Acute ABMR phenotypes shown in allografts treated with polyclonal DSA. (A) Control allografts treated with non-immune IgG do not show any histopathology in transplanted allograft kidney. (B) Allografts treated with 100µg/g polyclonal DSA induces the recruitment of leukocytes into the interstitial space in the allograft kidney. Recruitment of leukocytes is more intensive, mimicking acute ABMR, better than allografts treated with 25µg/g polyclonal DSA. (C) Allografts treated with 25µg/g polyclonal DSA show phenotypes of chronic ABMR, including tubular atrophy (black arrows) and glomerular basement membrane double contours (green arrows).

3.3 – Natural Killer cells cause apoptotic cell death and micro-inflammation in early mouse kidney allografts

3.3.1 – Overview

When examining our established mouse model of ABMR, we noticed a lack of inflammation and leukocyte recruitment in allograft kidneys treated with DSA, despite the presence of full complement activation to terminal MAC formation and the presence of pro-inflammatory molecules C3a and C5a. Furthermore, we noticed slight injury in control allograft kidneys treated with non-immune IgG in the form of increased serum creatinine at later time points (D20 post-transplant and later). Although observable histopathological injury was absent, we hypothesized that NK cells have a role in inducing the increased serum creatinine.

Rejection of kidney allografts in human patients is classified as either ABMR or TCMR, depending on cause of allograft injury and pathological features seen in the rejecting tissue (87). Current immunosuppression regimens can target B and T lymphocytes via inhibition of biochemical pathways or antibodies against the lymphocytes themselves. However, these treatments do not target innate inflammatory cells such as NK cells. This is a problem as studies have shown the involvement of NK cells in allograft injury (50).

The pathway by which NK cells invoke cell injury is different than that of T cells or antibodies. Unlike B cells or T cells, NK cells utilize apoptosis in order to eliminate target cells. There are two major pathways by which NK cells induce apoptosis. Firstly, with the release of perforin and granzyme, NK cells can first form pores in a targeted cell with the perforin protein, then release proteases such as granzyme into the target cell. Granzymes act within a cell to elicit the induction of apoptosis and cell death. The

second major method by which NK cells activate apoptosis is through death receptors such as the Fas receptor / Fas ligand pair. Fas receptors are expressed on the membrane of cells, and when it is bound with its Fas ligand pair expressed on the NK cell, the Fas receptor initiates the caspase cascade to begin the stages of apoptosis within that cell (76).

NK cells utilize the expression of cell surface antigens on target cells to determine whether or not cytotoxic action is required. Certain cell surface antigens (such as altered MHC I molecules (107)), or the Fc portion of IgG binding onto its Fcg3 receptor, have an activating effect for NK cells to induce apoptosis and release of cytokines, while other surface molecules such as the expression of normal MHC I has an inhibitory effect to prevent NK cell induced apoptosis (107).

Similar to NK cells, other innate inflammatory cells such as macrophages and neutrophils also express activating and inhibitory Fc receptors. Here, we focus on FcγR binding Fc portions of IgG antibodies. With four different forms of the FcγR, binding of the Fc portion of IgG onto the Fc receptor would have different immunomodulatory effects, depending on the specific FcγR bound.

In the first portion of this chapter, we examine the effects of NK cells on the recognition and injury to allograft tissues by establishing a MHC I mismatched kidney transplant model in mice. We performed MHC mismatched kidney transplantation by implanting wild-type H-2k CBA donor kidneys into T-cell/B-cell-null B6.Rag1-/- H-2b recipients. We also studied CBA into CBA kidney isografts, Rag1-/- into Rag1-/- kidney isografts, and normal CBA or Rag1-/- kidneys as controls. Transplanted kidneys were harvested on day 7 post-transplant and analyzed by histopathology, immunohistochemistry, and Affymetrix gene expression microarrays. Apoptosis was visualized by cleaved caspase-3 immunohistochemistry. Intrarenal burden of NK cells and macrophages was quantified by immunostaining using Ly49G2 and CD68 antibodies, respectively. By histopathology, Rag1-/- allografts did not show rejection

detected by conventional stains and were not different from controls. However, by microarrays Rag1-/- allografts displayed significantly increased expression of interferon-gamma gene, interferon-gamma inducible genes, and NK receptor genes when compared to normal kidneys, CBA isografts, and Rag1-/- isografts. By immunostaining, Rag1-/- allograft tissues displayed significantly higher numbers of NK cell infiltrates in the interstitium and increased cleaved caspase-3 (CC3) positive apoptotic tubular epithelial cells and glomerular cells in comparison to controls, including Rag1-/- isografts. The amounts of intragraft macrophages were not different among Rag1-/- allografts, Rag1-/- isografts, and CBA isografts. Our results indicate that T- and B-cell deficient mouse kidney recipients display signs of kidney allograft injury associated with NK cell activation causing allograft parenchymal apoptotic cell death and intragraft production of interferon-gamma. Thus, findings in this model suggest that NK cells recognize missing self MHC in allograft tissues and are capable to induce early allograft injury.

In the second portion of this chapter, we examine the FcγR effects in modulating the inflammatory response in ABMR. Utilizing our previously established ABMR model, we compared the inflammatory state of allograft recipients treated with 3000μg DSA for three days compared to control allografts treated with non-immune IgG. Briefly, MHC mismatched kidney transplantation were performed by implanting wild-type H-2k CBA donor kidneys into T-cell/B-cell-null B6.Rag1-/- H-2b recipients. 3000μg DSA were injected on days 5, 6, and 7 post-transplant, with allograft harvest on day 7. Control allografts were treated with either dose-matched non-immune IgG or PBS on days 5, 6, and 7 post-transplant, with allograft harvest on day 7. As evidenced by the first portion of this chapter, allografts with no DSA treatment experience NK cell recruitment, exposure to interferon gamma release, and apoptotic cell injury. We examined our ABMR model and compared the extent to which DSA binding onto allograft tissues could modulate inflammatory responses via interactions with FcγR. By gene expression analysis, our data shows significantly increased expression of inhibitory receptor FcγR2b in DSA treated allografts compared to control allografts. Furthermore, there is a significantly

decreased expression of inflammatory cytokines in DSA treated compared to control allografts. Our results suggest that the binding of DSA onto allograft tissues may induce a self-protective anti-inflammatory response, potentially via the increased expression of inhibitory FcγR2b.

Table 3.8 – Transplant and condition abbreviations applicable to section 3.3

Donor	Recipient	Condition	Treatment	Abbrev.	Day post tx	N of mice
CBA ($H\text{-}2^{k}$)	-	Normal CBA kidney	-	NCBA	-	29
CBA ($H\text{-}2^{k}$)	CBA ($H\text{-}2^{k}$)	Non-life supporting CBA/CBA isograft	-	CBA iso NLS	D7	9
B6.RAG1$^{-/-}$ ($H\text{-}2^{b}$)	-	Normal B6.RAG1$^{-/-}$ kidney	-	NRAG	-	5
B6.RAG1$^{-/-}$ ($H\text{-}2^{b}$)	B6.RAG1KO ($H\text{-}2^{b}$)	Non-life supporting RAG/RAG isograft	-	B6.RAG iso NLS	D7	4
CBA ($H\text{-}2^{k}$)	B6.RAG1KO ($H\text{-}2^{b}$)	Non-life supporting CBA/RAG allograft	-	CBA/ B6.RAG allo NLS	D7	12
CBA ($H\text{-}2^{k}$)	B6.RAG1KO ($H\text{-}2^{b}$)	Non-life supporting CBA/RAG allograft	0.2mL PBS / day, 3 day treatment	CBA/B6.RAG allo + PBS NLS	D7	6
CBA ($H\text{-}2^{k}$)	B6.RAG1KO ($H\text{-}2^{b}$)	Non-life supporting CBA/RAG allograft	0.25mL rabbit complement / day, 3 day treatment	CBA/B6.RAG allo + C' NLS	D7	5
CBA ($H\text{-}2^{k}$)	B6.RAG1KO ($H\text{-}2^{b}$)	Non-life supporting CBA/RAG allograft	3mg DSA / day, with or without complement, 3 day treatment	CBA/B6.RAG allo + 3x3mg NLS	D7	15
CBA ($H\text{-}2^{k}$)	B6.RAG1KO ($H\text{-}2^{b}$)	Life-supporting CBA/RAG allograft	3mg non-immune IgG / day	CBA/B6.RAG allo LS	varies (D25-40)	5
CBA ($H\text{-}2^{k}$)	B6.RAG1KO ($H\text{-}2^{b}$)	Life-supporting CBA/RAG allograft	3mg DSA / day	CBA/B6.RAG allo + 3x3mg LS	varies (D25-40)	5

3.3.2 – Results

NK cells recruited to allograft tissue and induce apoptosis

Allograft, isograft, and normal kidneys were harvested and stained with conventional histopathological stains, NK cell stains, and stains revealing apoptosis in order to determine the extent to which NK cells are activated in allograft transplants in the absence of lymphocytes.

By normal hematoxylin and eosin stain, there is no noticeable pathology or any signs of large-scale injury in any of the transplant or control conditions. When tissues were stained for NK cells via anti-Ly49G2 antibodies, no significant numbers of Ly49G2+ cells were seen in either B6.RAG or CBA isografts, nor were there any Ly49G2+ cells seen in normal kidney controls. However, there were significantly higher numbers of Ly49G2+ cells in allograft tissues, recruited to intragraft parenchymal space (Figure 3.18). In addition to Ly49G2 stains, we examined tissues for evidence of apoptosis by staining for cleaved caspase 3 (CC3). Similar to Ly49G2 stains, we found very little signs of CC3+ cells in isografts or normal kidney controls, but found significantly higher number of CC3+ cells in allografts (Figure 3.19).

Finally, we examined kidney tissues for signs of macrophage recruitment, as an indicator of tissue injury. Stains for Cd68 shows higher amounts of Cd68+ cells in both isograft transplants and allograft transplants compared to normal kidney controls (Figure 3.18 and Figure 3.19). Allografts showed the same amount of Cd68+ cells as CBA and B6.RAG isografts, most likely representing non-specific transplantation related injury.

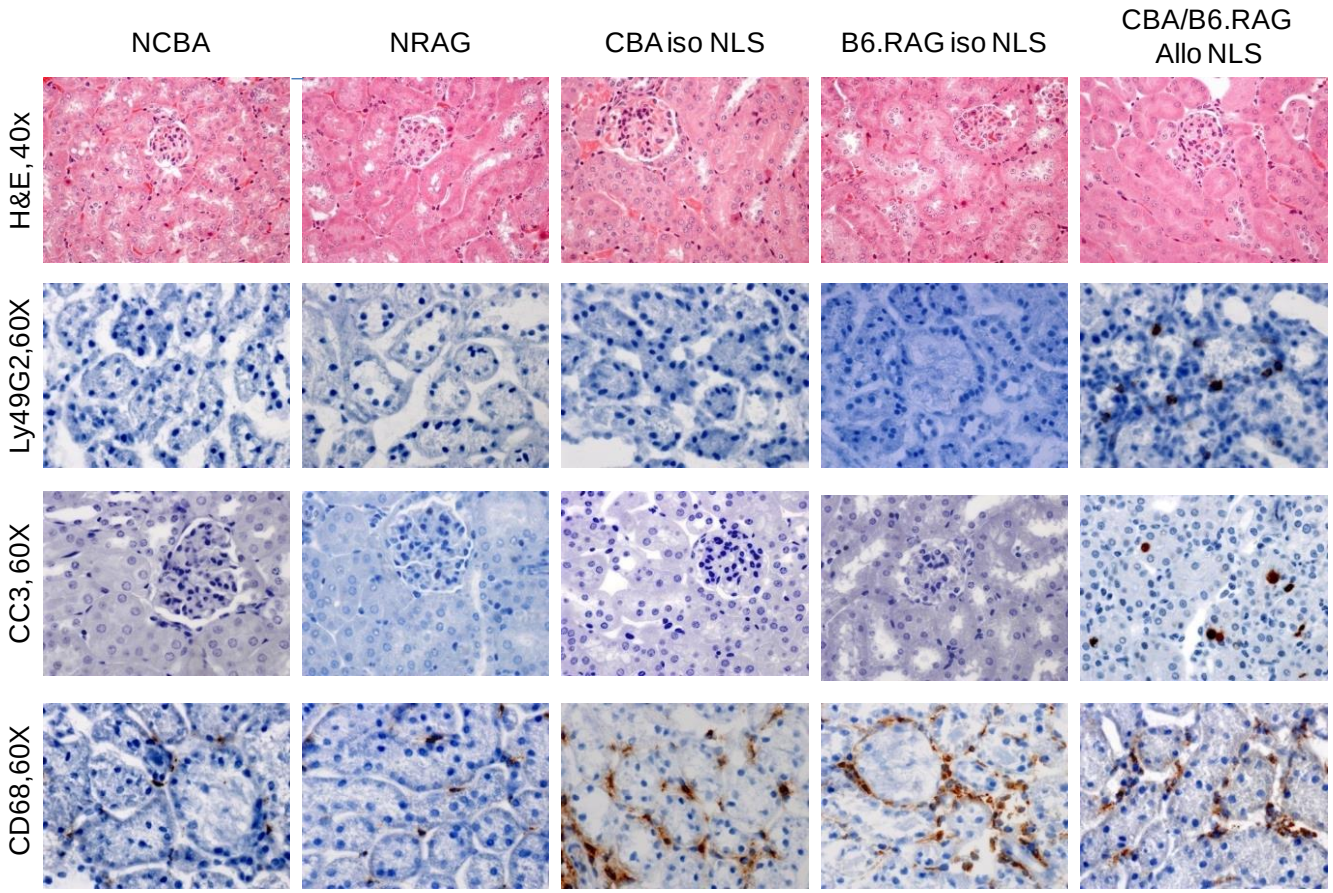

Figure 3.18 – Recruitment of Ly49G2+ cells in allograft tissues do not cause observable injury by H&E. CBA/B6.RAG allografts showed the presence of Ly49G2+ cells, CC3+ cells and Cd68+ cells, while isografts show only Cd68+ cells in graft tissue. Normal CBA and normal B6.RAG kidneys are negative for injury, Ly49G2, CC3, and Cd68 stained cells.

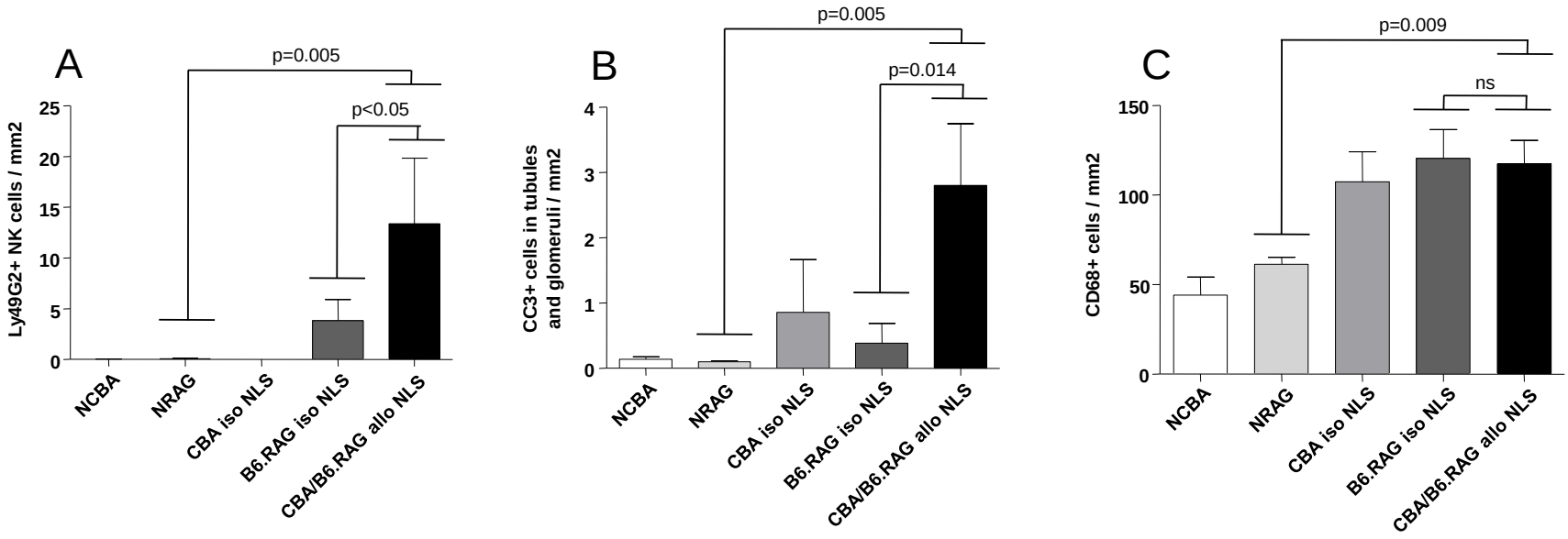

Figure 3.19 – Significantly increased Ly49G2+ and CC3+ cells in allografts compared to allograft controls and normal kidney controls. By quantifying stained cells in kidney sections, allograft tissues showed significantly higher ($p<0.05$) numbers of both Ly49G2+ and CC3+ cells compared to allograft controls or normal kidney controls. No significance (denoted by ns, not significant, $p>0.05$) is observed in Cd68+ staining between allograft and isograft kidneys, but there is significantly higher number of Cd68+ cells compared to normal kidney controls. Significance was determined by Mann-Whitney U-test. Values are represented as mean ± SEM.

Allograft tissues show increased expression of interferon gamma inducible genes

Since NK cells can carry out effector functions through the release of interferon gamma, we examined, by microarray, the extent to which interferon gamma is released in the Ly49G2+, CC3+ tissues by measuring expression of a previously established list (31) of interferon gamma-inducible genes.

By Kruskal-Wallis analysis comparing normal CBA kidney controls, CBA isografts, B6.RAG isografts, and CBA / RAG allografts, we found highly significant ($p=0.008$) differences in expression of interferon gamma-inducible genes between groups. Furthermore, by Mann-Whitney U test comparing expression of gamma interferon-inducible genes between CBA/B6.RAG allograft tissues and B6.RAG isografts, we found significantly ($p=0.021$) different expression between these two groups. Allograft tissues show a 7 fold increase in expression of interferon gamma-inducible genes compared to normal CBA kidneys, roughly 2.5 fold increased expression compared to CBA isografts, and 3.5 fold increased expression compared to B6.RAG isografts (Figure 3.20).

It is interesting to note the difference in expression of interferon gamma-inducible genes between CBA isografts and B6.RAG isografts. We originally expected very similar expression profiles between CBA and B6.RAG isografts.

Gene expression changes of macrophage associated transcripts confirm immunohistochemistry findings

By immunohistochemistry, we stained for Cd68 in kidney tissues, and found increased Cd68+ cells in tissues that have undergone transplant surgery compared to normal kidney controls. We examined gene expression of previously established macrophage associated transcripts gene list (30) to determine whether there are gene expression differences between CBA isografts, B6.RAG isografts, and CBA / RAG allografts which all show Cd68+ staining.

By Kruskal-Wallis analysis, we find significant (p=0.021) changes in expression of macrophage associated transcripts between normal CBA kidneys, CBA isografts, B6.RAG isografts, and CBA / B6.RAG allografts (Figure 3.20). However, when we compare expression differences between allograft and isograft tissues, we do not find statistical significance in expression differences when comparing CBA/B6.RAG allografts to either B6.RAG or CBA isografts (p= 0.2, 1.00, respectively).

NK cell receptor gene expression differs between transplant tissues

With increased recruited NK cell presence in allograft tissues visualized by significant increases in Ly49G2+ cells, we examined the gene expression of activating and inhibitory NK cell receptors to determine whether there is a shift in receptor expression to favor either activating or inhibitory receptors when NK cells are recruited into allograft tissues. Gene lists were constructed by literature review.

When comparing gene expression between all groups by Kruskal-Wallis, we found significant differences in gene expression of both activating NK cell receptors and inhibitory NK cell receptors (p=0.044 and p=0.013, respectively). However, increased expression of both activating and inhibitory NK cell receptors in allograft tissues are minimal in that Mann-Whitney comparisons between CBA/B6.RAG allografts to either CBA or B6.RAG isografts yield statistically insignificant values (Figure 3.20)

No significant molecular changes associated with injury

The measurement of molecular changes in injury-related genes has been previously shown to be a sensitive method in detecting the initial onset of allograft injury. Changes in gene expression can reveal itself prior to the manifestation of other pathology phenotypes (69). Here we examined the extent to which injury is present as a result of NK cell recruitment and activation of apoptosis.

We found no significant differences in gene expression of injury and repair associated transcripts, endothelium associated transcripts, or renal transcripts. Although

there is a trend towards increased expression of injury and repair associated transcripts in isografts and allograft kidneys compared to normal kidney controls, the changes did not achieve statistical significance.

Gene sets representing renal solute carriers show a decreasing trend in expression between normal kidney controls and allograft tissues. Although no direct significance between allograft tissues and isograft tissues is established, we attribute the trend of decreasing expression to micro-inflammation, apoptotic injury, and interferon-gamma effects in allograft kidneys.

It is also interesting to note an increased expression of cytotoxic T cell associated transcripts in allograft tissues compared to normal CBA kidneys and isograft tissues. Although statistical significance is not achieved, we do not expect any expression of lymphocyte associated transcripts in the B6.RAG recipient, as it has no mature T or B cells present due to the knockout in the Rag gene. The presence of the cytotoxic T cell associated transcripts in $RAG^{-/-}$ mice would most likely be due to the nature of the transcript list. Expression of cytotoxic T cell associated transcripts are not specific for T lymphocytes, as other cell types (such as NK cells) share overlapping molecular signatures represented here in the cytotoxic T cell associated transcript list.

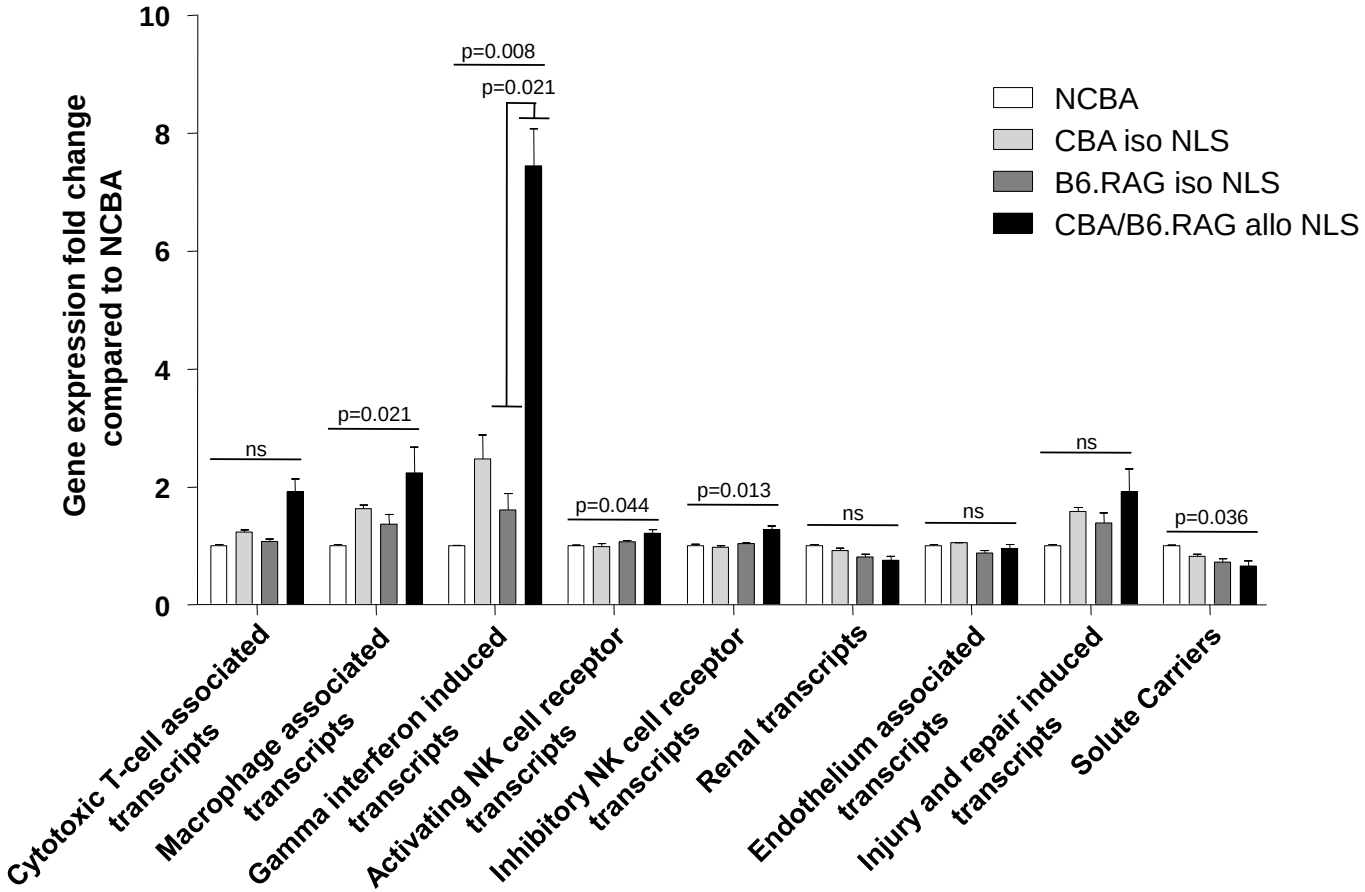

Figure 3.20 – Significantly increased interferon gamma inducible genes in allograft kidneys. By microarray, only expression differences in interferon gamma inducible genes reached significance by Mann-Whitney U-test (p=0.008) between allograft and isograft tissues. Kruskal-Wallis one way analysis of variance was performed as well, with several gene sets showing significantly differential expression.

NK cells favor Fas pathway to induce apoptosis in allograft tissues

After finding the presence of apoptotic cells in allograft tissues that are missing in isograft controls or normal kidney controls, we wished to determine which pathway NK cells utilized in order to bring about apoptosis. We examined gene expression associated with two major NK cell pathways: the perforin / granzyme pathway, and the Fas / Fas ligand pathway.

By microarray gene expression analysis, we found no significant differences or increases in expression in perforin (Figure 3.21) or granzyme B (not shown) in allograft tissues compared to isografts or normal kidneys. However, gene expression of Fas was significantly upregulated in CBA / B6.RAG allografts compared to B6.RAG isografts. Allografts also show an increased expression of Fas ligand, but it does not reach statistical significance.

As a means to confirm that the increase in expression of interferon gamma-inducible genes are indeed due to the presence of interferon gamma, we examined the gene expression of interferon gamma itself. In agreement with the increased expression of interferon gamma inducible genes, we found a significantly increase in gene expression of interferon gamma in allograft tissues compared to B6.RAG isografts.

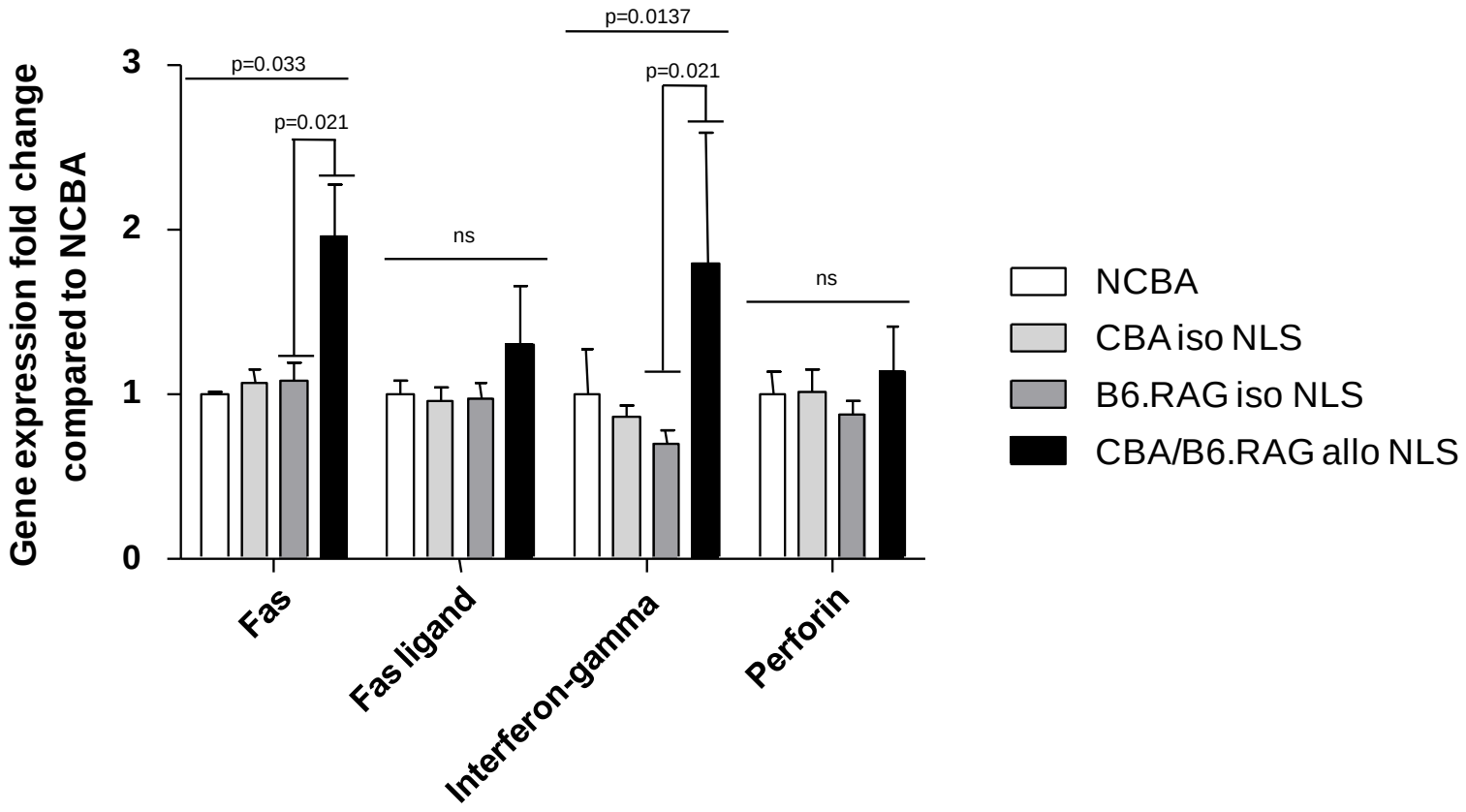

Figure 3.21 – Allograft tissues show significantly increased Fas, but not perforin expression. Allograft tissues show significant Fas (p=0.021) and Interferon-gamma (p=0.021) expression compared to isograft kidneys. Increased expression of Fas ligand in allograft tissues does not reach statistical significance (ns, not significant, p>0.05). Perforin expression does not show a meaningful trend. Each gene was analyzed by Mann-Whitney U-test and Kruskal-Wallis one way analysis of variance

Gene expression favors interferon gamma inducible genes

We examined broad-scale gene expression in allograft tissues in order to glean information as to biological pathways which could be involved in NK cell recruitment and activation of apoptosis in allograft tissues.

The top 5 most highly expressed genes in allografts compared to isografts show a higher expression of 15 to 30 fold increase compared to CBA or B6.RAG isografts. The expression of all 5 genes in allografts compared to isografts reached statistical significance. We found that the list of these genes confirm previous results in that expression heavily favors transcripts inducible by interferon gamma (Table 3.10).

Table 3.9 – Top 5 differentially expressed genes between allograft tissues compared to isograft tissues show propensity towards interferon gamma effects. Allografts show a 15-30 fold increase in expression of interferon-gamma inducible genes. Significance was measured by Mann-Whitney U-test.

Allograft: Isograft ratio	Corrected p value	Gene symbol	Description
30.10	0.0274	Ubd	Tags proteins for cellular processes / destruction
27.91	0.0434	Mpa2l (Gbp6)	Interferon gamma induced GTPase
23.52	0.0205	Gbp2	Interferon gamma induced GTPase
19.32	0.0334	Iigp1	Interferon gamma induced GTPase
15.27	0.0173	Cxcl10	Chemoattraction of monocytes/mac, NK, T cells

No significant changes in expression of activating Fc receptors FcγR1, FcγR3, FcγR4, but DSA induces increased expression of inhibitory Fc receptor FcγR2b in early time-points after transplantation

We examined the expression of Fcγ receptors in non-life supporting DSA-treated allograft tissues showing acute endothelial and tubular injury compared to control allografts with no distinguishable injury. Since DSA treated allograft recipients showed no noticeable inflammation despite endothelial and tubular injury, and the activation of the terminal MAC, we hypothesized that inhibitory Fc receptors may play a role in inhibiting inflammation.

By gene expression profiling, we found no significant differences in expression of activating Fcγ receptors between control allografts or allografts that was exposed to DSA treatment. However, expression of inhibitory Fc receptor FcγR2b was significantly increased in DSA treated allograft recipients compared to control allografts treated with PBS (Figure 3.22 and Table 3.11).

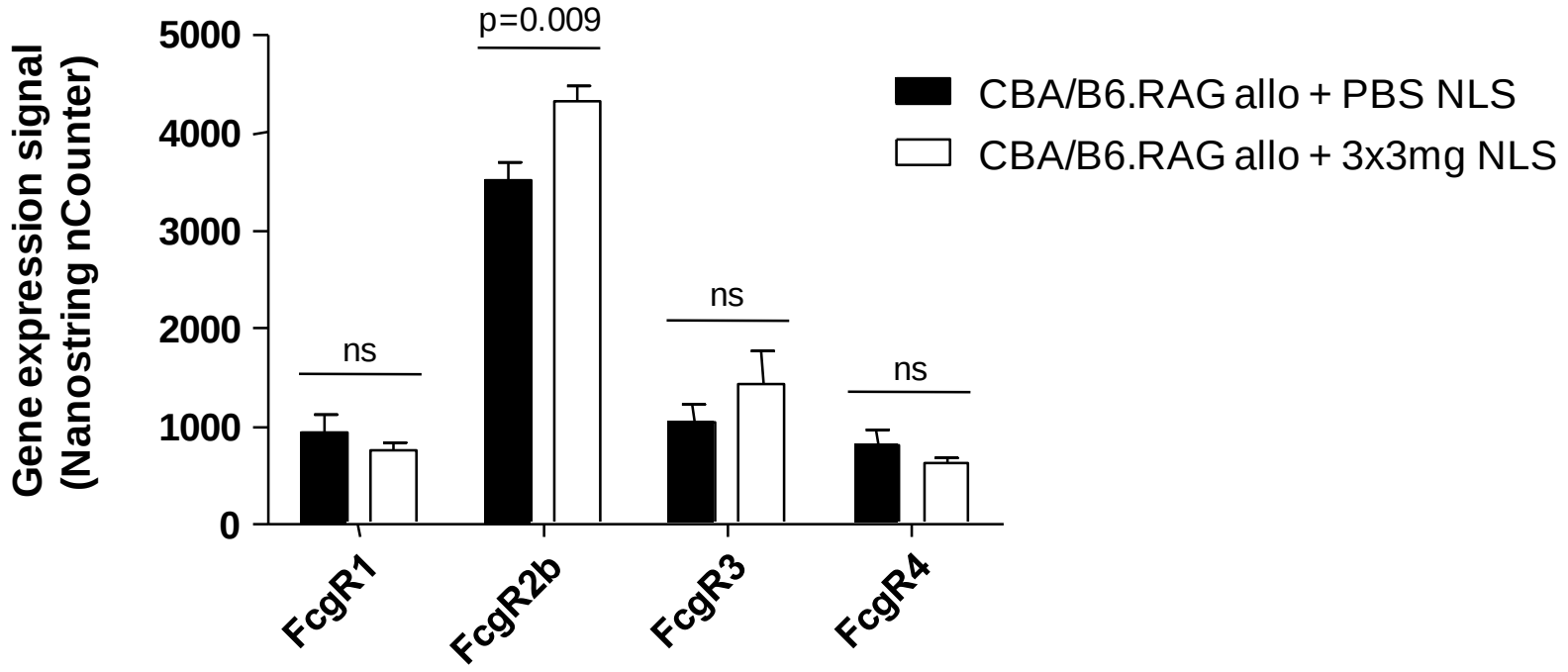

Figure 3.22 – Increased FcγR2b expression in DSA treated allografts. DSA treated allografts show significantly (p=0.009) increased expression of inhibitory receptor FcγR2b compared to PBS treated allograft controls. Expression of all other FcγR do not show significantly different expression (ns, not significant, p>0.05)

Expression of inflammatory cytokines decreases with treatment of DSA in early time-points after transplantation

With the increased expression of inhibitory FcγR2b in DSA treated non-life supporting allograft recipients, we further examined the expression profile of DSA treated allograft recipients in relation to inflammatory cytokines. Again, due to the lack of inflammation seen by histopathology in the DSA treated tissues, we hypothesized that DSA treated allografts express similar levels of inflammatory cytokines as control allograft tissues.

The data reveals that the expression of inflammatory cytokines such as the cxcl family, granzyme b / perforin, tumor necrosis factor related cytokines, and interferon gamma itself is significantly reduced in non-life supporting allografts treated with DSA in early time-points after transplantation (Table 3.11)

Table 3.10 – Increased expression of FcγR2b accompanied with decreased expression of inflammatory cytokines in 3x3mg DSA treated allografts early after transplantation. Allografts treated with 3mg DSA until D7 post-transplant show an anti-inflammatory response with increased inhibitory FcγR2b expression compared to PBS treated allograft controls. Genes were obtained by univariate analysis of expression values. FDR multiple test correction was applied for an additional, stricter filtered list (FDR<0.05, italicized)

Gene	Geometric mean of expression intensity				CBA/B6.RAG allo + PBS NLS vs. CBA/B6.RAG allo + 3x3mg NLS	
	NCBA	NRAG	CBA/B6.RAG allo + PBS NLS	CBA/B6.RAG allo + 3x3mg NLS	Adjusted p-value	FDR
Chemokine Ligand 10 (Cxcl10)	62	71	2822	557	0.00003	*0.001*
Granzyme B (Gzmb)	10	8	218	54	0.0002	*0.005*
Fas	130	101	232	144	0.0005	*0.008*
Chemokine ligand 11 (Cxcl11)	72	24	5065	1095	0.001	*0.016*
Tumor necrosis factor (ligand) superfamily, member 10 (Tnfsf10)	3594	1438	7096	2289	0.001	*0.016*
Lymphocyte protein tyrosine kinase (Lck)	48	28	350	133	0.002	*0.016*
Chemokine Ligand 9 (Cxcl9)	79	47	5927	1556	0.003	*0.026*
Interferon gamma (Ifng)	20	9	20	14	0.007	*0.042*
Caveolin 1 (Cav1)	989	763	836	1130	0.007	*0.042*
Fc-gamma receptor 2b (Fcgr2b)	3748	2242	3410	4269	0.009	*0.049*
Perforin 1 (Prf1)	8	10	63	34	0.012	0.056
Myeloperoxidase (Mpo)	6	5	28	17	0.013	0.056
Chemokine receptor 3 (Cxcr3)	53	41	151	94	0.023	0.090
T-box 21 (Tbx21)	8	4	22	14	0.039	0.143

Increased expression of FcγR2b is only an early time-point phenomenon

With an increased expression of inhibitory Fc receptor FcγR2b at day 7 post-transplant in DSA treated non-life supporting allografts, we explored whether this increased expression of inhibitory receptors is maintained into late timeframes after transplantation, represented by life-supporting transplants harvested between the days of approximately 25-40 post-transplant.

We found that the previously observed phenomenon showing significantly increased expression of FcγR2b is limited to early time points. The expression of FcγR2b at late time points in allograft recipients treated daily with 3mg DSA decreases to the point it has lower expression levels than non-immune IgG treated controls and normal CBA kidney controls (3310 vs. 3748 in NCBA and 3718 in non-immune treated recipients) (Table 3.12). As such, the increased expression of the same inhibitory receptor loses statistical significance when progressing from early post-transplant to later time points.

Decreased expression of inflammatory cytokines revealed in both early and late post-transplant

With the increased expression of FcγR2b waning with time in DSA treated allograft recipients, we examined whether the expression of inflammatory cytokines would increase in DSA treated life-supporting allograft recipients in late time points post-transplant as a result of reduced inhibitory receptors.

Surprisingly, despite the expression of inhibitory FcγR2b dropping to levels below baseline, we found that the decreased expression of pro-inflammatory cytokines in DSA treated allograft recipients (compared to non-immune IgG treated controls) seem to be maintained in late time-points post transplantation (Table 3.12). Although statistical significance is lost in some inflammation-related genes, especially after the more

stringent FDR multiple test correction, the overall trend of decreased expression of pro-inflammatory cytokines remains.

Table 3.11 – Anti-inflammatory effect remains in 3x3mg DSA treated life-supporting allografts despite lowered expression of FcγR2b. Allografts treated with 3mg DSA daily until graft dysfunction show decreased levels of FcγR2b expression compared to allograft controls or NCBA kidneys. However, gene expression of several pro-inflammatory cytokines are significantly decreased in life-supporting allograft recipients treated with DSA compared to non-immune IgG treated life-supporting allograft recipients. Genes were obtained by univariate analysis of expression values. FDR multiple test correction was applied for an additional, stricter filtered list (FDR<0.05, italicized)

	Geometric mean of expression intensity				CBA/B6.RAG allo + non-immune IgG LS vs. CBA/B6.RAG allo + 3x3mg + C' LS	
Gene	**NCBA**	**NRAG**	**CBA/B6.RAG allo LS**	**CBA/B6.RAG allo + 3x3mg LS**	**Adjusted p-value**	**FDR**
Fas ligand (Fasl)	37	35	60	32	0.001	*0.027*
Chemokine ligand 11 (Cxcl11)	72	24	804	140	0.001	*0.027*
Perforin 1 (Prf1)	8	10	33	13	0.001	*0.027*
Histocompatibility 2, K1 (H2-K1)	3091	5204	43863	10581	0.002	*0.035*
Chemokine Ligand 10 (Cxcl10)	62	71	704	164	0.005	*0.044*
Lymphocyte protein tyrosine kinase (Lck)	48	28	263	64	0.005	*0.044*
Chemokine receptor 3 (Cxcr3)	53	41	181	43	0.006	*0.044*
Histocompatibility 2, class II antigen A, alpha (H2-Aa)	4098	6969	50753	14666	0.008	0.050
Granzyme B (Gzmb)	10	8	45	11	0.010	0.050
Myeloperoxidase (Mpo)	6	5	21	7	0.011	0.050
Chitinase 3-like 3 (Chi3l3)	6	9	51	15	0.011	0.050
Chemokine Ligand 9 (Cxcl9)	79	47	1875	398	0.012	0.050

…table 3.11 continued on next page

…table 3.11 continued

Gene	Geometric mean of expression intensity				CBA/B6.RAG allo + non-immune IgG LS vs. CBA/B6.RAG allo + 3x3mg + C' LS	
	NCBA	NRAG	CBA/B6.RAG allo LS	CBA/B6.RAG allo + 3x3mg LS	Adjusted p-value	FDR
Fas ligand (Fasl)	37	35	60	32	0.001	*0.027*
Chemokine ligand 11 (Cxcl11)	72	24	804	140	0.001	*0.027*
Perforin 1 (Prf1)	8	10	33	13	0.001	*0.027*
Histocompatibility 2, K1 (H2-K1)	3091	5204	43863	10581	0.002	*0.035*
Chemokine Ligand 10 (Cxcl10)	62	71	704	164	0.005	*0.044*
Lymphocyte protein tyrosine kinase (Lck)	48	28	263	64	0.005	*0.044*
Chemokine receptor 3 (Cxcr3)	53	41	181	43	0.006	*0.044*
Histocompatibility 2, class II antigen A, alpha (H2-Aa)	4098	6969	50753	14666	0.008	0.050
Granzyme B (Gzmb)	10	8	45	11	0.010	0.050
Myeloperoxidase (Mpo)	6	5	21	7	0.011	0.050
Chitinase 3-like 3 (Chi3l3)	6	9	51	15	0.011	0.050
Chemokine Ligand 9 (Cxcl9)	79	47	1875	398	0.012	0.050

Chapter 4:

Discussion

4.1 – Correlation between dosages of DSA to extent of allograft injury

Complement split product C4d deposition in human organ transplants is a biomarker of classical complement activation triggered by antibody binding to donor antigens, but this process does not always result in allograft rejection. In cases such as ABO blood group mismatched transplants, deposition of C4d can occur in the absence of any detectable injury in the transplanted organ. We tested the hypothesis that antibody-induced complement activation fails to produce allograft rejection if distal complement effector products are not generated. We transplanted wild-type H-2^k donor kidneys into T-cell/B-cell-null Rag1$^{-/-}$ H-2^b recipients. Adoptive transfer of donor specific anti-class I antibodies into allograft recipients was followed by intragraft antibody deposition and triggered initiation of classical complement activation resulting diffuse C4d staining in allograft peritubular capillaries. However, by histopathology, antibody-induced complement activation did not cause detectable allograft injury or inflammation. Furthermore, using expression microarrays, there is a lack of molecular signs of injury, inflammation, and endothelial activation in C4d positive allografts compared to control allografts, confirming the lack of allograft injury and inflammation by histology. Because intragraft C4d deposition was not accompanied by graft inflammation, we asked if potent chemoattractant complement effectors i.e., C5a were generated. Supporting our hypothesis, serum levels of distal complement effector product C5a were not increased in mice with C4d positive allografts. Thus, bound DSA induced the initiation of complement activation (as indicated by intragraft C4d staining), but this process did not progress to distal stages of the complement cascade, but was terminated, implying rapid termination of complement cascade by natural regulators.

By quantitative histopathology, the data shows that the dosage of DSA treatments is significantly correlated with complement C5a generation as well as certain

forms of acute tubular and microvascular injury. However, the extent of inflammation in transplanted kidneys is not correlated. In this way, the data suggests that the absence of tissue injury in C4d positive (but C5a and C5b-9 negative) transplants is related to the absence of distal complement effector products. With the presence of both circulating DSA and diffuse C4d staining in transplanted allograft tissue, one can see that the phenotype shown in the DSA treated mice satisfy two Banff requirements for the positive diagnosis of ABMR. However, without the presence of morphologic evidence of injury, ABMR is not present in these mice.

ELISA experiments specific for mouse IgG clearly showed the presence of DSA in sera, denoting the successful transfer of injected DSA into circulation. It is interesting to note that trace amounts of IgG was detected in sera of control B6.RAG mice with allografts which did not receive antibody transfer. This was an interesting observation because B6.RAG mice do not have mature B cells and endogenous antibodies. The trace serum IgG detected in control B6.RAG mice with allografts was approximately 0.2% of serum IgG amount found in healthy wild-type B6 mice (17;29;75) and thus, likely represents passage of donor IgG originating from the vascular lumens of transplanted wild-type CBA donor kidney into the recipient's circulation.

The apparent lack of allograft inflammation and injury and absence of C5a activation in the presence of bound donor specific antibody and C4d suggests that complement cascade terminated prior to the conversion of C5. The low amount and monoclonal nature of the transferred donor specific antibody in this model were likely limiting factors for generation of acute rejection. This would lead to a weak complement activation that was easily quelled by normal regulation. Since the activation of the complement cascade is normally tightly regulated, the extent of progression through the complement cascade may have been terminated by naturally present complement inhibitors (131). The regulatory step truncating the complement cascade seems to be after the formation of C4d but prior to formation of C5a. Without C5a, downstream

complement-induced effects such as intragraft endothelial activation, injury, and inflammation did not occur.

Microarray findings suggest that there was also no local C5a formation in the allografts. Furthermore, allograft tissues showed no changes in transcript expression of pro-inflammatory cytokines and endothelial activation molecules inducible by C5a (4;43;49;55;95). Thus, combined with total serum C5a levels and intragraft microarray findings, our data indicate that C5a was not generated. The prevention of C5a formation does not seem to be due to a resistance to antibody binding onto transplanted graft tissue, but more likely due to the effects of the basal levels of complement regulatory proteins (131). The data suggest that DSA treatment did not elicit an active complement inhibitory response by increased complement regulatory protein expression, as transcript levels of intragraft complement regulators did not change after donor specific antibody exposure, suggesting that normal levels of complement regulatory proteins are capable of halting complement activation by DSA treatment.

Analysis of allograft tissues by histopathology and microarrays shows that C4d is an inert molecule incapable of causing allograft injury. Clinical studies already identified a number of limitations of the C4d stain as a biomarker for antibody-mediated rejection: C4d is neither specific nor sensitive for detecting antibody-mediated rejection (47;70;74;102;104). Analyzed on its own, C4d deposition is not a sign of graft injury, but merely denotes the initiation of the classical complement cascade. It should be used in conjunction with morphological and/or molecular assessments in order to determine whether allograft tissue is suffering from inflammation and/or injury. It is noteworthy that our observations in the C4d positive mouse kidney allografts with no injury/inflammation and no C5a are analogous to ABO incompatible transplants in humans, and to the C4d positive kidney allografts with no histological features of antibody-mediated rejection in highly sensitized patients who were treated with anti-C5 (eculizumab) (111). In comparison to ABO incompatible transplants, the mouse model described here elicit C4d

deposition through IgG antibody recognition of peptide antigens present on MHC I molecules, whereas C4d deposition in ABO incompatible transplants are due primarily to IgM antibodies recognizing carbohydrate blood group antigens (53).

C4d deposition in this model was not associated with a protective molecular phenotype in allografts. Resistance to antibody-mediated injury has been observed in a number of xenografts and human ABO-incompatible or crossmatch-positive allografts, a condition termed 'accommodation,' implying that the endothelium has developed resistance to antibody-mediated injury (82;116). Lately, graft accommodation is defined as acquired resistance of an organ transplant to immune-mediated injury (116). A handful of previous studies found increased expression levels of survival or cytoprotective genes such as bcl2, bcl2l1, hmox1, tnfaip3 (7;48;82), and complement regulatory genes such as Cd59 (20) in accommodation of ABO-incompatible allografts or xenografts. DSA treated allograft tissues with positive C4d deposition do not show any changes in gene expression of cytoprotective or accommodation-associated transcripts. In this way, the data suggests that the deposition of C4d on graft tissue in the presence of donor specific antibodies does not induce expression of accommodation-associated genes to confer a protective effect on allograft kidney tissues.

Injections of increasing DSA dosages show a significant correlation with both serum C5a levels and extent of observable histopathology. This dose dependency of injury hints that allograft injury may require a threshold level of DSA binding on any given allograft cell. With increasing DSA dosages, greater numbers of cell surface antigens are recognized, thereby increasing bound DSA density on allograft cells until a threshold is reached, and the full complement cascade to terminal MAC formation is achieved. Along this train of thought, greater allograft injury may be achieved in our mouse ABMR model by increasing bound DSA density on allografts. Further increasing DSA injection dosages could be one method to increase DSA density, but may eventually yield diminishing returns for increasing DSA dosages at a certain point. However, we

hypothesize that increasing the number of antigens recognized by DSAs instead of merely increasing the injection dosage of DSA may have a significant effect in the generation of pathology in allograft tissue. By increasing the number of DSA clones, or by utilizing polyclonal DSA instead of a combination of several monoclonal DSAs, a greater variety of allograft cell surface antigens could be recognized, leading to a greater density of DSAs bound onto allograft cells.

The lack of inflammation and leukocyte recruitment to allograft tissues in DSA treated B6.RAG recipients may be due to the nature of the RAG mutation. Since T helper cells aid in the activation of lymphocytes, it can be postulated that T lymphocytes are also required here in leukocyte recruitment and generation of inflammation. We tested this hypothesis by performing allograft kidney transplantation from wild-type CBA/J into wild-type C57BL/6 mice with treatment of DSA antibodies. Despite the presence of intact T lymphocytes with treatment of DSA antibodies, no noticeable ABMR injury was seen in short term post-transplant, prior to the onset of TCMR, demonstrating that the lack of T lymphocytes may not be crucial to the production of ABMR phenotypes. However, in this experiment, time may be an important factor which cannot be examined with kidney allografts between wild-type CBA/J and wild-type C57BL/6 mice. Since T lymphocytes are intact in the C57BL/6 recipient mice, TCMR manifests fairly rapidly, thereby potentially rejecting the graft prior to the onset of ABMR. In this way, examination of allograft transplants between wild-type mice was limited to short timeframes post-transplant, prior to the onset of TCMR.

4.2 – Mouse model demonstrating allograft rejection

With increasing dosages of DSA correlated with increasing amounts of detectable injury in kidney allografts, the mouse model of antibody-mediated kidney allograft rejection is based on MHC I mismatched kidney transplant model between wild type H-2^k expressing CBA kidneys into H-2^b expressing B6 mice with a knockout in the

Rag gene, with injections of 3mg DSA with addition of rabbit complement. Due to the current lack of suitable small animal models of pure ABMR in kidney allografts, we aim to utilize this mouse model to reproduce pathological features as seen in human allografts undergoing ABMR.

By ELISA measuring C5a / C5b-9 proteins, the treatment of monoclonal DSA in MHC I mismatched transplant is sufficient to activate the complement pathway to terminal C5a / C5b-9 formation. Furthermore, allograft injury and graft dysfunction is demonstrated in the form of measuring changes in serum creatinine levels in graft recipients. With the presence of these signs of graft injury, we further examine tissue samples for pathological evidence of ABMR.

By histopathology and gene expression, the data confirms the validity of the ABMR model, as it demonstrates activation and injury to the microvascular endothelium, which are pathological hallmarks of human acute ABMR. Taken together with the presence of DSA and C4d deposition, our animal model satisfies the consensus Banff diagnostic criteria for type I acute ABMR, designated by C4d positivity, presence of donor specific antibodies in circulation, and ATN-like phenotypes with minimal inflammation, representing morphological features of acute tissue injury. (85;86;105). In addition to evoking endothelial circulation injury in transplanted kidney allografts, there was also the presence of tubular injury as well. However, as described in the previous experiment, despite the presence of potent pro-inflammatory agents and chemokines such as complement C5a, we were unable to generate a strong inflammatory response or recruit large numbers of leukocytes to allograft tissue. We hypothesized that greater antigen recognition and antibody binding onto donor cells would be required in order to enhance pathology phenotypes.

Polyclonal DSA treatments were performed on allograft recipients in order to test this hypothesis. Through preliminary experimental data, the hypothesis seems to be confirmed, as both histopathological observations and measurement of graft function

demonstrates that polyclonal antibody treatment induces greater antibody-mediated allograft injury compared to monoclonal antibody treatment. Further experimentation is required to test the reproducibility of these results. However, taken together, it seems as though the increased recognition of donor MHC I molecules by polyclonal antibodies does indeed lead to increased pathological phenotypes. This may be due to an increased density of bound antibodies onto donor tissue. The greater antibody density and closer proximity of individual antibodies would then be conducive to antibody cross-linking to further promote antibody-mediated immune responses.

Control allografts injected with non-immune IgG showed a slight gradual increase in serum creatinine, denoting a slow decrease in graft function over time. Since the allograft recipient had sufficient time to recover from the initial transplant surgery, and it did not undergo DSA treatments, nor does it have mature T or B lymphocytes, we hypothesize that graft injury is originating from NK cells present in the transplant recipient. We explore this observation in subsequent experiments in this thesis.

The pathology in DSA treated mice show promising results as phenotypes are purely ABMR pathology in the absence of TCMR pathology. The mouse model also shows diagnostic criteria for ABMR, including the presence of DSA, diffuse C4d staining, and morphological changes in transplanted kidney tissue. This model is based on IgG antibodies specific against donor MHC class I antigens. Although this model is based on one immunoglobulin sub-type, immunoglobulin subtype distribution in humans is skewed heavily favoring high levels of IgG. Furthermore, recognizing only donor MHC class I molecules is not a limitation to the mouse model itself due to two reasons: Firstly, mice do not express MHC II molecules on endothelial cells (57), and secondly, ABMR of renal allografts is predominately an MHC class I driven disease in humans(124).

4.3 – Inflammatory trend in allograft transplants

Currently, the specific involvement of NK cells and the role they play in allograft injury is largely unknown. Here we tested the hypothesis that NK cells play an active role to independently cause early kidney allograft injury. We transplanted wild-type H-2^k expressing CBA mice kidneys into T-cell / B-cell null Rag$1^{-/-}$ H-2^b expressing B6 mice. Resultant analysis of early allograft injury in the MHC I mismatched transplant by conventional histopathological stains show no signs of broad-scale tissue injury despite the recruitment of NK cells into the allograft and induction of tubular apoptosis. Although statistically significant, we believe that the amount of tubular apoptosis in allograft tissues is too few and far between to form distinctly visible large scale injury in the transplanted allograft. The lack of histopathological signs of tissue injury may also be due to the insufficient time in which NK cells were able to act on allograft tissue (tissues were harvested 7 days post-transplant). When examining previous experiments (Fig 3.13), the kidney function of control allografts with no DSA treatment began deteriorating over time, as seen in the gradual increase in serum creatinine. Since there were no DSA introduced to the allograft, nor were there any T lymphocytes present, a likely source of injury could be through NK cell action. The increase in serum creatinine of control allografts did not occur until later time points (day 10-15+ post-transplant), and as such, we believe that the lack of injury caused by NK cells in allograft tissues harvested on day 7 post-transplant is in part due to reduced time for the injury to manifest itself. The recruitment of macrophages into transplanted kidney tissues was constant within all groups undergoing transplantation; therefore it seems that the localization of macrophages to renal tissue is to clean up cellular debris caused by the transplantation surgery itself, and not due to allorecognition or rejection of the graft. We believe that, similar to the induction of apoptosis, the recruitment of monocytes / macrophages by activated NK cells (via secretion of cytokines such as interferon gamma) is on a small scale. As such, any recruitment of macrophages by activated NK cells would be masked by the effects of macrophage localization due to general injury arising from surgery procedures, as described above.

Gene expression analysis reveals that interferon gamma is present and seems to have a large impact on gene expression in allograft tissues. Since T lymphocytes are absent in the recipient mice due to the Rag gene knockout, we attribute the source of the interferon gamma as from NK cells. As expected from an increased expression of interferon gamma in allografts, a large response in the form of increased expression of interferon gamma inducible genes in allografts is seen as well. It is interesting to note, however, that there is variation in expression of interferon gamma inducible genes in CBA and B6.RAG isografts even though they were not transplanted with allogeneic kidneys. We attribute this finding as due to expression variation and differences present between two different strains of mice.

Changes in gene expression within several transcript gene sets are most likely a result of non-specific effects arising due to the experimental design. For example, we believe that the increase of T cell associated transcripts in allograft conditions are not due to the presence of T lymphocytes present in the animal, but instead due to the presence of genes in the gene set that are associated with NK cell activation as well. Furthermore, increases in both macrophage-associated and injury and repair-associated transcripts are primarily due to general non-specific injury sustained during transplantation surgery, and not due to allospecific injury / rejection. Thus, contributions of NK cells in recruiting macrophages or inducing injury and repair responses (as seen through gene expression) may be masked by the high background of expression in these transcript sets.

Activated NK cells show a propensity towards the Fas / Fas ligand pathway to induce apoptosis, demonstrated by gene expression changes, which are also inducible by interferon gamma (8;81;115). The upregulation of Fas / Fas ligand expression in the absence of expression in other apoptotic pathways (namely the perforin / granzyme pathway) suggests that the Fas / Fas ligand pathway is the primary way by which apoptosis is activated in allograft recognition, and that interferon gamma release only

enhances the apoptotic effects of Fas / Fas ligand binding (119). Further experiments will be required in order to confirm these findings.

Examining Fcγ receptor and inflammatory cytokine gene expression in DSA treated allografts yielded interesting results. The data shows that treatment of DSA in allograft recipients induces significantly increased expression of the inhibitory FcγR2b early after transplantation, but decreases with time, to the point where expression of the inhibitory receptor is below baseline levels in DSA-treated allograft recipients harvested at days 25-40 post-transplant. FcγR2b is typically expressed on inflammatory cells such as macrophages, neutrophils, and dendritic cells (14). However, in our animal model of allograft injury, there are very few numbers of infiltrating cells observable by histology in both early and late time-point DSA treated allografts. As such, we hypothesize that the increase in FcγR2b early after transplantation is arising from kidney mesangial cell expression. Furthermore, we hypothesize that the binding of DSA onto allograft tissue induces the expression of a 'self-protecting' phenotype namely by decreasing inflammation. Studies by Sharp et al., Callaghan et al., and Radeke et al. (16;88;98) have shown similar findings of increased FcγR2b expression in renal mesangial cells when stressed, leading to a protective effect on renal tissue. Although our comparison between DSA treated allograft recipients and PBS treated allograft recipients in early post-transplant timeframes could be improved to include early post-transplant harvested allograft recipients treated with non-immune IgG, the data still shows a decreased inflammatory response in both early and late time points post-transplant in these controls. Although the anti-inflammatory cytokine effect is reduced in late time-points post-transplant, we suspect this reduction in number of cytokines reaching statistical significance through FDR multiple test correction may be due, in part, to the reduced levels of inhibitory FcγR2b expression.

These findings contribute interesting insights towards the further development of the ABMR model. Allografts seem to naturally express a slight innate inflammatory

phenotype to recruit NK cell to allograft tissue. This NK cell recruitment is capable of inducing small amounts of apoptotic injury and interferon gamma release. Although NK cell induced injury is not detectable by general histology, the effects of NK cell recruitment gradually accumulate and show noticeable graft dysfunction in allografts in later time points. However, when treated with DSA, the allograft's anti-inflammatory response in addition to increased FcγR2b expression is a possible reason why leukocyte recruitment and inflammation is absent in our mouse ABMR model.

Chapter 5: Conclusions and Future directions

5.1 – Conclusions

Here, we developed a mouse model demonstrating pure ABMR in response to MHC mismatched kidney transplantation and anti-donor MHC class I antibodies. We examined the complement components and inflammatory components that combine to form ABMR phenotypes as seen in our model. The data shows that the fluid phase level of DSA and terminal complement effector proteins C5a and C5b-9 is correlated with the extent of ABMR pathology in mouse renal allografts. The presence of C4d deposition in the absence of the formation of terminal complement components C5a and C5b-9 is not indicative of pathological phenotypes, and, on its own, is not a marker for ABMR; it merely indicates the activation of the initial portions of the complement cascade. In this way, the basis to which C4d is deposited without allograft injury can be explained by the lack of distal complement effector proteins. The mouse model of ABMR developed here is very promising as it mimics human endothelial and tubular injury, as seen in ABMR. However, optimization is required as there is weak inflammation shown. This model can be improved on by increasing antigen recognition by DSA, such as through the use of polyclonal antibodies. Here, preliminary data shows that the increased recognition of donor antigens led to greater graft dysfunction with increased inflammation and recruitment of leukocytes to allograft tissues.

With this observation, we examined the recruitment of inflammatory cells and generation of pro-inflammatory cytokines in the ABMR model. The data shows that NK cells are capable of allorecognition (possibly via the 'missing self' hypothesis), and are capable of causing tubular apoptotic injury in allografts, most likely via the Fas / Fas ligand pathway. Finally, gene expression data suggests that, contrary to expectations, the biding of high levels of DSA onto allograft tissue seems to induce a 'self-protective' phenotype by reducing the expression of pro-inflammatory cytokines and inhibiting the inflammatory process, despite experiencing visible endothelial and tubular injury. The data suggests that inhibitory receptor FcγR2b is possibly playing a role to inhibit the

inflammatory response in the presence of DSA, and thereby reduce leukocyte recruitment in this model at early post-transplantation timeframes.

5.2 – Future Directions

Having a model of ABMR in mice has provided new insights into the mechanisms and progression of pathology in this disease, but further development of this animal model is required. As the development of pathology has been shown to be correlated with serum levels of DSA, we plan to examine the effects of increasing DSA recognition and binding of cell surface antigens. We aim to optimize the use of polyclonal DSA in the generation of ABMR injury, as opposed to the use of monoclonal DSA, which cannot successfully induce inflammation or recruit leukocytes into allograft tissue.

Further study into NK cell involvement of ABMR is necessary. General importance of NK cells can be determined through depletion experiments, through the use of antibodies such as NK1.1 to eliminate the presence of NK cells (52). Similarly, the importance of interferon-gamma in the progression of ABMR can be studied by examining the effects from eliminating interferon-gamma in the model system through the use of antibodies such as Xmg1.2 antibody targeting against mouse interferon gamma. Furthermore, additional exploration into the importance of inhibitory FcγR2b will provide valuable insights into the development of inflammation in ABMR. We aim towards more concrete evidence of FcγR2b expression through immunohistochemical staining and ELISA, and to improve gene profiling analysis by incorporating allograft recipients treated with non-immune IgG early post-transplant. We aim to potentially examine the effects of non-DSA IgG in circulation, as it may shed insights into the mechanisms by which treatments of non-immune IgG in human patients (namely IVIG) induce anti-inflammatory and immunomodulatory effects.

Reference List

1. K/DOQI clinical practice guidelines for chronic kidney disease: evaluation, classification, and stratification. Am J Kidney Dis 2002, 39: 1-266

2. U.S. Renal Data System, USRDS 2008 Annual Data Report: Atlas of Chronic Kidney Disease and End-Stage Renal Disease in the United States, National Institutes of Health, National Institute of Diabetes and Digestive and Kidney Diseases, Bethesda, MD. 2008.
   Ref Type: Report

3. Canadian Institute for Health Information Annual Report 2011-2012. 1-59. 6-28-2012.
   Ref Type: Report

4. Allen MD, McDonald TO, Himes VE, Fishbein DP, Aziz s, and Reichenbach DD: E-selectin expression in human cardiac grafts with cellular rejection. Circulation 1993, 88: II243-II247

5. Anderson SK, Ortaldo JR, and McVicar DW: The ever-expanding Ly49 gene family: repertoire and signaling. Immunol Rev 2001, 181: 79-89

6. Anglicheau D and Suthanthiran M: Noninvasive prediction of organ graft rejection and outcome using gene expression patterns. Transplantation 2008, 86: 192-199

7. Bach FH, Ferran C, Hechenleitner P, Mark W, Koyamada N, Miyatake T, Winkler H, Badrichani A, Candinas D, and Hancock WW: Accommodation of vascularized xenografts: expression of "protective genes" by donor endothelial cells in a host Th2 cytokine environment. Nat Med 1997, 3: 196-204

8. Badie B, Schartner J, Vorpahl J, and Preston K: Interferon-gamma induces apoptosis and augments the expression of Fas and Fas ligand by microglia in vitro. Exp Neurol 2000, 162: 290-296

9. Bauer J and Valet G: Conformational changes of the subunits C1q, C1r and C1s of human complement component C1 demonstrated by 125I labeling. Biochim Biophys Acta 1981, 670: 129-133

10. Bohmig GA, Exner M, Habicht A, Schillinger M, Lang U, Kletzmayr J, Saemann MD, Horl WH, Watschinger B, and Regele H: Capillary C4d deposition in kidney allografts: a specific marker of alloantibody-dependent graft injury. J Am Soc Nephrol 2002, 13: 1091-1099

11. Bruhns P: Properties of mouse and human IgG receptors and their contribution to disease models. Blood 2012, 119: 5640-5649

12. Bruhns P: Properties of mouse and human IgG receptors and their contribution to disease models. Blood 2012, 119: 5640-5649

13. Bruhns P: Properties of mouse and human IgG receptors and their contribution to disease models. Blood 2012, 119: 5640-5649

14. Caligiuri MA: Human natural killer cells. Blood 2008, 112: 461-469

15. Callaghan CJ, Win TS, Motallebzadeh R, Conlon TM, Chhabra M, Harper I, Sivaganesh S, Bolton EM, Bradley JA, Brownlie RJ, Smith KGC, and Pettigrew GJ: Regulation of Allograft Survival by Inhibitory Fc gamma RIIb Signaling. Journal of Immunology 2012, 189: 5694-5702

16. Chang JH, Cha HR, Chang SY, Ko HJ, Seo SU, and Kweon MN: IFN-gamma secreted by CD103+ dendritic cells leads to IgG generation in the

mesenteric lymph node in the absence of vitamin A. J Immunol 2011, 186: 6999-7005

17. Cohen D, Colvin RB, Daha MR, Drachenberg CB, Haas M, Nickeleit V, Salmon JE, Sis B, Zhao MH, Bruijn JA, and Bajema IM: Pros and cons for C4d as a biomarker. Kidney Int 2012, 81: 628-639

18. Colvin RB: Antibody-mediated renal allograft rejection: diagnosis and pathogenesis. J Am Soc Nephrol 2007, 18: 1046-1056

19. Dalmasso AP, Benson BA, Johnson JS, Lancto C, and Abrahamsen MS: Resistance against the membrane attack complex of complement induced in porcine endothelial cells with a Gal alpha(1-3)Gal binding lectin: up-regulation of CD59 expression. Journal of Immunology 2000, 164: 3764-3773

20. Dharnidharka VR: Renal transplantation: the present and the future. Indian J Pediatr 2005, 72: 785-788

21. Eckels DD: Alloreactivity: allogeneic presentation of endogenous peptide or direct recognition of MHC polymorphism? A review. Tissue Antigens 1990, 35: 49-55

22. Eckels DD: Alloreactivity: allogeneic presentation of endogenous peptide or direct recognition of MHC polymorphism? A review. Tissue Antigens 1990, 35: 49-55

23. Einecke, G, Sis, B, Reeve J, Mengel, M, Hidalgo, L, Kaplan, B, and Halloran, P. Antibody Mediated Microcirculation Damage Is the Major Cause of Late Kidney Transplant Loss. American Journal of Transplantation 9[s2], 383. 2009.
Ref Type: Abstract

24. Einecke G, Broderick G, Sis B, and Halloran PF: Early loss of renal transcripts in kidney allografts: relationship to the development of histologic lesions and alloimmune effector mechanisms. Am J Transplant 2007, 7: 1121-1130

25. Einecke G and Halloran PF: Antibody-Mediated Microcirculation Injury Is the Major Cause of Late Kidney Transplant Failure: Response to Dr. Loupy et al. Am J Transplant 2010, 10: 953

26. Einecke G, Melk A, Ramassar V, Zhu LF, Bleackley RC, Famulski KS, and Halloran PF: Expression of CTL associated transcripts precedes the development of tubulitis in T-cell mediated kidney graft rejection. Am J Transplant 2005, 5: 1827-1836

27. El Zoghby ZM, Stegall MD, Lager DJ, Kremers WK, Amer H, Gloor JM, and Cosio FG: Identifying specific causes of kidney allograft loss. Am J Transplant 2009, 9: 527-535

28. Enoksson SL, Grasset EK, Hagglof T, Mattsson N, Kaiser Y, Gabrielsson S, McGaha TL, Scheynius A, and Karlsson MC: The inflammatory cytokine IL-18 induces self-reactive innate antibody responses regulated by natural killer T cells. Proc Natl Acad Sci U S A 2011, 108: E1399-E1407

29. Famulski KS, Broderick G, Hay K, Cruz J, Sis B, Mengel M, and Halloran PF: Transcriptome analysis reveals heterogeneity in the injury response of kidney transplants. Am J Transplant 2007, 7: 2483-2495

30. Famulski KS, Einecke G, Reeve J, Ramassar V, Allanach K, Mueller T, Hidalgo LG, Zhu L-F, and Halloran PF: Changes in the transcriptome in allograft rejection: IFN-γ induced transcripts in mouse kidney allografts. Am J Transplant 2006, 6: 1342-1354

31. Feucht HE, Felber E, Gokel MJ, Hillebrand G, Nattermann U, Brockmeyer C, Held E, Riethmuller G, Land W, and Albert E: Vascular deposition of complement-split products in kidney allografts with cell-mediated rejection. Clin Exp Immunol 1991, 86: 464-470

32. Feucht HE, Schneeberger H, Hillebrand G, Burkhardt K, Weiss M, Riethmüller G, Land W, and Albert E: Capillary deposition of C4d complement fragment and early renal graft loss. Kidney Int 1993, 43: 1333-1338

33. Fidler ME, Gloor JM, Lager DJ, Larson TS, Griffin MD, Textor SC, Schwab TR, Prieto M, Nyberg SL, Ishitani MB, Grande JP, Kay PA, and Stegall MD: Histologic findings of antibody-mediated rejection in ABO blood-group-incompatible living-donor kidney transplantation. Am J Transplant 2004, 4: 101-107

34. Fleury S, Lamarre D, Meloche S, Ryu SE, Cantin C, Hendrickson WA, and Sekaly RP: Mutational analaysis of the interaction between CD4 and class II MHC: class II antigens contact CD4 on a surface opposite the gp 120-binding site. Cell 1991, 66: 1037-1049

35. Forquet F, Hadzija M, Semple JW, Speck E, and Delovitch TL: Naturally processed heterodimeric disulfide-linked insulin peptides bind to major histocompatibility class II molecules on thymic epithelial cells. Proc Natl Acad Sci U S A 1994, 91: 3936-3940

36. Gaboriaud C, Thielens NM, Gregory LA, Rossi V, Fontecilla-Camps JC, and Arlaud GJ: Structure and activation of the C1 complex of complement: unraveling the puzzle. Trends Immunol 2004, 25: 368-373

37. Game DS and Lechler RI: Pathways of allorecognition: implications for transplantation tolerance. Transpl Immunol 2002, 10: 101-108

38. Game DS and Lechler RI: Pathways of allorecognition: implications for transplantation tolerance. Transpl Immunol 2002, 10: 101-108

39. Game DS and Lechler RI: Pathways of allorecognition: implications for transplantation tolerance. Transpl Immunol 2002, 10: 101-108

40. Game DS and Lechler RI: Pathways of allorecognition: implications for transplantation tolerance. Transpl Immunol 2002, 10: 101-108

41. Gaston RS, Cecka JM, Kasiske BL, Fieberg AM, Leduc R, Cosio FC, Gourishankar S, Grande J, Halloran P, Hunsicker L, Mannon R, Rush D, and Matas AJ: Evidence for antibody-mediated injury as a major determinant of late kidney allograft failure. Transplantation 2010, 90: 68-74

42. Gennaro R, Simonic T, Negri A, Mottola C, Secchi C, Ronchi S, and Romeo D: C5a fragment of bovine complement. Purification, bioassays, amino-acid sequence and other structural studies. Eur J Biochem 1986, 155: 77-86

43. Golan MD, Burger R, and Loos M: Conformational changes in C1q after binding to immune complexes: detection of neoantigens with monoclonal antibodies. J Immunol 1982, 129: 445-447

44. Groot E, de Groot PG, Fijnheer R, and Lenting PJ: The presence of active von Willebrand factor under various pathological conditions. Curr Opin Hematol 2007, 14: 284-289

45. Guild WR, Harrison JH, Merrill JP, and Murray J: Successful homotransplantation of the kidney in an identical twin. Trans Am Clin Climatol Assoc 1955, 67: 167-173

46. Guo RF and Ward PA: Role of C5a in inflammatory responses. Annu Rev Immunol 2005, 23: 821-852

47. Haas M, Rahman MH, Racusen LC, Kraus ES, Bagnasco SM, Segev DL, Simpkins CE, Warren DS, King KE, Zachary AA, and Montgomery RA: C4d and C3d staining in biopsies of ABO- and HLA-incompatible renal allografts: Correlation with histologic findings. Am J Transplant 2006, 6: 1829-1840

48. Haas M, Segev DL, Racusen LC, Bagnasco SM, Locke JE, Warren DS, Simpkins CE, Lepley D, King KE, Kraus ES, and Montgomery RA: C4d deposition without rejection correlates with reduced early scarring in ABO-incompatible renal allografts. J Am Soc Nephrol 2009, 20: 197-204

49. Hancock WW, Buelow R, Sayegh MH, and Turka LA: Antibody-induced transplant arteriosclerosis is prevented by graft expression of anti-oxidant and anti-apoptotic genes. Nature Medicine 1998, 4: 1392-1396

50. Hauser IA, Riess R, Hausknecht B, Thuringer H, and Sterzel RB: Expression of cell adhesion molecules in primary renal disease and renal allograft rejection. Nephrol Dial Transplant 1997, 12: 1122-1131

51. Hidalgo LG, Sis B, Sellares J, Campbell PM, Mengel M, Einecke G, Chang J, and Halloran PF: NK cell transcripts and NK cells in kidney biopsies from patients with donor-specific antibodies: evidence for NK cell involvement in antibody-mediated rejection. Am J Transplant 2010, 10: 1812-1822

52. Hindmarsh EJ and Marks RM: Complement activation occurs on subendothelial extracellular matrix in vitro and is initiated by retraction or removal of overlying endothelial cells. J Immunol 1998, 160: 6128-6136

53. Hood L, Steinmetz M, and Malissen B: Genes of the major histocompatibility complex of the mouse. Ann Rev Immunol 1983, 1: 529-568

54. Hsu MH, Wang M, Browning DD, Mukaida N, and Ye RD: NF-kappaB activation is required for C5a-induced interleukin-8 gene expression in mononuclear cells. Blood 1999, 93: 3241-3249

55. Hussain R, Dawood G, Abrar N, Toossi Z, Minai A, Dojki M, and Ellner JJ: Selective increases in antibody isotypes and immunoglobulin G subclass responses to secreted antigens in tuberculosis patients and healthy household contacts of the patients. Clin Diagn Lab Immunol 1995, 2: 726-732

56. Hussain R, Dawood G, Abrar N, Toossi Z, Minai A, Dojki M, and Ellner JJ: Selective increases in antibody isotypes and immunoglobulin G subclass responses to secreted antigens in tuberculosis patients and healthy household contacts of the patients. Clin Diagn Lab Immunol 1995, 2: 726-732

57. Janeway CA, Jr., Travers P, and Walport M: The complement system and innate immunity. Immunobiology: The Immune System in Health and Disease. New York, Garland Science, 2001,

58. Jin YP, Jindra PT, Gong KW, Lepin EJ, and Reed EF: Anti-HLA class I antibodies activate endothelial cells and promote chronic rejection. Transplantation 2005, 79: S19-S21

59. Jindra PT, Hsueh A, Hong L, Gjertson D, Shen XD, Gao F, Dang J, Mischel PS, Baldwin WM, III, Fishbein MC, Kupiec-Weglinski JW, and Reed EF: Anti-MHC class I antibody activation of proliferation and survival signaling in murine cardiac allografts. J Immunol 2008, 180: 2214-2224

60. Jordan SC, Reinsmoen N, Peng A, Lai CH, Cao K, Villicana R, Toyoda M, Kahwaji J, and Vo AA: Advances in diagnosing and managing antibody-mediated rejection. Pediatr Nephrol 2010, 25: 2035-2045

61. Kinderlerer AR, Pombo G, I, Hamdulay SS, Ali F, Steinberg R, Silva G, Ali N, Wang B, Haskard DO, Soares MP, and Mason JC: Heme oxygenase-1 expression enhances vascular endothelial resistance to complement-mediated injury through induction of decay-accelerating factor: a role for increased bilirubin and ferritin. Blood 2009, 113: 1598-1607

62. Kissmeyer-Nielsen F, Olsen S, Peterson VP, and Fjeldborg O: Hyperacute rejection of kidney allografts associated with pre-existing humoral antibodies against donor cells. Lancet 1966, 2: 662-665

63. Lanier LL: NK cell receptors. Ann Rev Immunol 1998, 16: 359-393

64. Lanier LL: NK cell recognition. Annu Rev Immunol 2005, 23: 225-274

65. Lerut E, Naesens M, Kuypers DR, Vanrenterghem Y, and Van Damme B: Subclinical peritubular capillaritis at 3 months is associated with chronic rejection at 1 year. Transplantation 2007, 83: 1416-1422

66. Ley K: Molecular mechanisms of leucocyte rolling and adhesion to microvascular endothelium. Eur Heart J 1993, 14 Suppl I: 68-73

67. Ley K: Molecular mechanisms of leukocyte recruitment in the inflammatory process. Cardiovasc Res 1996, 32: 733-742

68. Ley K: Molecular mechanisms of leukocyte recruitment in the inflammatory process. Cardiovasc Res 1996, 32: 733-742

69. Ley K: Molecular mechanisms of leukocyte recruitment in the inflammatory process. Cardiovasc Res 1996, 32: 733-742

70. Lipman ML, Shen Y, Jeffery JR, Gough J, McKenna RM, Grimm PC, and Rush DN: Immune-activation gene expression in clinically stable renal allograft biopsies: molecular evidence for subclinical rejection. Transplantation 1998, 66: 1673-1681

71. Loupy A, Hill GS, Suberbielle C, Charron D, Anglicheau D, Zuber J, Timsit MO, Duong JP, Bruneval P, Vernerey D, Empana JP, Jouven X, Nochy D, and Legendre CH: Significance of C4d Banff scores in early protocol biopsies of kidney transplant recipients with preformed donor-specific antibodies (DSA). Am J Transplant 2011, 11: 56-65

72. Loupy A, Suberbielle-Boissel C, Hill GS, Lefaucheur C, Anglicheau D, Zuber J, Martinez F, Thervet E, Mejean A, Charron D, van Huyen JP, Bruneval P, Legendre C, and Nochy D: Outcome of subclinical antibody-mediated rejection in kidney transplant recipients with preformed donor-specific antibodies. Am J Transplant 2009, 9: 2561-2570

73. Meier-Kriesche HU, Schold JD, Srinivas TR, and Kaplan B: Lack of improvement in renal allograft survival despite a marked decrease in acute rejection rates over the most recent era. Am J Transplant 2004, 4: 378-383

74. Mengel M, Bogers J, Bosmans JL, Seron D, Moreso F, Carrera M, Gwinner W, Schwarz A, De Broe M, Kreipe H, and Haller H: Incidence of C4d stain in protocol biopsies from renal allografts: results from a multicenter trial. Am J Transplant 2005, 5: 1050-1056

75. Mengel M, Husain S, Hidalgo L, and Sis B: Phenotypes of antibody-mediated rejection in organ transplants. Transpl Int 2012, 25: 611-622

76. Nagai H, Ueda Y, Ochi T, Hirano Y, Tanaka H, Inagaki N, and Kawada K: Different role of IL-4 in the onset of hapten-induced contact hypersensitivity in BALB/c and C57BL/6 mice. Br J Pharmacol 2000, 129: 299-306

77. Nagata S: Fas ligand-induced apoptosis. Annu Rev Genet 1999, 33: 29-55

78. Ortaldo JR, Mason AT, Winkler-Pickett R, Raziuddin A, Murphy WJ, and Mason LH: Ly-49 receptor expression and functional analysis in multiple mouse strains. J Leukoc Biol 1999, 66: 512-520

79. Ortaldo JR and Young HA: Mouse Ly49 NK receptors: balancing activation and inhibition. Mol Immunol 2005, 42: 445-450

80. Ossina NK, Cannas A, Powers VC, Fitzpatrick PA, Knight JD, Gilbert JR, Shekhtman EM, Tomei LD, Umansky SR, and Kiefer MC: Interferon-gamma modulates a p53-independent apoptotic pathway and apoptosis-related gene expression. J Biol Chem 1997, 272: 16351-16357

81. Park WD, Grande JP, Ninova D, Nath KA, Platt JL, Gloor JM, and Stegall MD: Accommodation in ABO-incompatible kidney allografts, a novel mechanism of self-protection against antibody-mediated injury. Am J Transplant 2003, 3: 952-960

82. Pettigrew GJ, Lovegrove E, Bradley JA, Maclean J, and Bolton EM: Indirect T cell allorecognition and alloantibody-mediated rejection of MHC class I-disparate heart grafts. Journal of Immunology 1998, 161: 1292-1298

83. Puttarajappa C, Shapiro R, and Tan HP: Antibody-mediated rejection in kidney transplantation: a review. J Transplant 2012, 2012: 193724

84. Racusen LC, Colvin RB, Solez K, Mihatsch MJ, Halloran PF, Campbell PM, Cecka MJ, Cosyns JP, Demetris AJ, Fishbein MC, Fogo A, Furness P, Gibson IW, Glotz D, Hayry P, Hunsickern L, Kashgarian M, Kerman R, Magil AJ, Montgomery R, Morozumi K, Nickeleit V, Randhawa P, Regele H, Seron D, Seshan S, Sund S, and Trpkov K: Antibody-mediated rejection criteria - an addition to the Banff 97 classification of renal allograft rejection. Am J Transplant 2003, 3: 708-714

85. Racusen LC, Halloran PF, and Solez K: Banff 2003 meeting report: new diagnostic insights and standards. Am J Transplant 2004, 4: 1562-1566

86. Racusen LC, Solez K, Colvin RB, Bonsib SM, Castro MC, Cavallo T, Croker BP, Demetris AJ, Drachenberg CB, Fogo AB, Furness P, Gaber LW, Gibson IW, Glotz D, Goldberg JC, Grande J, Halloran PF, Hansen HE, Hartley B, Hayry PJ, Hill CM, Hoffman EO, Hunsicker LG, Lindblad AS, Marcussen N, Mihatsch MJ, Nadasdy T, Nickerson P, Olsen TS, Papadimitriou JC, Randhawa PS, Rayner DC, Roberts I, Rose S, Rush D, Salinas-Madrigal L, Salomon DR, Sund S, Taskinen E, Trpkov K, and Yamaguchi Y: The Banff 97 working classification of renal allograft pathology. Kidney Int 1999, 55: 713-723

87. Radeke HH, Janssen-Graalfs I, Sowa EN, Chouchakova N, Skokowa J, Loscher F, Schmidt RE, Heeringa P, and Gessner JE: Opposite regulation of type II and III receptors for immunoglobulin G in mouse glomerular mesangial cells and in the induction of anti-glomerular basement membrane (GBM) nephritis. J Biol Chem 2002, 277: 27535-27544

88. Ravetch JV and Kinet JP: Fc receptors. Annu Rev Immunol 1991, 9: 457-492

89. Regele H, Bohmig GA, Habicht A, Gollowitzer D, Schillinger M, Rockenschaub S, Watschinger B, Kerjaschki D, and Exner M: Capillary deposition of

complement split product C4d in renal allografts is associated with basement membrane injury in peritubular and glomerular capillaries: a contribution of humoral immunity to chronic allograft rejection. J Am Soc Nephrol 2002, 13: 2371-2380

90. Reis-Filho JS and Pusztai L: Gene expression profiling in breast cancer: classification, prognostication, and prediction. Lancet 2011, 378: 1812-1823

91. Roopenian DC and Akilesh S: FcRn: the neonatal Fc receptor comes of age. Nat Rev Immunol 2007, 7: 715-725

92. Rotman S, Collins AB, and Colvin RB: C4d deposition in allografts: Current concepts and interpretation. Transplant Rev 2005, 19: 65-77

93. Sellares J, De Freitas D, Mengel M, Reeve J, Einecke G, Sis B, Hidalgo L, Famulski K, Matas A, and Halloran P: Understanding the causes of kidney transplant failure: the dominant role of antibody-mediated rejection and non-adherence. Am J Transplant 2012, 12: 388-399

94. Selvan RS, Kapadia HB, and Platt JL: Complement-induced expression of chemokine genes in endothelium: regulation by IL-1-dependent and -independent mechanisms. J Immunol 1998, 161: 4388-4395

95. Shakib F and Stanworth DR: Human IgG subclasses in health and disease. (A review). Part I. Ric Clin Lab 1980, 10: 463-479

96. Shakib F and Stanworth DR: Human IgG subclasses in health and disease. (A review). Part II. Ric Clin Lab 1980, 10: 561-580

97. Sharp PEH, Martin-Ramirez J, Mangsbo SM, Boross P, Pusey CD, Touw IP, Cook HT, Verbeek JS, and Tarzi RM: Fc gamma RIIb on Myeloid Cells

and Intrinsic Renal Cells Rather than B Cells Protects from Nephrotoxic Nephritis. Journal of Immunology 2013, 190: 340-348

98. Sis B: Endothelial Molecules Decipher the Mechanisms and Functional Pathways in Antibody-Mediated Rejection. Hum Immunol 2012, 73: 1218-1225

99. Sis B, Einecke G, Chang J, Hidalgo LG, Mengel M, Kaplan B, and Halloran PF: Cluster analysis of lesions in kidney transplant biopsies: Microcirculation changes, tubulointerstitial inflammation, and scarring. Am J Transplant 2010, 10: 421-430

100. Sis B, Famulski KS, Allanach K, Zhu L-F, and Halloran PF: IFN-γ prevents early perforin-granzyme-mediated destruction of kidney allografts by inducing donor class I products in the kidney. Am J Transplant 2007, 7: 2301-2310

101. Sis B and Halloran PF: Endothelial transcripts uncover a previously unknown phenotype: C4d-negative antibody-mediated rejection. Curr Opin Organ Transplant 2010, 15: 42-48

102. Sis B, Jhangri G, Bunnag S, Allanach K, Kaplan B, and Halloran PF: Endothelial gene expression in kidney transplants with alloantibody indicates antibody-mediated damage despite lack of C4d staining. Am J Transplant 2009, 9: 2312-2323

103. Sis B, Jhangri GS, Riopel J, Chang J, de Freitas DG, Hidalgo L, Mengel M, Matas A, and Halloran PF: A new diagnostic algorithm for antibody-mediated microcirculation inflammation in kidney transplants. Am J Transplant 2012, 12: 1168-1179

104. Smyth MJ, Cretney E, Kelly JM, Westwood JA, Street SE, Yagita H, Takeda K, van Dommelen SL, gli-Esposti MA, and Hayakawa Y: Activation of NK cell cytotoxicity. Mol Immunol 2005, 42: 501-510

105. Smyth MJ, Cretney E, Kelly JM, Westwood JA, Street SE, Yagita H, Takeda K, van Dommelen SL, gli-Esposti MA, and Hayakawa Y: Activation of NK cell cytotoxicity. Mol Immunol 2005, 42: 501-510

106. Smyth MJ, Cretney E, Kelly JM, Westwood JA, Street SE, Yagita H, Takeda K, van Dommelen SL, gli-Esposti MA, and Hayakawa Y: Activation of NK cell cytotoxicity. Mol Immunol 2005, 42: 501-510

107. Smyth MJ, Cretney E, Kelly JM, Westwood JA, Street SE, Yagita H, Takeda K, van Dommelen SL, gli-Esposti MA, and Hayakawa Y: Activation of NK cell cytotoxicity. Mol Immunol 2005, 42: 501-510

108. Smyth MJ, Cretney E, Kelly JM, Westwood JA, Street SE, Yagita H, Takeda K, van Dommelen SL, gli-Esposti MA, and Hayakawa Y: Activation of NK cell cytotoxicity. Mol Immunol 2005, 42: 501-510

109. Smyth MJ, Cretney E, Kelly JM, Westwood JA, Street SE, Yagita H, Takeda K, van Dommelen SL, gli-Esposti MA, and Hayakawa Y: Activation of NK cell cytotoxicity. Mol Immunol 2005, 42: 501-510

110. Stegall MD, Chedid MF, and Cornell LD: The role of complement in antibody-mediated rejection in kidney transplantation. Nat Rev Nephrol 2012, 8: 670-678

111. Stegall MD, Chedid MF, and Cornell LD: The role of complement in antibody-mediated rejection in kidney transplantation. Nat Rev Nephrol 2012, 8: 670-678

112. Stegall MD, Chedid MF, and Cornell LD: The role of complement in antibody-mediated rejection in kidney transplantation. Nat Rev Nephrol 2012, 8: 670-678

113. Stegall MD, Dean PG, and Gloor J: Mechanisms of alloantibody production in sensitized renal allograft recipients. Am J Transplant 2009, 9: 998-1005

114. Stegall MD, Diwan T, Raghavaiah S, Cornell LD, Burns J, Dean PG, Cosio FG, Gandhi MJ, Kremers W, and Gloor JM: Terminal complement inhibition decreases antibody-mediated rejection in sensitized renal transplant recipients. Am J Transplant 2011, 11: 2405-2413

115. Steinle A, Li P, Morris DL, Groh V, Lanier LL, Strong RK, and Spies T: Interactions of human NKG2D with its ligands MICA, MICB, and homologs of the mouse RAE-1 protein family. Immunogenetics 2001, 53: 279-287

116. Stevens J, Wiesmuller KH, Walden P, and Joly E: Peptide length preferences for rat and mouse MHC class I molecules using random peptide libraries. Eur J Immunol 1998, 28: 1272-1279

117. Sumitran-Holgersson S: HLA-specific alloantibodies and renal graft outcome. Nephrol Dial Transplant 2001, 16: 897-904

118. Tamura T, Ueda S, Yoshida M, Matsuzaki M, Mohri H, and Okubo T: Interferon-gamma induces Ice gene expression and enhances cellular susceptibility to apoptosis in the U937 leukemia cell line. Biochem Biophys Res Commun 1996, 229: 21-26

119. Tang AH and Platt JL: Accommodation of grafts: implications for health and disease. Hum Immunol 2007, 68: 645-651

120. Taylor RC, Cullen SP, and Martin SJ: Apoptosis: controlled demolition at the cellular level. Nat Rev Mol Cell Biol 2008, 9: 231-241

121. Tinckam KJ and Chandraker A: Mechanisms and role of HLA and non-HLA alloantibodies. Clin J Am Soc Nephrol 2006, 1: 404-414

122. Tsutsui H, Nakanishi K, Matsui K, Higashino K, Okamura H, Miyazawa Y, and Kaneda K: IFN-γ-inducing factor up-regulates Fas ligand-mediated cytotoxic activity of murine natural killer cell clones. Journal of Immunology 1996, 157: 3967-3973

123. Uehara S, Chase CM, Cornell LD, Madsen JC, Russell PS, and Colvin RB: Chronic Cardiac Transplant Arteriopathy in Mice: Relationship of Alloantibody, C4d Deposition and Neointimal Fibrosis. Am J Transplant 2007, 7: 57-65

124. Ueno T, Tanaka K, Jurewicz M, Murayama T, Guleria I, Fiorina P, Paez JC, Augello A, Vergani A, Wong M, Smith RN, and Abdi R: Divergent role of donor dendritic cells in rejection versus tolerance of allografts. J Am Soc Nephrol 2009, 20: 535-544

125. Unkeless JC, Scigliano E, and Freedman VH: Structure and function of human and murine receptors for IgG. Annu Rev Immunol 1988, 6: 251-281

126. Vo AA, Petrozzino J, Yeung K, Sinha A, Kahwaji J, Peng A, Villicana R, Mackowiak J, and Jordan SC: Efficacy, outcomes, and cost-effectiveness of desensitization using IVIG and rituximab. Transplantation 2013, 95: 852-858

127. Wang H, Jiang J, Liu W, Kubelik D, Chen G, Gies D, Garcia B, Zhong R, and Rother RP: Prevention of acute vascular rejection by a functionally

blocking anti-C5 monoclonal antibody combined with cyclosporine. Transplantation 2005, 79: 1121-1127

128. Wehner J, Morrell CN, Reynolds T, Rodriguez ER, and Baldwin WM, III: Antibody and complement in transplant vasculopathy. Circ Res 2007, 100: 191-203

129. Wiebe C, Gibson IW, Blydt-Hansen TD, Karpinski M, Ho J, Storsley LJ, Goldberg A, Birk PE, Rush DN, and Nickerson PW: Evolution and clinical pathologic correlations of de novo donor-specific HLA antibody post kidney transplant. Am J Transplant 2012, 12: 1157-1167

130. Williams GM, Hume DM, Hudson RP, Morris PJ, Kano K, and Milgrom F: Hyperacute renal-homograft rejection in man. N Engl J Med 1968, 279: 611-618

131. York IA and Rock KL: Antigen processing and presentation by the class I major histocompatibility complex. Annu Rev Immunol 1996, 14: 369-396

132. Zhang X and Reed EF: Effect of antibodies on endothelium. Am J Transplant 2009, 9: 2459-2465

133. Zipfel PF and Skerka C: Complement regulators and inhibitory proteins. Nat Rev Immunol 2009, 9: 729-740

Appendix A – Pathology Scoring Guide

Lesions	Score			
	0	1	2	3
Interstitial inflammation (100;105;108)	Interstitial mononuclear inflammatory cells in 0-9% of cortex	Interstitial mononuclear inflammatory cells in 10-25% of cortex	Interstitial mononuclear inflammatory cells in 26-50% of cortex	Interstitial mononuclear inflammatory cells in >50% of cortex
Tubulitis (100;105;108)	No tubulitis	1-4 mononuclear inflammatory cells / tubular cross-section	5-10 mononuclear inflammatory cells / tubular cross-section	>10 mononuclear inflammatory cells / tubular cross-section
Intimal arteritis (100;105;108)	No arteritis	Subendothelial mononuclear inflammatory cells involving <25% of luminal area	Subendothelial mononuclear cells involving >25% of luminal area, no necrosis	Transmural inflammation and/or arterial fibrinoid necrosis with mononuclear cells
Glomerulitis (100;105;108)	No glomerulitis	Mononuclear cells in <25% of glomeruli	Mononuclear cells in 26-75% of glomeruli	Mononuclear cells in >75% of glomeruli
Peritubular capillaritis (41;100;105;108)	Absent or <10% of cortical peritubular capillaries with inflammatory cells	3-4 luminal inflammatory cells in ≥10% of cortical peritubular capillaries	5-10 luminal inflammatory cells in ≥10% of cortical peritubular capillaries	>10 luminal inflammatory cells in ≥10% peritubular capillaries
C4d peritubular capillary staining (100;105;108)	0% of biopsy area that has a linear, circumferential staining in peritubular capillaries	1-9% of biopsy area that has a linear, circumferential staining in peritubular capillaries	10-50% of biopsy area that has a linear, circumferential staining in peritubular capillaries	>50% of biopsy area that has a linear, circumferential staining in peritubular capillaries
Transplant glomerulopathy (100;105;108)	Double contours in <10% of capillary loops in most severely affected glomerulus	Double contours in 10-25% of capillary loops in most severely affected glomerulus	Double contours in 26-50% of capillary loops in most severely affected glomerulus	Double contours in >50% of capillary loops in most severely affected glomerulus

Interstitial fibrosis (100;105;108)	Interstitial fibrosis in 0-5% of cortex	Interstitial fibrosis in 6-25% of cortex	Interstitial fibrosis in 26-50% of cortex	Interstitial fibrosis in >50% of cortex
Tubular atrophy (100;105;108)	No tubular atrophy	Tubular atrophy in 1-25% of cortical tubules	Tubular atrophy in 26-50% of cortical tubules	Tubular atrophy in >50% of cortical tubules
Arterial fibrous intimal thickening (100;105;108)	No arterial fibrous intimal thickening	Arterial fibrous intimal thickening with 1-25% luminal narrowing	Arterial fibrous intimal thickening with 26-50% luminal narrowing	Arterial fibrous intimal thickening with >50% luminal narrowing
Arteriolar hyalinosis (100;105;108)	No arteriolar hyalinosis	Mild-moderate hyalinosis in at least one arteriole	Moderate-severe hyalinosis in more than one arteriole	Severe hyalinosis in many arterioles
Capillary endothelial swelling (100;105;108)	Absence of prominent (larger of hyperchromatic) cortical PTC endothelial cell nucleus compared to those in normal left kidney	Presence of prominent (larger of hyperchromatic) cortical PTC endothelial cell nucleus compared to those in normal left kidney	n/a	n/a
Capillary dilation (100;105;108)	Cortical peritubular capillary dilation present in 0-9% of cortex	Cortical peritubular capillary dilation present in 10-25% of cortex	Cortical peritubular capillary dilation present in 25-50% of cortex	Cortical capillary dilation present in >50% of cortex
% Tubular cytoplasmic vacuolation (11)	Approximate visual estimation of the cytoplasmic vacuolization of tubular epithelial cells in a section of mouse kidney (see comment)			
% Epithelial cell flattening	Approximate visual estimation of the flattening/thinning of tubular epithelial cells in a section of mouse kidney (see comment)			
% Necrosis of tubules (9)	The number of tubular cross sections with necrosis of tubular epithelial cells per 3285 tubular cross sections (average number of cross sections in a longitudinal / sagittal section of mouse kidney) (see comment)			
% Capillaritis (41)	% of cortical peritubular capillaritis			

Comments:

- We counted the number of cortical tubular sections in 4 transplanted kidneys and calculated the median number. We used this number as a denominator for tubular lesions

- Tubular sections (longitudinal) in 4 transplanted kidneys are as follows: 3049, 3284, 3286, 3350. The median is 3285 tubular sections (longitudinal). For 12 cases we did an absolute count of various parameters and an approximate visual estimation for each and then correlated the values. To assess the reproducibility, we calculated the coefficient of variance for the various parameters.